Random combinatorial processes

Jacob Richey

A dissertation submitted in partial fulfillment of
the requirements for the degree of

Doctor of Philosophy

University of Washington

2020

Reading Committee:
Christopher Hoffman, Chair
Krzysztof Burdzy
Soumik Pal

Program Authorized to Offer Degree:

Mathematics

University of Washington

Abstract

Random combinatorial processes

Jacob Richey

Chair of the Supervisory Committee:
Chris Hoffman
Department of Mathematics

We study four problems in combinatorial probability, namely: activated random walk, an interacting particle process; a phase transition for Wishart matrices, a model of a random geometric graph; the Boolean intersection model, an intersection of random sets in $\mathbb{R}^d$; and rumor spreading algorithms on the d-regular tree.

Acknowledgements

Thanks to Chris and Miki, whose mentorship propelled me to grow and challenge myself; to Jon Wellner, who helped me make the leap from curious student to well-armed mathematician; to Amy, Courtney, Jon, Kevin, Sean, and all the other friends who never refused an impromptu brainstorming session; and to all my collaborators, including Leo, Shirshendu, Riddhi, and Amites, without whom none of this research would have been possible.

Contents

Part 1. Introduction

Discrete probabilistic models and methods have continuously grown in their usefulness and ubiquity since the early 20th century. Today we are lucky to have a plethora of questions, coming from classical results and problems, from other fields – notably in my own research, statistical mechanics – and from natural variants on well studied processes. In a nutshell, I study the limiting behavior of systems that obey simple (stochastic) rules. The areas of particular interest to me include: interacting particle systems, random walks, percolation, random graphs, and poisson processes.

Working in this field involves a satisfying mix of inventing and polishing. Answering some open questions requires creative re-thinking of old probabilistic models: re-inventing the wheel, with a twist. Recent work on activated random walk (ARW) – a stochastic particle system – is an example where this approach has been successful: a sequence of papers tightening the phase transition for ARW rely on viewing the underlying particle dynamics in new and insightful ways. Asking new questions about old models can lead to deeper understanding, and if you're lucky, to valuable results! These new techniques for studying ARW are a roadmap for how particle systems with long range interactions (both in time and space) can be analyzed rigorously. See section 2 for results related to ARW on the cycle.

The big probabilistic models of interest are never really 'solved:' we understand them over time by attacking from many different angles, like polishing a stone until it gleams. In my work on random matrix theory, we found new evidence for a universality phenomenon – a phase transition common to an ensemble of random graphs – by showing that it holds for random intersection graphs. This came as a surprise, since there is no obvious connection between these graphs and the matrices originally shown to have a similar phase transition, namely Wishart matrices. Unifying these approaches and models is an interesting open problem, with applications to detecting geometry in large random graphs, and for applications of random matrices. See section 3 for a result related to the behavior at criticality.

Much of my work is motivated by what is interesting and natural. (A 'natural' question or problem is one that fits the model, in that the associated calculations are easy, or that it is the first question someone learning about the model might ask.) My project on intersections of random sets is such an example: we considered a new random set model, the Boolean intersection model, which is easy to define and relatively easy to calculate with. We proved that it shares a scaling limit with a class of well-studied models, namely the Boolean model and tessellation models. (See section 4.)

In the process, we scratched the surface of the underlying geometric and combinatorial structure of the intersection model, which deserves further study. The intersection model is connected to the theory of coverage processes.

My work on rumor source detection is also motivated by a simple question: can the source of a diffusion be found easily? Our attempts to find a satisfying answer led to a more nuanced statistical understanding of the performance of rumor spreading algorithms. (See section 5.) Although our results apply to the theoretical situation where the underlying network is a regular tree, recent work has shown that properties of these algorithms also hold on randomly generated (preferential attachment) trees, and it seems likely that our results are also valid on these real-world networks.

Part 2. Activated random walk on a cycle

Consider the following interacting particle system on a one dimensional lattice. Given a configuration of particles, initially all active, the dynamics, which conserves the particles, proceeds as follows. Each active particle independently does a simple symmetric random walk at rate one in continuous time and falls asleep at rate $\lambda > 0$. Each sleepy particle is awakened when an active particle occupies the same site. This model, known as Activated Random Walk (ARW), has attracted interest in non-equilibrium statistical mechanics as well as probability literature in recent years in connection with studying fixed energy sandpile models [14, 57, 58, 12, 59, 15, 42]. The motivation of studying this model is two-fold. ARW can be regarded as a special case of driven diffusive epidemic process introduced by Spitzer in 1970s, and studied later in [30, 31, 32, 33]. ARW was also introduced in the physics literature as a more mathematically tractable approximation of the Stochastic Sandpile Model (SSM), and is one of the paradigm examples of the widely studied phenomenon of self-organized ciriticality (SOC) [40, 41, 13, 11].

ARW is believed to manifest self-organized criticality when run in a finite volume with carefully controlled driven diffusive dynamics. However, the rigorous study of ARW has so far been mostly restricted to the case of infinite volume limit where the counterpart of SOC is known as Absorbing state Phase Transition (APT) (although some recent results have called into question the exact relationship between these two notions [24, 36, 25]). Absorbing state Phase Transition was rigorously established for ARW on $\mathbb{Z}$ a few years ago in the fundamental work of Rolla and Sidoravicius [42]. Let us briefly explain their result. Consider ARW started with initial configuration of particles coming from a product measure with density μ; denote this process by ARW(μ, λ). One would expect that for a fixed λ, if μ is very small, then all the particles will eventually fall asleep, whereas for large μ the activity would go on forever. Indeed, in [42] it was shown that for each $\lambda > 0$, there exists $\mu_c(\lambda) \in [\frac{\lambda}{\lambda+1}, 1]$ such that for $\mu < \mu_c$ the process ARW(μ, λ) on $\mathbb{Z}$ fixates (i.e., the total number of jumps at origin is finite) almost surely, and for $\mu > \mu_c$ the process remains almost surely active forever. Observe that it is easy to understand heuristically why $\mu_c \leq 1$. If $\mu > 1$, there are "more particles than sites" and hence not all particles can eventually fall asleep [47, 1, 42]. Complementing the results of [42], the first three authors showed in [4] that for any fixed $\mu > 0$, the process almost surely does not fixate if λ is sufficiently small; thus showing $\mu_c \to 0$ as $\lambda \to 0$, and answering a question from [15, 42]. Subsequently, a statement similar to the latter was proven for transient Euclidean lattices in [53], which also analyzed ARW dynamics on transitive graphs where

the random walk is ballistic. However, to rigorously establish the critical or near-critical behaviour in these models seems far out of reach of the current mathematical techniques.

The results in [42, 4] are in the setting of ARW on the inifinite lattice $\mathbb{Z}$. Indeed, there has been a flurry of recent mathematically rigorous results on ARW following the breakthrough work [42], but most of them have been in the context of Euclidean lattices or other infinite graphs [47, 1, 48, 54, 55, 53]. From the point of view of understanding self-organized criticality, it is interesting to study this model on a finite lattice, with say a periodic boundary condition. On a finite graph, if the total number of particles is more than the number of vertices, then the process will continue for ever. If the total number of particles is at most the number of vertices, this is an absorbing Markov chain, so all the particles will almost surely fall asleep after a finite time. One would expect the Absorbing state Phase Transition to be manifested in the finite process as a phase transition for the absorption time. For many finite systems of these type, it is generally believed that absorption time has three different scalings with the system size, polynomial (with different exponents) for the sub-critical and critical systems, and exponential for the super-critical system. Indeed a version of the above statement in the set up of [42] and [4] respectively are the main results of this paper. In physics literature there are many non-rigorous and numerical results about the critical and near-critical scaling of this and related quantities for SSM and its many variants (see e.g. [38] and references therein). However, as with the infinite system, rigorous analysis of the critical scaling behaviour remains a challenging problem.

0.1. **Main Results.** Consider an n-cycle $\mathbb{Z}/n\mathbb{Z}$ with nearest neighbour edges. Fix $\lambda > 0$ and $\mu \in (0,1)$. Consider the initial configuration with independent $\mathrm{Ber}(\mu)$ many particles at each site. (We will denote the product Bernoulli measure by $\mathbb{P}^\mu$). Consider ARW started with this configuration with sleep rate λ; denote this process by $\mathrm{ARW}(\mu,\lambda)$. As mentioned before, this is an absorbing Markov chain and hence the process reaches the absorbing state of all sleepy particles (the set of all such configuration will be henceforth called the cemetery set and written Δ) after a finite time almost surely. Let $T_n(\mu,\lambda)$ denote the total number of attempts by any active particle to either jump or to try to sleep. Note that the continuous time ARW dynamics can be coupled naturally to the following discrete time dynamics: at every positive integer time, pick an active particle uniformly at random. With probability $\frac{1}{2(1+\lambda)}$ each, the particle jumps to one of the neighbouring sites, and with probability $\frac{\lambda}{1+\lambda}$ it tries to fall asleep. It is easy to see that under the natural coupling, $T_n(\mu,\lambda)$ is the absorption time of the latter dynamics.

Our first result shows that if the particle density μ is sufficiently small compared to λ then $T_n(\mu,\lambda)$ is linear up to poly-logarithmic correction factors.

Theorem 1. *Consider* ARW(μ,λ) *on* $\mathbb{Z}/n\mathbb{Z}$. *For any* $\lambda>0$ *and* $\mu<\frac{\lambda}{1+\lambda}$, *there exist positive constants* C_0, b *depending on* μ *and* λ, *such that for all large enough* n,

$$\mathbb{P}(T_n(\mu,\lambda)>C_0 n\log^2 n)\le\frac{1}{n^b}.$$

Observe that $\mu<\frac{\lambda}{\lambda+1}$ is precisely the regime in which [42] showed fixation on $\mathbb{Z}$. It is also easy to observe that the bound is tight up to the polylogarithmic factor. To see this, observe that the expected total number of jumps a particle takes before trying to fall asleep is $\frac{1+\lambda}{\lambda}$. Thus, if the number of particles is linear in n, the total number of jumps is also at least linear in n.

In the heavily super-critical regime, i.e., when λ is sufficiently small compared to μ, we have the following complementary result (This result should be compared to [4, Theorem 1].).

Theorem 2. *For any* $0<\mu<1$, *there exists* $\lambda_0>0$ *and* $c>0$ *such that for any* $\lambda<\lambda_0$, *and all large enough* n,

$$\mathbb{P}(T_n(\mu,\lambda)<e^{cn})<e^{-cn}.$$

Theorem 1 relies heavily on the uniformity of the locations of the particles in the initial configuration (note however, that the arguments in this paper do not depend on the specific nature of the Bernoulli distribution of the initial configuration). In fact, it can be shown that $T_n(\mu,\lambda)$ is at least of order n^3 when all the particles start at the origin. An exponential upper bound for $T_n(\mu,\lambda)$ is also relatively easy to establish. See Remarks 2.13 and 3.6 for further elaboration.

We list below the new contributions in this paper and relations to existing results: Although the linear to exponential phase transition for absorption time is widely expected in the statistical physics literature, to the best of our knowledge this is the first rigorous result establishing such a transition for some variant of fixed energy sandpile models. We rely crucially on the recent progress [42, 4] in understanding ARW on the infinite line. However one needs certain new ideas to deal with the finite case. Following the argument of [42], the main obstacle in showing fast fixation for low particle density is the wrapping around issue, that is to make sure the particles do not wrap around the cycle, and wake up already settled particles. We get around this by a block argument and a two-sided variant of the stabilizing algorithm in [42]. In the process of attaining the quantitatively optimal result Theorem 1, we encounter a particle system similar to internal erosion (see [36]).

For the slow fixation part i.e., Theorem 2, we first recall that the argument from [4] essentially tells us that when we stabilize a certain density of particles on $\mathbb{Z}/n\mathbb{Z}$ until they hit 0, for small enough sleep rate only a small fraction of the particles fall asleep. The key observation in this paper is that the above step can be applied iteratively for exponentially many rounds. A naive application of the iteration scheme only allows the number of steps to be logarithmic in n since a constant fraction of particles fall asleep in every round. However the finiteness of the environment allows us to recycle particles which fell asleep in earlier rounds once they get woken up in later rounds. To this end we strengthen the argument in [4] by showing that with exponentially small failure probability all the particles that were asleep at the start of the round get woken before the end of the round and not too many particles fall asleep. Thus we can sustain the process for exponentially many steps.

In the next section we elaborate on the above ideas further.

0.2. **Sketch of the proofs.** A crucial property of many interacting particle systems that serve as models of distributed networks is the Abelian Property. Informally it means that the final outcome of a certain probabilistic experiment does not depend on the order in which operations at different sites are performed.

In the context of ARW, one exploits the Abelian Property via the Diaconis-Fulton representation, which is roughly the following (see Section 1.1 for a more formal description). At every site in $\mathbb{Z}/n\mathbb{Z}$, we have a sequence of i.i.d. instructions (referred to as the "stack of instructions") to either jump to one of the two neighbours, with probability $\frac{1}{2(1+\lambda)}$ each, or to fall asleep, with probability $\frac{\lambda}{1+\lambda}$. Given these stacks, one way to run the process is: as long as there is some active particle, pick an arbitrary site $x \in \mathbb{Z}/n\mathbb{Z}$ with at least one active particle, and use the first unused instruction from the stack to topple the site. That is, if the instruction is a jump instruction, then the particle jumps to a neighbouring site accordingly, and otherwise tries to fall asleep.

The Abelian Property then states that the final configuration of particles after every particle has fallen asleep does not depend on the order in which the sites were toppled. Thus in this language $T_n(\mu, \lambda)$ is the total number of instructions across all the stacks used until the end of the toppling process.

We also rely on the following monotonicity property of the ARW dynamics: given a set of stacks of instructions, while toppling sites, if we ignore any sleep instruction, then the total number of topplings required to reach Δ can only increase. Here 'ignoring a sleep instruction' means the

configuration does not turn an active particle to a sleepy particle, even though the instruction is a sleep instruction. This monotonicity is certainly heuristically plausible and, indeed, is a well-known consequence of the Abelian Property. (See Lemma 1.3 and the discussion preceding it for formal definitions.)

0.2.1. *Sketch of the proof of Theorem 1.* Given the above two properties, to prove Theorem 1 we will provide a toppling scheme which will end with a configuration in the cemetery set Δ. Our toppling procedure will ignore certain sleep instructions and hence by the monotonicity property, the total number of instructions used in the actual process in the Diaconis-Fulton representation is upper bounded by the number of instructions used in our scheme. The basic idea is to break the cycle $\mathbb{Z}/n\mathbb{Z}$ in to sub-intervals $I_1, I_2, \ldots$ of size $c_0 \log n$ for some constant c_0. Our toppling scheme is then a combination of toppling schemes, one for each of the sub-intervals. The toppling scheme for I_i is designed to stabilize particles inside I_i for $i = 1, 2, \ldots, \frac{n}{c_0 \log n}$. The toppling scheme in each of the intervals is a variant of the trap-setting procedure appearing in [42]. We prove that with very small failure probability (exponential in the size of the interval) the toppling procedure in the interval succeeds to stabilize everything. A union bound over all the intervals show that with high probability the procedure succeeds simultaneously for all the intervals, and hence stabilizes the system. Recall that the failure probability for each interval is exponential in the size of the interval which forces us to choose the size of the intervals to be logarithmic (in n) as otherwise the union bound over polynomially (in n) many such intervals will fail; this also explains the logarithmic correction term in the statement of Theorem 1.

We now briefly describe our toppling scheme. It consists of broadly two parts.

(1) Phase 1: Given the initial configuration, the first step is to gather particles which are initially located uniformly over $\mathbb{Z}/n\mathbb{Z}$, to a set of points we call **Sources**. We will take this set to be $\{\frac{c_0}{2} \log n, \frac{3c_0}{2} \log n, \ldots\}$ for some carefully chosen value of c_0, depending on the parameters μ and λ. Thus we first ignore all the sleep instructions and allow the particles to do independent random walks till they hit an element of **Sources**. Large deviation estimates imply that with high probability the number of particles at each **Source** at the end of this process is roughly $c_0 \mu \log n$. Recall that we are using the monotonicity property mentioned above, and hence we can ignore certain sleep instructions.

(2) Phase 2: The intervals $I_1, I_2 \ldots$ inside which we run our toppling scheme are of size $c_0 \log n$, and centred at the sources. The proof proceeds by showing that there is a toppling procedure

which carefully ignores certain sleep instructions allowing the particles to fall asleep only at certain well chosen 'traps' which prevents interaction with other particles. The remainder of the proof then shows that the above scheme succeeds with high probability.

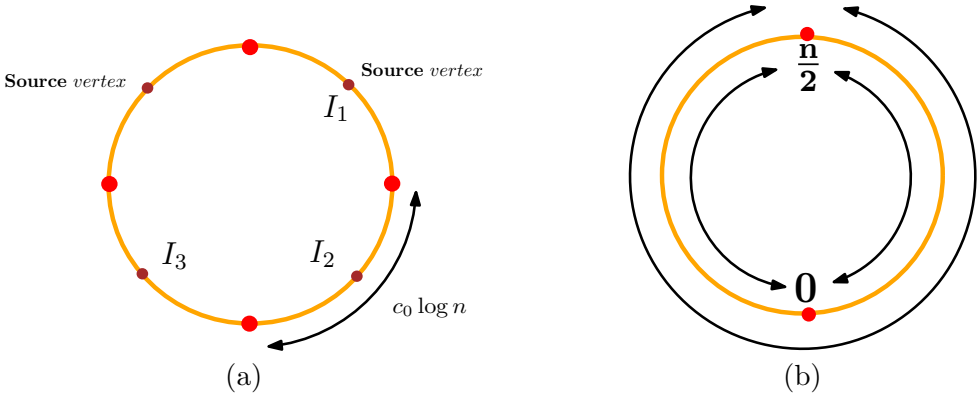

FIGURE 1. (a) The toppling scheme for fixation in the sub-critical regime: in the first step of the stabilization scheme, we ignore sleep instructions to get every particle to a nearby source vertex. Particles at a particular source are then stabilized inside an interval of length $c_0 \log n$ using a trap-setting procedure. (b) The toppling scheme for non-fixation in the supercritical regime: 0 and $n/2$ are the north and south 'poles' of the cycle. We run several rounds of the following stabilization loop where we first try to topple all particles located away from 0 or $n/2$ until they fall asleep or hit $\{0, n/2\}$. Then we try to topple particles starting from 0 until they hit $n/2$ or fall asleep, and afterwards do the same at $n/2$, namely topple all particles starting from $n/2$ until they hit 0 or fall asleep. These three actions are repeated until all particles are asleep: our proof shows that this loop can be sustained for exponentially many steps (in n) with high probability.

Even though the trap setting scheme is inspired from [42], the argument in the latter was particularly tailored to the ARW process on the infinite line and does not directly work on the cycle: this is because on the cycle, each particle has a chance of order $\frac{1}{n}$ to wrap around the cycle before falling into the trap and thereby waking up the already asleep particles. To circumvent this we introduce a two sided version, which, relying on estimates for random walk on the interval, can be shown to work in our setting.

0.2.2. *Sketch of the proof of Theorem 2.* For the proof of Theorem 2 we rely on the non-fixation result from [4]. The technical core of that paper (see the proof of [4, Lemma 18]) was to establish the following non-fixation phenomenon. Consider a sufficiently large interval $[0, r]$ with at least μr many active particles, and stabilize the particle system inside the interior of the interval $[0, r]$, i.e., the particles are stopped upon hitting $\{0, r\}$. Then, given $\varepsilon > 0$, for any mass density μ, and for all

small enough λ, at the end of the stabilization procedure, the number of particles accumulating at $\{0, r\}$ is at least $(1-\varepsilon)$ fraction of the total number, with failure probability exponentially small in r. This was used in [4] to show infinite activity on the line, by considering a growing sequence of r and then using the above statement to show that particles from arbitrary far away would hit the origin, thus implying non-fixation. For a finite system, we cannot rely on an argument which uses particles arbitrarily far away. Instead we use the following 'recycling particles' approach: represent the cycle $\mathbb{Z}/n\mathbb{Z}$ as the interval $[-n/2, n/2]$ with endpoints identified. We run the following rounds of particle stabilization:

(1) We first treat the 'poles' 0 and $n/2$ as boundary points, and topple particles not at those sites until they fall asleep or land at one of the sites 0 or $n/2$. By the arguments in [4], a constant fraction of all particles will make it to either 0 or $n/2$ with exponentially high probability.

(2) We topple particles that ended up at 0 in the previous stage until they fall asleep or hit $n/2$. The particles that did not start at 0 do not move, but they can be woken up by other active particles during this stage. Using ideas from [4, Lemma 18], we show that most particles will make it to the boundary before falling asleep with exponentially high probability.

(3) Just as the previous step, we only topple particles that started at $n/2$ at the end of the previous stage, running the dynamics until all such particles are asleep or at 0.

Since all these steps keep most particles awake with exponentially high probability, we can run the loop exponentially many times. Moreover, since each loop takes at least one stack instruction to run, the Abelian Property implies that $T_n(\mu, \lambda)$ is at least exponential in n.

Acknowledgements

The authors thank Lionel Levine, Vladas Sidoravicius and Lorenzo Taggi for useful conversations, and Leonardo Rolla for comments on a previous version of the paper. Research of RB is partially supported by a Simons Junior Faculty Fellowship and a Ramanujan Fellowship from the Govt. of India. SG is supported by a Miller Research Fellowship.

1. Abelian Property for Activated Random Walk

For brevity, we will denote $\mathbb{Z}/n\mathbb{Z}$ by $\mathcal{C}_n$. We follow [42] in formally describing the set up of ARW. To avoid unnecessary notational overhead we describe the bare minimum of the formalism

necessary. We always work with ARW on $\mathcal{C}_n$ for some fixed but large n, and the notation is adapted accordingly. In particular, for the remainder of this section, addition and subtraction will be considered modulo n whenever appropriate and we shall not mention that explicitly every time.

For any time $t \geq 0$ and location $x \in \mathcal{C}_n$, $\eta_t(x)$ denotes the state of the system at location x at time t. We write $\eta_t(x) = \rho$ if there is one sleepy particle at $x \in \mathcal{C}_n$ at time t. If there is not a sleepy particle present we let $\eta_t(x) \in \mathbb{N}$ denote the number of particles at $x \in \mathcal{C}_n$ at time t. Then $\eta_t = \{\eta_t(x)\}_{x \in \mathcal{C}_n}$ denotes the state of the system at time t.

We shall use two operations (called topplings) on the space of configurations. For $x \in \mathbb{Z}$ and $y = x \pm 1$, let $\tau_{x,y}(\eta)$ denote the configuration obtained by moving one of the active particles from x to y. This operation will be called **illegal** (for the configuration) if there are no active particles at x and the system remains unchanged. Let $\tau_{x,\rho}(\eta)$ denote the configuration obtained from η by making the solitary particle at x fall asleep. Moreover if x has more than one active particle, the sleep instruction has no effect, so $\tau_{x,\rho}(\eta) = \eta$. Again if there are no particles at x, this instruction is called illegal and the system is not changed.

Now we can formally define ARW as a finite state space continuous time Markov chain with transitions $\eta \to \tau_{x,y}\eta$ at rate $A(\eta_t(x))\frac{1}{2}\mathbf{1}_{y=x\pm1}$, and $\eta \to \tau_{x,\rho}\eta$ at rate $\lambda A(\eta_t(x))$ where $A(\eta(x))$ denote the number of active particles at site x in configuration η. Let $\mathbb{P}^\nu$ denote the law of the process started from an initial configuration distributed according to ν.

1.1. **Diaconis-Fulton representation.** We will now describe the Diaconis-Fulton representation of the ARW dynamics which will be convenient for our purposes. For an extensive discussion of the Diaconis-Fulton representation of ARW dynamics, the Abelian Property and its consequences, see [42]. For completeness we recall the relevant results from [42], suitably adapted to the setting of a finite cycle.

The Diaconis-Fulton representation [10, 19] maps the ARW process to sequence of instructions attached to the sites. The advantage of this representation is the Abelian Property, which allows one to disregard the order in which different steps were performed in certain settings. We start by introducing a series of notations. Recall the operations $\tau_{x,y}$ and $\tau_{x,\rho}$ from above. Now consider the

following array of random variables:

$$\mathscr{I} = \begin{matrix} \cdots & \xi_{(-2,1)} & \xi_{(-1,1)} & \xi_{(0,1)} & \xi_{(1,1)} & \xi_{(2,1)} & \cdots \\ \cdots & \xi_{(-2,2)} & \xi_{(-1,2)} & \xi_{(0,2)} & \xi_{(1,2)} & \xi_{(2,2)} & \cdots \\ \vdots & \vdots & \vdots & \vdots & \vdots & \vdots & \vdots \end{matrix} \tag{1.1}$$

where $\xi_{(x,j)}$ are independent for any $x \in \mathcal{C}_n$ and $j \in \mathbb{N}$ and moreover,

$$\xi_{(x,j)} = \begin{cases} \tau_{x,x-1} & \text{with probability } \frac{1}{2(\lambda+1)} \\ \tau_{x,x+1} & \text{with probability } \frac{1}{2(\lambda+1)} \\ \tau_{x,\rho} & \text{with probability } \frac{\lambda}{\lambda+1}. \end{cases} \tag{1.2}$$

We will now show that using these instructions one can define a discrete time version of the ARW process. In fact we can define many such versions. But they will all have the same configuration when it is finally stabilized and the same set of instructions that have been implemented.

We call the $\xi_{(x,j)}$'s instructions at the site x and the underlying product measure $\mathscr{P}$.

Given a configuration η at each discrete time step t, one can choose (arbitrarily) an unstable site x and use the first unused element from the stack $\xi_{(x,\cdot)}$ and use it to perform the transition to a configuration η' at time step $(t+1)$. As mentioned in Section 0.2, we call such an operation "toppling" at site x. We keep track of the number of topplings at every site. Let η be the configuration after applying $h(x)$ many topplings at each site $x \in \mathcal{C}_n$. Let us denote

$$h := (h(x) : x \in \mathbb{Z}/n\,\mathbb{Z}) \tag{1.3}$$

which we will call the odometer function. Let $\Phi_x(\eta)$ denote the configuration obtained by toppling the site x next, i.e., we apply the instruction $\xi_{x,h(x)+1}$, and also increase h at x by one (h at other sites does not change). We say Φ_x is legal for η if x is unstable in η. For any sequence $\alpha = (x_1, x_2, \ldots, x_k)$ we define the sequence of topplings at x_1, followed by x_2 and so on through until x_k by Φ_α, i.e. $\Phi_\alpha = \Phi_{x_k} \ldots \Phi_{x_1}$. We now say that α is a **legal sequence** for initial configuration η if Φ_{x_i} is legal for $\Phi_{x_{i-1}} \ldots \Phi_{x_1}(\eta)$ for all $i = 1, \ldots k$. We abuse notation a little to denote by h_α the odometer function after performing the sequence of toppling given by α, i.e. for any $x \in \mathcal{C}_n$,

$$h_\alpha(x) = \sum_{i=1}^{k} \mathbf{1}(\alpha_i = x). \tag{1.4}$$

Given the above preparation we can now formally state the Abelian Property, which says that given two sequence of legal topplings that result in the same odometer function (see (1.4)), the final configuration is the same in both the cases, i.e. the order in which topplings are performed does not matter.

Lemma 1.1. *(Abelian Property,* [42, Lemma 2]*) Given any two legal sequence of topplings α and α' such that $h_\alpha = h_{\alpha'}$, then*

$$\Phi_\alpha(\eta) = \Phi_{\alpha'}(\eta).$$

The next lemma is a consequence of the Abelian Property. It shows that any legal sequence of topplings must occur in any stabilizing sequence (i.e., a legal sequence which leads to all stable sites).

Lemma 1.2. *(Least Action Principle,* [42, Lemma 1]*) Let α, α' be two legal sequences of topplings such α stabilizes η, then $h_{\alpha'} \leq h_\alpha$, i.e. all the topplings in α' are also needed in α.*

Observe that Lemma 1.2 immediately implies that any two stabilizing sequence must lead to the same odometer function, and in turn by Lemma 1.1 this implies that the final configuration after stabilization is also independent of the stabilizing sequence. This will imply that for any stabilizing sequence α, for an initial configuration of product Ber(μ) many particles, we have

$$T_n(\mu, \lambda) = \sum_{x \in \mathcal{C}_n} h_\alpha(x).$$

This will be the fundamental tool used in our proofs. Finally we need another lemma to compare the stabilizing sequences which formalizes the intuitively plausible statement: for a stabilizing sequence where we ignore some of the sleep instructions, the total number of jumps is larger than if we hadn't ignored those sleep instructions. Formally we need to introduce a new notation to define precisely the meaning of ignoring a sleep instruction. Recall the stack of instructions $\mathscr{I}$ from (1.1) and the action of the instructions $\tau_{x,\rho}$ and $\tau_{x,x\pm1}$ on the particle configuration η. Let us introduce a null instruction $\mathfrak{n}$ which acts on a configuration to create no change, i.e., $\mathfrak{n}\eta = \eta$ for all η. Now given a stack of instructions, $\mathscr{I} = \{\xi_{(\cdot,\cdot)}\}$, as in (1.1), let $\mathscr{I}' = \{\xi'_{(\cdot,\cdot)}\}$, be another stack, with the property that for each (x, j) either , $\xi_{(x,j)} = \xi'_{(x,j)}$, or $\xi_{(x,j)} = \tau_{x,\rho}$, and $\xi'_{(x,j)} = \mathfrak{n}$. Thus informally $\mathscr{I}'$ is any set of toppling instructions obtained from $\mathscr{I}$ by ignoring certain sleep instructions.

Lemma 1.3. [42, Lemma 5] *Given any $\mathscr{I}, \mathscr{I}'$ as above, and any initial configuration η, let α and α' be two legal toppling sequences stabilizing η, using instructions from $\mathscr{I}$ and $\mathscr{I}'$, respectively. Let $h_\alpha(\cdot)$ and $h_{\alpha'}(\cdot)$ be the respective odometer functions. Then $h_{\alpha'}(x) \geq h_\alpha(x)$ for every $x \in \mathcal{C}_n$.*

Often our argument will be based on running the ARW dynamics on certain sub-intervals of $\mathcal{C}_n$, and hence to be completely formal one needs to introduce stacks corresponding to such intervals. However to avoid introducing additional notation, we will identify the latter in the natural way with the corresponding subset of stacks of $\mathscr{I}$.

2. Fast fixation under low density

We prove Theorem 1 in this section. By the discussion at the end of last section and Lemma 1.3, we shall provide an algorithm for toppling which will ignore some sleep instruction and which stabilizes all sites in $\mathcal{C}_n$ within $O(n \log^2 n)$ many topplings with high probability. (Note that the probability here is over both the random initial configuration and also the random stack of instructions.) We shall formalize the sketch provided in Section 0.2 to build the toppling procedure.

Let η be a initial configuration of particles on $\mathcal{C}_n$ distributed according to law $\mathbb{P}^\mu$. Also fix a realization $\mathscr{I}$ of the stack of instructions. For the remainder of this section, we shall always talk about toppling the configuration η sequentially using instructions from $\mathscr{I}$.

2.1. Random Walk estimates.

As explained before, the first phase will be to topple any unstable site that is not a **Source** and ignore any sleep instructions encountered in the process. So at the end of this phase of the toppling all the particles will be herded at the **Source** vertices. Let $\eta^{(1)}$ denote the configuration at the end of this phase, which is supported on **Source** vertices. Because we ignore the sleep instructions, this procedure is the same as letting all the particles in η be independent simple symmetric random walks stopped at hitting one of the sources. Thus we shall need a couple of basic random walk estimates to estimate the distribution $\eta^{(1)}$, as well as the total number of jumps to reach that configuration.

Recall that the i^{th} source is located at the vertex $z_i := (i - \frac{1}{2})c_0 \log n$. Let $\eta_i^{(1)}$ denote the number of particles $\eta^{(1)}$ has in this vertex. Also recall that to reduce notation we assumed that n is an integer multiple of $c_0 \log n$, which itself is an even integer. Let $K = \frac{n}{c_0 \log n}$ be the number of sources. In the general case we can take all the intervals to be $\lfloor c_0 \log n \rfloor$ except possibly one which has length between $\lfloor c_0 \log n \rfloor$ and $2\lfloor c_0 \log n \rfloor$.

The following lemma is our first random walk estimate.

Lemma 2.1. *For each $\varepsilon > 0$, there exists $a > 0$ such that for all large enough c_0 and n,*

$$\mathbb{P}\left(\sup_{1\le i\le K} |\eta_i^{(1)} - \mu c_0 \log n| \ge \varepsilon c_0 \log n\right) \le e^{-ac_0 \log n}.$$

Proof. For this proof we shall forget about $\mathscr{I}$ and the toppling procedure, and treat $\eta^{(1)}$ as the configuration obtained from letting all the particles of η perform independent simple symmetric random walks stopped at hitting any of the source vertices (thus particles initially located at source vertices do not move at all). We first recall a standard concentration inequality for sums of independent but not necessarily identically distributed Bernoulli variables that we will use later in the proof. Let $X_1, \ldots, X_k$ be independent Bernoulli variables with means $p_1, \ldots, p_k$ respectively. Let $\nu = p_1 + \ldots + p_k$. Then

$$\mathbb{P}\left(\left|\sum_i^k X_i - \nu\right| \ge \delta\nu\right) \le e^{-\frac{\delta^2\nu^2}{k}}. \tag{2.1}$$

Let us consider the first source z_1. Clearly, any particle that ended up at z_1 in $\eta^{(1)}$ must have been located at some $j \in V_1 = (-\frac{c_0}{2}\log n, \frac{3c_0}{2}\log n)$. Let Z_j denote the indicator of the event that there was a particle at j in η and that ended up at z_1 in $\eta^{(1)}$. Clearly

$$\eta_i^{(1)} = \sum_{j\in V_1} Z_j.$$

Observe that a standard Gambler's ruin calculation yields that the probability that a random walk started at $j \in V_1$ would reach z_1 before reaching either z_0 or z_2 is $g(j) = 1 - \frac{|j - \frac{c_0}{2}\log n|}{c_0 \log n}$. It follows that Z_j's are independent Bernoulli variables with mean $\mu g(j)$. Observe that

$$\left|\sum_{j\in V_1} g(j) - c_0 \log n\right| \le 1,$$

and hence using (2.1) we get that for each $\varepsilon > 0$, and for all n sufficiently large

$$\mathbb{P}\left(|\eta_1^{(1)} - \mu c_0 \log n| \ge \varepsilon c_0 \log n\right) \le e^{-2ac_0 \log n} \tag{2.2}$$

for some a depending on μ, ε (but not on c_0). By the rotational symmetry of $\mathcal{C}_n$ and of the law of the initial configuration $\mathbb{P}^\mu$, we have the same bound for all $\eta_i^{(1)}$ for all $1 \le i \le K$. Now since the number of source vertices is less than n, using (2.2) and a union bound over all source vertices, we

get

$$\mathbb{P}\left(\sup_{1\le i\le K}|\eta_i^{(1)}-\mu c_0\log n|\ge \varepsilon c_0\log n\right)\le ne^{-2ac_0\log n}\le e^{-ac_0\log n}$$

where we have chosen c_0 sufficiently large (depending on μ,ε) so that the last inequality holds. This completes the proof of the lemma. □

Recall the basic setting of toppling sites using instructions from stack $\mathscr{I}$. The next lemma will prove that the total number of instructions explored until the end of phase one is at most order $n\log^2 n$ with high probability.

Lemma 2.2. *Let $T^{(1)}(\mu,\lambda)$ denote the total number of instructions that have been explored until the end of phase one. Then there exists $C_2,\theta>0$ such that*

$$\mathbb{P}\left(T^{(1)}(\mu,\lambda)>C_2 n\log^2 n\right)\le n^{-\theta}.$$

For this step we shall need a concentration result for sums of geometric random variables. Although the result we need at this step is pretty standard, we shall need a more complicated variant later on, and we also need a concentration for some of exponential random variables for a later part of the argument. For convenience we quote, at this point, the following result from [26] which shall cover all our needs (see theorems 2.1 and 5.1 there).

Lemma 2.3. *The following concentration results hold:*

(i) Fix $p\in(0,1)$, and let $Y_1,Y_2,\dots$ be i.i.d. geometric random variables with parameter p, so $\mathbb{E}Y_1=1/p$. Then for any $\delta>0$ and any $M\in\mathbb{N}$,

$$\mathbb{P}\Big(\Big|\sum_{i=1}^{M}Y_i-M/p\Big|\ge\delta\frac{M}{p}\Big)\le 2\exp\Big(-(\delta-\log(1+\delta)))\frac{M}{p}\Big).$$

(ii) Suppose $Z_1,Z_2,\dots$ are independent exponential random variables with means $a_1,a_2,\dots$, and set $a_*=\inf_i a_i$, $\kappa=\sum_{1\le i\le M}a_i$. Then for any $\delta>0$ and $M\in\mathbb{N}$,

$$\mathbb{P}\Big(\Big|\sum_{i=1}^{M}Z_i-\kappa\Big|\ge\delta\kappa\Big)\le 2\exp\Big(-a_*\kappa(\delta-\log(1+\delta))\Big).$$

For the proof of Lemma 2.2 we need the following result.

Lemma 2.4. *Let n be an integer multiple of r and consider fixed locations at distance r on $\mathcal{C}_n$ (without loss of generality take them to be multiples of r). Let k independent identically distributed*

lazy symmetric random walks started from arbitrary locations on $\mathcal{C}_n$ and stopped on hitting the nearest integer multiple of r. Let T_i be the total number of steps taken by the i^{th} walk (including the lazy steps). Then there exists $C > 0$ such that

$$\mathbb{P}\left(\sum_{i=1}^{k} T_i \geq Cr^2k\right) \leq e^{-Ck},$$

where C depends on the laziness parameter, (i.e., the probability of not jumping).

Proof. Standard simple random walk estimates show that if τ is the hitting time of $\{0, r\}$ for a lazy simple random walk on $\mathbb{Z}$ (with laziness p), then for each $x \in [\![0, r]\!]$, we have $\mathbb{P}_x(\tau < Cr^2) \geq \frac{1}{2}$ where $\mathbb{P}_x$, denotes the probability measure for the random walk started at x and C depends only on the laziness parameter. It follows then that for any arbitrary location of the k particles, each T_i is stochastically dominated by r^2G where G is a geometric random variable with mean 2. The statement now follows from part (i) of Lemma 2.3. □

We are now ready to prove Lemma 2.2.

Proof of Lemma 2.2. First notice that the total number of instructions used by the particles ignoring the sleep instructions is the same as the total number of steps taken when the particles do independent lazy symmetric random walks on $\mathcal{C}_n$, where the laziness (probability of not jumping) is $\frac{\lambda}{1+\lambda}$ (exactly the probability that an instruction is a sleep instruction). Now as an easy consequence of (2.1), for any $\varepsilon > 0$, the total number of particles in η is in $(\mu - \varepsilon, \mu + \varepsilon)n$ with probability at least $1 - e^{-cn}$ for some $c = c(\varepsilon, \mu) > 0$. We can therefore condition on the number of particles being $m \in (\mu - \varepsilon, \mu + \varepsilon)n$. Let T^* denote the total number of steps taken by these particles until the end of phase one. Using Lemma 2.4 with $r = c_0 \log n$,we get that $\mathbb{P}(T^* > Cn \log^2 n) \leq e^{-cn}$. □

2.2. **Phase two: Stabilizing from the sources.** We describe the second phase of our toppling scheme now. Recall that we start with the configuration $\eta^{(1)}$ that is supported on the **Source** vertices. Throughout the section we shall assume that $\eta^{(1)}$ satisfies the high probability event described in Lemma 2.1, where ε will be chosen sufficiently small depending on μ and λ later. Recall the intervals $I_i = [(i-1)c_0 \log n, ic_0 \log n]$ for $1 \leq i \leq K$. Observe that the i^{th} source z_i is the midpoint of the interval I_i.

As mentioned before, for each $1 \leq i \leq K$, we start stabilizing particles at z_i sequentially, in any arbitrary manner of toppling, until one of the particles hit the boundary of I_i, in which case we

term the process a failure. On the contrary, we denote by $\mathcal{S}_i$ the event that all the $\eta_i^{(1)}$ particles all fall asleep before hitting the boundary of I_i: call this event **Success at source** z_i. Clearly on the event that $\mathcal{S}_i$ occurs for all i, the system stabilizes. The main step is to show that $\mathcal{S}_i$ occurs with high enough probability so that one can take a union bound over all intervals I_i. Because of the underlying symmetry, we state the following result for a generic interval $[-\frac{r}{2}, \frac{r}{2}]$, where we assume r is even to avoid rounding issues.

Proposition 2.5. *Consider* ARW, *with sleep rate* λ, *on* $[-\frac{r}{2}, \frac{r}{2}]$, *started with* m *particles at the origin. Let* $\varepsilon > 0$ *be such that* $\mu + 2\varepsilon < \frac{\lambda}{1+\lambda}$, *and let* $m \leq (\mu + \varepsilon)r$. *Let* $\mathcal{S}$ *denote the event that all the particles fall asleep before any particle hits* $\{-\frac{r}{2}, \frac{r}{2}\}$. *Then there exists* $c > 0$, *such that for all* r *sufficiently large we have* $\mathbb{P}(\mathcal{S}^c) \leq e^{-cr}$.

Proposition 2.5 is the most technically complicated result that goes into the proof of Theorem 1, and the proof will be spread over the next two subsections. Before delving into this proof, we want to complete the remaining steps in the argument proving Theorem 1. First we need to prove the following easy lemma.

Lemma 2.6. *Consider* ARW *with sleep rate* λ, *started from* $\eta^{(1)}$. *Let* $T^{(2)} = T^{(2)}(\mu, \lambda)$ *denote the total number of steps taken by all the particles until stabilization. Then there exists* $C_3 > 0$, *and* $\theta > 0$, *such that on the event* $\cap \mathcal{S}_i$, *we have*

$$\mathbb{P}\left(T^{(2)} \geq C_3 n \log^2 n\right) \leq n^{-\theta}$$

for all n *sufficiently large.*

Proof. Observe that arguing as in the proof of Lemma 2.4, taking $r = c_0 \log n$, on $\mathcal{S}_i$, the number of steps taken by each particle started from z_i is dominated by $Cc_0^2 \log^2 n G$ where G is a geometric random variable with mean 2 and C depends on λ. The rest of the proof is identical to that of Lemma 2.4 and its application in the proof of Lemma 2.2. We skip the details. □

We can now complete the proof of Theorem 1.

Proof of Theorem 1. Fix $\mu < \frac{\lambda}{1+\lambda}$ and recall our two phase stabilization procedure. Recall $T^{(1)}$ from Lemma 2.2 and $T^{(2)}$ from Lemma 2.6, and the stack of instructions $\mathscr{I}$ from (1.1). Note that our toppling scheme produces a stack of instructions $\mathscr{I}^*$ obtained from $\mathscr{I}$, where the sleep instructions which are ignored by our toppling scheme are replaced by $\mathfrak{n}$ instructions (see the

definitions before Lemma 1.3). Moreover, given the stack $\mathscr{I}^*$, by the Abelian Property (Lemma 1.1), on the event $\cap \mathcal{S}_i$, the total number of instructions needed to stabilize is $T^{(1)} + T^{(2)}$, since our toppling scheme uses exactly those many instructions from $\mathscr{I}^*$. Finally, using Lemma 1.3, the total number of instructions used to stabilize, for the stack $\mathscr{I}$, is upper bounded by $T^{(1)} + T^{(2)}$. Thus it will suffice to show that

$$\mathbb{P}(T^{(1)} + T^{(2)} > C_0 n \log^2 n) \leq n^{-b}. \tag{2.3}$$

We first fix $\varepsilon > 0$ so that the hypothesis of Proposition 2.5 is satisfied. Then fix c_0, C_2, a so that the conclusions of Lemma 2.1 (with the same ε) and Lemma 2.2 hold. Thus, the event

$$\mathcal{A} = \left\{ \sup_{1 \leq i \leq K} |\eta_i^{(1)} - \mu c_0 \log n| \leq \varepsilon c_0 \log n \right\} \cap \left\{ T^{(1)}(\mu, \lambda) < C_2 n \log^2 n \right\}$$

occurs with probability at least $1 - n^{-\theta}$ for some $\theta > 0$.

On $\mathcal{A}$, by definition, for each $1 \leq i \leq K$, $\eta_i^{(1)}$ satisfies the hypothesis of Proposition 2.5, and hence applying the latter with $r = c_0 \log n$ and a union bound we get

$$\mathbb{P}(\cap \mathcal{S}_i) \geq 1 - n e^{-h c_0 \log n} \geq 1 - n^{-\theta}$$

for some $h > 0$, and by choosing c_0 sufficiently large the final inequality holds for some $\theta > 0$. We can now infer (2.3) for all sufficiently large n, from Lemma 2.6, choosing C_0 sufficiently large compared to C_2 and C_3 and choosing b sufficiently small. □

2.3. **Setting the Traps.** It remains to prove Proposition 2.5. For this proof we shall work with the Diaconis-Fulton representation of ARW on $[-\frac{r}{2}, \frac{r}{2}]$ using the stack of instructions $\mathscr{I}$ as explained at the end of Section 1.

For the remainder of this section, we shall be in the set-up of Proposition 2.5. Also without loss of generality we shall assume that the total number of particles at the origin is $m = \mu r$, and we run ARW with sleep rate λ where $\mu < \frac{\lambda}{1+\lambda}$. Using Abelian Property (Lemma 1.1), our goal will be to provide a toppling procedure (with some possibly ignored sleep instructions) that, when it succeeds, will lead to a stable configuration before any of the particles reach $\{-\frac{r}{2}, \frac{r}{2}\}$. Our job will be finished once we show that the algorithm succeeds with high probability. Next we describe in detail the steps of our algorithm, which employs a variant of the algorithm in [42, Section 5], along with a more complicated trap setting procedure in the finite setting. We elaborate on the differences from [42] and their necessity later, but first we describe the procedure.

2.3.1. *Exploration, and locating the traps.* Recall that the number of particles at the origin is m. Let us enumerate the particles $y_1, y_2, \ldots, y_m$. The algorithm consists of applying a settling procedure to each particle. This procedure explores $\mathscr{I}$ until it identifies a suitable trap for the particle. The exploration follows the path that the particle would perform if we always toppled the site it occupies, and stops when the trap has been chosen. In the absence of a suitable trap, we declare the algorithm to have failed. We set two initial barriers $a_0 = -\frac{r}{2}, b_0 = \frac{r}{2}$. We will recursively define barrier processes $a_0 < a_1 < \ldots$ and $b_0 > b_1 > \ldots$ that are functions of $\mathscr{I}$. Having defined a_i and b_i, we define a_{i+1} and b_{i+1} as follows:

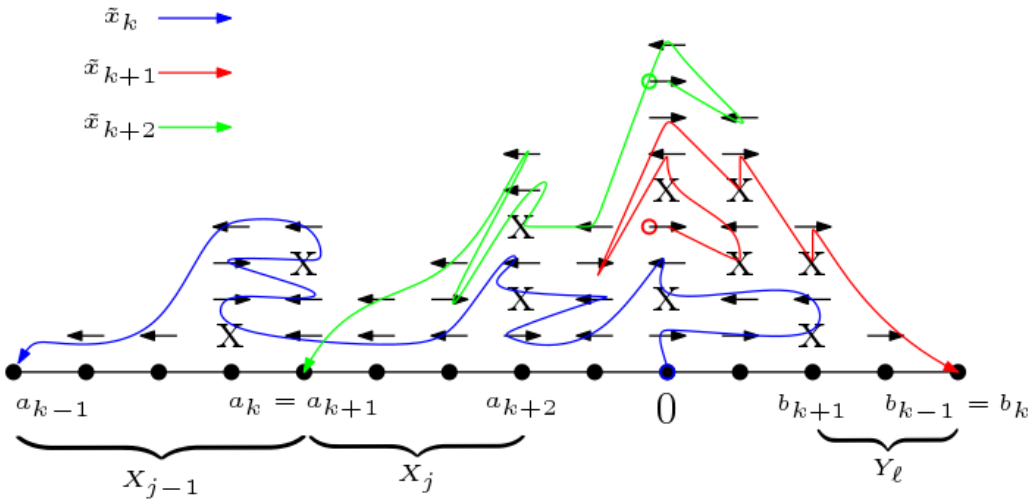

FIGURE 2. This figure is similar to the one appearing in [42]. The blue, red and green paths are the exploration trajectories for three consecutive particles labelled $\tilde{x}_k, \tilde{x}_{k+1}, \tilde{x}_{k+2}$ respectively, starting at the origin. The $\leftarrow, \rightarrow$ denote jump instructions whereas X denotes a sleep instruction. The first particle is stopped on hitting the barrier a_{k-1} and hence it advances to a_k which is the closest site where the second last instruction was a sleep instruction ignored. The particle now falls asleep at a_k instead of exploring the path beyond a_k. As shown in Lemma 2.9, $a_k - a_{k-1}$ is dominated by a Geometric variable of mean $\frac{1+\lambda}{\lambda}$. However the barrier b_{k-1} stays as it is and is renamed b_k. The second particle hits barrier b_k which now advances to b_{k+1} where the particle uses the previously ignored sleep instruction to fall asleep, whereas a_k is renamed a_{k+1}. Thus the trap setting scheme proceeds to find traps for each individual particle to fall asleep.

Topple the particle y_{i+1} using the previously unexplored instructions in $\mathscr{I}$ until it hits either a_i or b_i: that is, we always topple the site where this particle is currently located. At this stage we ignore all the sleep instructions. Eventually the particle hits either a_i or b_i, call the site hit q_i. Let us suppose $q_i = a_i$ and the exploration process hits q_i at step τ_i. We set $b_{i+1} = b_i$ and explore the accessed sites backwards from a_i, until we reach zero. If we reach a site v where the second to last

instruction accessed was a sleep instruction (notice that the last instruction must have been a step towards a_i) that was ignored, then we set $a_{i+1} = v$, and call $a_{i+1} = \mathbf{Trap}_{i+1}$. If no such site exists we declare the procedure to have failed. Observe that provided we can successfully set the barriers then they are moving towards the origin from both sides. We declare the trap setting scheme a success if $a_m < 0 < b_m$. Note that this is a sufficient condition for us to be able to set barriers for all the m particles.

In [42], the argument is based on considering the infinite half line and hence in that setting, it suffices to only consider a single barrier process $a_0 < a_1 < \dots$ In contrast, in our setting, we want the particles to not exit the interval $[-\frac{r}{2}, \frac{r}{2}]$, and hence do not want the situation where a certain random walk hits the barrier process $a_0 < a_1 < \dots,$, after a long excursion outside the interval of our interest. This creates the necessity to have another barrier process, $\dots < b_1 < b_0$, which the particle would hit instead on such a journey, preventing its exit from the interval.

2.3.2. *Running the dynamics.* Let us suppose that the realization of $\mathscr{I}$ is such that the trap setting procedure is a success. On this event, let us give a toppling scheme which will utilize the traps to stabilize all the particles before they hit a_0 or b_0. We topple the particles sequentially. Assuming the particles up to y_{i-1} have been settled, we start the toppling of the particle y_i, ignoring all the sleep instructions until the particle hits $\mathbf{Trap}_i$ for the last time before hitting a_{i-1} or b_{i-1}. Observe that because the instructions used were never used in the in exploration process of the previous particles, the path of this particle is the same as the exploration path, up until it hits $\mathbf{Trap}_i$ for the last time. We let the sleep instruction that was the second to last one accessed at $\mathbf{Trap}_i$ be executed and this settles the particle y_i at $\mathbf{Trap}_i$. The key thing to notice here is that all the subsequent instructions accessed by the exploration process (but not in the actual dynamics) are located outside (a_i, b_i), hence the future exploration processes will never try to access them by definition. This implies that the procedure can be continued with all the particles settled at their respective traps if the trap setting procedure succeeds, and additionally the consecutive exploration paths are independent of each other. This fact will be crucial for us when we try to estimate the growth of the barrier processes.

We summarize the upshot of the toppling procedure and the discussion above in the following lemma.

Lemma 2.7. *In the set-up of Proposition 2.5, suppose the trap setting procedure described above succeeds. Then $\mathcal{S}$ occurs.*

Proof. The proof is a straightforward consequence of Lemmas 1.3 and 1.1. □

Using Lemma 2.7, the proof of Proposition 2.5 will now be complete, if we show that the probability that the trap setting procedure fails is exponentially small in r. As mentioned before, our toppling scheme succeeds if $a_m < 0 < b_m$ where m is the total number of particles initially at 0. The proof of Proposition 2.5 follows from the next lemma.

Lemma 2.8. *Let $m = \beta r$ be the total number of particles at the origin, and consider the trap setting procedure described above. For $\beta < \frac{\lambda}{1+\lambda}$, there exists $c = c(\beta, \lambda) > 0$ such that for all sufficiently large r we have*

$$\mathbb{P}(a_m < 0 < b_m) \geq 1 - e^{-cr}.$$

Let us first provide a brief outline of our argument. Observe that at each stage i, exactly one of the barriers advances towards the origin. The probability of this being the left one or the right one is equal by symmetry at step 1 and hence equal to $\frac{1}{2}$. The proof now involves showing that it remains close to $\frac{1}{2}$ throughout. Also we show that the distance a barrier moves at each step has mean $\frac{1+\lambda}{\lambda}$. So the total distance covered by the barriers after βr many moves is approximately $\frac{1}{2}\beta r \frac{1+\lambda}{\lambda}$, which is smaller than $\frac{r}{2}$ because of the assumption on β and λ. Since the initial location of the barriers were at $-\frac{r}{2}$ and $\frac{r}{2}$, the above implies that none of the barriers cross the origin.

We now make the above argument formal. The first lemma we need is the following. A similar observation was already present in [42].

Lemma 2.9. *At the i^{th} stage, the distance of $\mathbf{Trap}_i$ from the barrier q_{i-1} hit by the i^{th} exploration process is dominated by a geometric random variable with mean $1 + \frac{1}{\lambda}$ independent of everything else.*

Proof. Without loss of generality we assume that $q_{i-1} = a_{i-1}$. Recall from (1.2) that each instruction $\xi_{(x,j)}$ in $\mathscr{I}$ is a sleep instruction with probability $\frac{\lambda}{1+\lambda}$ and jump instruction otherwise, independent of everything else. Thus, conditioning on the i^{th} exploration path, the number of sleep instructions ignored at any site $x \in \mathcal{C}_n$ between successive jumps at x are i.i.d. random variables distributed as $\text{Geom}(\frac{1}{1+\lambda}) - 1$ (we adopt the standard notation of denote a Geometric random variable with mean p^{-1} by $\text{Geom}(p)$). In particular the number of sleep instructions between successive jumps is zero

with probability $\frac{1}{1+\lambda}$. Thus at any site, the probability that there was a sleep instruction ignored before the last jump instruction is $\frac{\lambda}{1+\lambda}$. Thus $\mathbf{Trap}_i - a_{i-1}$ is dominated by Geom($\frac{1+\lambda}{\lambda}$) variable, independent of everything else. Note that this is not a distributional identity, as $\mathbf{Trap}_i - a_{i-1}$ is bounded above by $r - a_{i-1}$. □

The next step is to show that roughly half of the particles hit the barriers on either side. For $i = 1, 2, \ldots, m$, let U_i denote the indicator that the i-th particle exploration process hits the left barrier first, i.e., $q_{i-1} = a_i$. Also let $V_i = 1 - U_i$. We have the following lemma.

Lemma 2.10. *In the above set-up, for each $\delta > 0$, there exists $c = c(\delta) > 0$ such that*

$$\mathbb{P}\left(\sum_{i=1}^{m} U_i \geq \Big(\frac{1}{2} + \delta\Big)m\right) \leq e^{-cr}; \quad \mathbb{P}\left(\sum_{i=1}^{m} V_i \geq \Big(\frac{1}{2} + \delta\Big)m\right) \leq e^{-cr}.$$

The proof of Lemma 2.10 is involved and requires a somewhat complicated coupling to a different process; we postpone it to the next subsection. Using this, however, the proof of Lemma 2.8 is almost immediate and we complete that part of the argument now.

Proof of Lemma 2.8. Let $X_1, X_2, \ldots$ and $Y_1, Y_2, \ldots$ be two independent sequences of i.i.d. Geom($\frac{\lambda}{1+\lambda}$) variables independent of the sequences $\{U_i\}_{i=1}^m$ defined above. It follows from Lemma 2.9 that a_m is stochastically dominated by $-\frac{r}{2} + \sum_{i=1}^m X_i U_i$, and similarly b_m stochastically dominates $\frac{r}{2} - \sum_{i=1}^m Y_i V_i$. Now clearly, using Lemma 2.3 it follows that for all $\delta, \delta' > 0$ there exists $c = (\delta, \delta') > 0$ such that

$$\mathbb{P}\left(\sum_{i=1}^{(\frac{1}{2}+\delta)m} X_i \geq (1+\delta')\frac{1+\lambda}{\lambda}(\frac{1}{2}+\delta)m\right) \leq e^{-cr}.$$

Choosing δ and δ' sufficiently small so that $(1+\delta')\frac{1+\lambda}{\lambda}(\frac{1}{2}+\delta)\beta < \frac{1}{2}$ (this is possible since $\beta < \frac{\lambda}{1+\lambda}$ and $m = \beta r$) it follows using Lemma 2.10 that $\mathbb{P}(a_m < 0) \geq 1 - e^{-cr}$. By symmetry an identical bound holds for $\mathbb{P}(0 < b_m)$ and we are done by taking a union bound. □

2.4. **Coupling with an internal erosion process.** It only remains to prove Lemma 2.10. As alluded to before to this end we shall use a coupling to a process called internal erosion, (see [37] for a nice exposition on the latter). Let $X_1, X_2, \ldots$ and $Y_1, Y_2, \ldots$ be two independent sequences of i.i.d. Geom($\frac{\lambda}{1+\lambda}$) variables. Let $S_i = \sum_{j=1}^i X_j$ and $T_i = \sum_{j=1}^i Y_j$ denote the sequence of partial sums. Let τ_1 (resp. τ_2) denote the largest positive integer i such that S_i (resp. T_i) is less than $\frac{r}{2}$. Now let $\{Z_i\}_{1 \leq i < \tau_1}$ (resp. $\{W_i\}_{1 \leq i < \tau_2}$) be a sequence of independent exponential random variables with means $f(i)$ (resp. $g(i)$) where $f(i) = \frac{r}{2} - S_i$ (resp. $g(i) = \frac{r}{2} - T_i$). Consider the two following

continuous time counting processes:

$$N^{(1)}(t) = \sup\{n \geq 0 : \sum_{i=1}^{n} Z_i \leq t\}; \quad N^{(2)}(t) = \sup\{n \geq 0 : \sum_{i=1}^{n} W_i \leq t\}.$$

Set also $N(t) = N^{(1)}(t) + N^{(2)}(t)$. We shall crucially use the following connection of the above process with the trap setting procedure described in the previous subsection.

Lemma 2.11. *Consider the barrier processes $\{a_i\}, \{b_i\}$ and the internal erosion process described above. There is a coupling between the two processes satisfying the following: for all $t \geq 0$ such that $N^{(1)}(t) < \tau_1$ and $N^{(2)}(t) < \tau_2$, one has $a_{N(t)} = -\frac{r}{2} + \sum_{i=1}^{N^{(1)}(t)} X_i$ and $b_{N(t)} = \frac{r}{2} - \sum_{i=1}^{N^{(2)}(t)} Y_i$. Moreover, $N^1(t)$ is the number of times the barrier $a_0 < a_1 < \ldots$ is hit among the first $N(t)$ particles.*

Proof. The proof is a consequence of the memoryless property of Exponential variables. Recall from the proof of Lemma 2.9 that the consecutive non-zero increments of the process $a_0 \leq a_1 \leq \ldots$, are distributed as $X_1, X_2, \ldots$, truncated at certain values which are functions of both the barrier processes. However note that while neither barrier process has reached zero, the issue of truncation does not arise. And hence we can couple the increments of the $\{a_i\}_{i\geq 1}$ exactly to the process $\{X_i\}_{i\geq 1}$ for the first τ_1 increments. Similarly the decrements of the process $\{b_i\}_{i\geq 1}$ can be coupled exactly to the process $\{Y_i\}_{i\geq 1}$ for the first τ_2 decrements (see Figure 2 for an illustration.).

Thus to finish the proof of the lemma, we have to argue that the probability of the j^{th} particle hitting the barrier a_{j-1} instead of b_{j-1} is the same as the process $N^1(t)$ increasing before $N^2(t)$ when $N(t) = j-1$ for any j such that both $N^1(t) < \tau_1$ and $N^2(t) < \tau_2$. Note that the probability of the $(N(t)+1)^{th}$ particle hitting the barrier $a_{N(t)}$ as opposed to $b_{N(t)}$ has probability

$$\frac{b_{N(t)}}{b_{N(t)} - a_{N(t)}} = \frac{g(N^{(2)}(t))}{f(N^{(1)}(t)) + g(N^{(2)}(t))}. \tag{2.4}$$

Note that given the filtration up to time t, N^1_t increases before $N^2(t)$ if and only if

$$\sum_{i=1}^{N^1(t)+1} Z_i - t \leq \sum_{i=1}^{N^1(t)+1} W_i - t.$$

Now given the filtration up to time t, using the memoryless property, it follows that

$$\sum_{i=1}^{N^1(t)+1} Z_i - t \text{ is distributed as } Z_{N^1(t)+1},$$

and similarly $\sum_{i=1}^{N^2(t)+1} W_i - t$ is distributed as $W_{N^2(t)+1}$. Thus using the fact that

$$\mathbb{P}(Z_{N^1(t)+1} < Z_{N^2(t)+1}) = \frac{g(N^{(2)}(t))}{f(N^{(1)}(t)) + g(N^{(2)}(t))},$$

the proof is complete using (2.4). □

Using Lemma 2.11 to prove Lemma 2.10, it suffices to prove the following lemma. Recall that $m = \beta r$ is the total number of particles.

Lemma 2.12. *Let $\beta < \frac{\lambda}{1+\lambda}$ and let $\delta > 0$ be fixed (and sufficiently small as a function of $\frac{\lambda}{1+\lambda} - \beta$). Let $M_1 = (\frac{1}{2} - \delta)\beta r$, $M_2 = (\frac{1}{2} + \delta)\beta r$. Let $\mathcal{E}$ denote the event that there exists t such that $\{N^{(1)}(t) \geq M_2, N^{(2)}(t) \leq M_1\}$ or $\{N^{(2)}(t) \geq M_2, N^{(1)}(t) \leq M_1\}$. Then there exists $c > 0$ such that $\mathbb{P}(\mathcal{E}) \leq e^{-cr}$.*

Proof. First observe that, by Lemma 2.3, $\max(S_{M_2}, T_{M_2}) \leq \frac{r}{2}$ (since δ is sufficiently small) with exponentially small failure probability and hence we have $\min(\tau_1, \tau_2) \geq M_2$ with exponentially small failure probability. Thus we can safely restrict our analysis to the latter event. Observe next that it suffices to prove that with exponentially (in r) small failure probability, we have

$$\sum_{i=1}^{M_2} Z_i > \sum_{i=1}^{M_1} W_i; \quad \sum_{i=1}^{M_2} Z_i > \sum_{i=1}^{M_1} W_i. \tag{2.5}$$

Conditional on the sequences S_i and T_i, the concentration estimates in Lemma 2.3 imply that the terms $A_1 := \sum_{i=1}^{M_1} Z_i$, $A_2 := \sum_{i=1}^{M_1} W_i$, $A_3 := \sum_{i=1}^{M_2} Z_i$, $A_4 := \sum_{i=1}^{M_2} Z_i$ are all concentrated near their means p_1, p_2, p_3, p_4, with exponentially small failure probability. The proof is then essentially completed by comparing the means. Note that the means are themselves random (functions of S_i and T_i) and hence the last detail is to show that the means themselves are concentrated.

Formally we first observe that $p_1 = M_1 \frac{r}{2} - \sum_{i=1}^{M_1} i S_{M_1 - i + 1}$ and similar expressions holds for p_2, p_3 and p_4. Note that $\mathbb{E}(p_1) = M_1 \frac{r}{2} - \frac{1+\lambda}{\lambda} \frac{M_1^2}{2} + O(M)$. There are several ways to prove concentration of p_1 and below we sketch a way to use Lemma 2.3 to achieve this. Note that the latter only allows for sums of geometric variables, whereas we have a linear combination of them. Since we can afford to be rather crude with our estimates, we use the following decomposition

$$p_1 = M_1 \frac{r}{2} - \sum_{i=1}^{M_1} \sum_{j=1}^{i} S_j.$$

Thus by union bound, after applying Lemma 2.3 to each of the terms of form $\sum_{j=1}^{i} S_j$, it follows that: for all ε_1 small enough, there exists c depending on all the parameters except r, such that

$$\mathbb{P}\left(|p_1 - \mathbb{E}(p_1)| \geq \varepsilon_1 r^2\right) < e^{-cr}.$$

Similar analysis allows us to conclude similar bounds as above for p_2, p_3, p_4. By choice of M_1 and M_2, note that there exists ε_1 such that $\mathbb{E}(p_3) - \mathbb{E}(p_1) \geq 4\varepsilon_1 r^2$ and similarly $\mathbb{E}(p_4) - \mathbb{E}(p_2) \geq 4\varepsilon_1 r^2$. Thus we see that with probability at least $1 - e^{-cr}$, the sequences S_i, T_i are such that

$$p_3 - p_1 > 2\varepsilon_1 r^2 \text{ and } p_4 - p_2 > 2\varepsilon_1 r^2.$$

Moreover, conditioned on the above events, for $j = 1, 2, 3, 4$, Lemma 2.3 implies the following concentration estimates:

$$\mathbb{P}\left(|A_j - p_j| \geq \frac{\varepsilon_1}{2} r^2\right) > e^{-cr}. \tag{2.6}$$

Thus combining the above inequalities and union bound the lemma follows. □

We are now ready to complete the proof of Lemma 2.10.

Proof of Lemma 2.10. We shall use the coupling described in Lemma 2.11. Let M_1, M_2 be as in Lemma 2.12. Now by the coupling discussed above and Lemma 2.12, it follows that with exponential (in r) failure probability, M_1 particles hit both barriers before M_2 particles hit any barrier.

Since the total number of of particles is $m \leq M_1 + M_2$ it follows that, with exponentially high probability neither $\sum_{i=1}^{m} U_i$ nor $\sum_{i=1}^{m} V_i$ can exceed M_2. Since $\beta < \frac{\lambda}{1+\lambda}$, we can safely ignore the exponentially (in r) unlikely event that $M_2 \geq \min(\tau_1, \tau_2)$ and hence assume that coupling in Lemma 2.11 does not fail. □

Remark 2.13. *It can be shown that $T_n(\mu, \lambda)$ will be of order n^3, if all the particles (approximately μn) were initially located at the same site and hence Theorem 1 relies heavily on the location of the particles in the initial configuration being uniform. To see this, note that by the above discussion regarding topplings, when a linear in n, say αn, number of particles start at the origin, then to stabilize, due to lack of space, at least $\frac{\alpha n}{2}$ particles must move outside an interval of size $\frac{\alpha n}{2}$ centred at the origin. Since a random walk path takes time $\Theta(n^2)$ on average to exit such an interval, the observation follows.*

3. Slow fixation for low sleep rate

In this section we prove Theorem 2. That is, we prove that for any $\mu > 0$ and sufficiently small sleep rate λ, ARW(μ, λ) on $\mathcal{C}_n$ takes at least exponentially many steps before reaching the absorbing state with failure probability exponentially small in n.

3.1. **The Stabilization Loop.** We shall now describe the toppling scheme outlined in Section 0.2 in more detail. Let $\mu \in (0, 1)$ be fixed and λ be sufficiently small. By Lemma 1.1 it suffices to exhibit a sequence of legal topplings with exponentially many steps. We shall show that our procedure satisfies this property with exponentially high probability if λ is sufficiently small.

While running this scheme, particles will switch between two different states, which we call states X and Y. Particles in state X follow normal ARW dynamics among themselves as described in Section 1.1, and can wake up sleeping Y-particles. Y-particles, on the other hand, do not move, and have no effect on the states of any other particles. Thus a state of the system during this toppling scheme consists of all the particles, each in state X or state Y, and each asleep or awake. When a site is toppled, only X-particles at that site follow the corresponding stack instructions from $\mathscr{I}$ (see Section 1.1). So Y-particles only undergo the transition from sleepy to active when an active X-particle reaches the same site.

As described in Section 0.2, our toppling procedure will run multiple rounds of what we call stabilization loop. Formally, starting from a particle configuration η – i.e. the values $\eta_t(x)$ for $x \in \mathcal{C}_n$ – stabilizing the system in a subset $\mathcal{D}$ of sites in $\mathcal{C}_n$ means choosing some particles to be in state X and the rest to be in state Y. Then running the particle dynamics described above, only toppling sites inside $\mathcal{D}$, until all X-particles are asleep in $\mathcal{D}$ or are outside $\mathcal{D}$. Now the obvious strong Markov property of the above dynamics makes the different stabilization rounds conditionally independent which would be crucial in our calculations.

It will be convenient to identify $\mathcal{C}_n$ with the interval $[-r, r]$ with $-r$ and r identified, i.e., assume $n = 2r$ for integer r. We shall denote the origin by $\mathbf{0}$ and the identified vertex $r = -r$ will be denoted by $\mathbf{r}$. The stabilization steps we run will alternate between taking $\mathcal{D} = \mathcal{C}_n \setminus \{\mathbf{0}, \mathbf{r}\}$, $\mathcal{D} = \mathcal{C}_n \setminus \{\mathbf{0}\}$ and $\mathcal{D} = \mathcal{C}_n \setminus \{\mathbf{r}\}$.

1. **Stabilization Step A:** Stabilize all the particles in $\mathcal{C}_n \setminus \{\mathbf{0}, \mathbf{r}\}$. That is, treat particles in $\mathcal{C}_n \setminus \{\mathbf{0}, \mathbf{r}\}$ as X-particles, stopped upon hitting $\{\mathbf{0}, \mathbf{r}\}$, and all other particles as Y-particles. So at the end of this procedure all active particles will be at $\mathbf{0}$ or $\mathbf{r}$.

2. **Stabilization Step B:** Reset the X and Y labels: the particles initially at $\mathbf{0}$ become X-particles, and all other particles become Y-particles. Then stabilize all X-particles with particles stopped at $\mathbf{r}$. With the identification of $\mathcal{C}_n$ with $[-r, r]$, this step is the same as stabilizing the ARW dynamics in the interior of $[-r, r]$ where the initial particle configuration is supported at the center of the interval, a special case of the more general process analyzed later in Lemma 3.5 using results from [4].
3. **Stabilization Step C:** This is identical to the **Stabilization Step B** above with the roles of $\mathbf{0}$ and $\mathbf{r}$ interchanged.

The algorithm receives an initial particle configuration η on $\mathcal{C}_n$ drawn from $\mathbb{P}^\mu$ as an input. Then we perform the **Stabilization Loop**, which is **Stabilization Step A**, followed by **Stabilization Step B** and **Stabilization Step C**. We repeat the **Stabilization Loop** until all of the particles are asleep.

We now state the main lemma about the **Stabilization Loop** and use it to prove Theorem 2.

Lemma 3.1. *Fix $\mu \in (0, 1)$, $\varepsilon \in (0, 2\mu/5)$ and any particle configuration η with at least $(\mu - \varepsilon)n$ particles, and suppose at least $\mu n/2$ particles are active in η. Let $\widetilde{\eta}$ denote the configuration after we have performed the **Stabilization Loop**. Then for $\lambda = \lambda(\mu) > 0$ sufficiently small, there exists $c > 0$ such that*

$$\mathbb{P}(\widetilde{\eta} \text{ has less than } \mu n/2 \text{ active particles}) < e^{-cn}.$$

Using this lemma we now prove Theorem 2.

Proof of Theorem 2. By the Abelian Property it suffices to demonstrate that with high probability there is a toppling algorithm that does not terminate before exponentially many steps are executed. By a Chernoff bound for any μ and ε the probability that there are at least $(\mu - \varepsilon)n$ particles is exponentially close to one. In the initial stage at least $\mu n/2$ of the particles are awake. By Lemma 3.1, the number of consecutive rounds that the **Stabilization Loop** is performed is at least $e^{\frac{c}{2}r}$ with probability at least $1 - e^{-\frac{c}{2}r}$ before all the particles are asleep. Each time the **Stabilization Loop** is performed, there must be at least one jump or sleep instruction occurring in it. As $n = 2r$ this completes the proof of Theorem 2. □

To prove Lemma 3.1 we rely on two results that are proved by adapting the analysis in [4]. Our first goal is to show that with exponentially high probability after performing **Stabilization Step A** there are at least $\mu n/4$ active particles. By definition these active particles are all at **0** or **r**.

Lemma 3.2. *Fix $\mu \in (0,1), \varepsilon \in (0, 2\mu/5)$ and any particle configuration η with at least $(\mu - \varepsilon)n$ particles of which at least $\mu n/2$ are active.*

*Let $\widetilde{\eta}^A$ denote the configuration after we have performed the **Stabilization Step A**. Then for $\lambda = \lambda(\mu) > 0$ sufficiently small, there exists $c > 0$ such that*

$$\mathbb{P}\left(\widetilde{\eta}^A \text{ has less than } \mu n/4 \text{ active particles}\right) < e^{-cn}.$$

Thus after performing **Stabilization Step A** there are likely to be either at least $\mu n/8$ active particles at **0** or at least $\mu n/8$ active particles at **r**. Suppose there at least $\mu n/8$ active particles at **0**. Our next result says that with high probability after running **Stabilization Step B** at least 90% of active particles that were at **0** are now active particles at **r**. Also all Y particles are now active.

Lemma 3.3. *Fix $\mu > 0$ and any particle configuration η with at least $A \geq \mu n/8$ active particles at **0**.*

*Let $\widetilde{\eta}^B$ denote the configuration after we have performed **Stabilization Step B**. Then for $\lambda = \lambda(\mu) > 0$ sufficiently small, there exists $c > 0$ such that*

$$\mathbb{P}\left(\widetilde{\eta}^B \text{ has all } Y \text{ particles active and at least } .9A \text{ active particles at } \mathbf{r}\right) > 1 - e^{-cn}.$$

We postpone the proofs of Lemma 3.2 and Lemma 3.3 for now and complete the proof of Lemma 3.1.

Proof of Lemma 3.1. After performing **Stabilization Step A**, by Lemma 3.2 there are at least $\mu n/4$ active particles at either **0** or **r** except exponentially small failure probability. On this high probability event, after performing **Stabilization Step B** then except for exponentially small failure probability there are at least $\mu n/8$ active particles at **r** by Lemma 3.3. (Note that this is true no matter how the active particles were split among **0** and **r** at the start of **Stabilization Step B**). On the event that, the high probability event happens at both of these steps, when we start **Stabilization Step C** there are at least $\mu n/8$ active particles at **r**. Thus we can apply

Lemma 3.3, and it follows that, again except for exponentially small failure probability, at the end of **Stabilization Step C** all Y particles are active and at least 90% of the X particles are active. Since, by hypothesis, the total number of particles is at least $(\mu - \varepsilon)n$ and $\varepsilon < 2\mu/5$, easy algebra shows that on the event that none of the three steps resulted in the failure events of exponentially small probability, the loop results in a particle configuration with at least $\mu n/2$ active particles. The lemma now follows by taking a union bound over the three failure events. (Note that implicitly we are using the obvious strong Markov property of the above dynamics.) □

3.2. **Proving Lemmas 3.2 and 3.3.** Now we show how to derive Lemmas 3.2 and 3.3 from [4]. The following lemma will be the key in both arguments.

Lemma 3.4. *Fix $\delta_0 \in (0,1)$ and $c_0 > 0$. Consider ARW with sleep rate λ on the interval $[-r, r]$ starting from an initial configuration η with at least $\delta_0 r$ active particles. Let S denote the number of sleepy particles in $(-r, r)$ after stabilizing. There exists $C = C(\delta_0, c_0)$ and $\lambda_0 = \lambda_0(\delta_0, c_0) > 0$ such that for all $\lambda < \lambda_0$*

$$\mathbb{P}(S \geq c_0 r) \leq e^{-Cr}.$$

for all r sufficiently large.

Proof. This lemma comes from calculations contained in [4]. Recall the odometer function from (1.3) and let $h(0)$ denote the odometer at the origin at the end of the stabilization process and let $\mathcal{E} = \{h(0) \leq r^6\}$. We break up $\{S \geq c_0 r\}$ in two parts

$$\{S \geq c_0 r\} \subset (\{S \geq c_0 r\} \cap \mathcal{E}) \cup \mathcal{E}^c.$$

First we use random walk estimates to prove $\mathbb{P}(\mathcal{E}^c) \leq e^{-Cr}$. This is the same as the argument presented in [4] (Lemma 32) but we provide the short proof for completeness. To start, note that the probability that a lazy random walk started arbitrarily inside $[-r, r]$ does not hit $\{-r, r\}$ in Kr^2 steps is at most $e^{-Kc'}$, where c' depends on the laziness parameter. Now there are at most $2r$ particles, each of which moves along an independent, $\frac{\lambda}{1+\lambda}-$lazy, random walk trajectory. So the probability that any of these particles take more than $0.5r^5$ steps before hitting $\{-r, r\}$ is exponentially small. A union bound then implies that the sum of the number of steps taken by all the particles before reaching $\{-r, r\}$ is exponentially unlikely to be more than r^6 and hence we get

$$\mathbb{P}(\mathcal{E}) = \mathbb{P}(h(0) \leq r^6) \geq 1 - e^{-Cr}.$$

Fix c_1 such that $c_0/4 > c_1 > 0$. Equation (6.21) in [4] shows for λ sufficiently small (and r sufficiently large)

$$\mathbb{E}\left((e^{S_1} + e^{S_2})\mathbf{1}_{\mathcal{E}}\right) \leq e^{c_1 r}$$

where S_1 and S_2 denote the number of sleepy particles in $(-r, 0]$ and $[0, r)$ respectively. Thus by Markov's inequality,

$$\mathbb{P}(\{S \geq c_0 r\} \cap \mathcal{E}) \leq \frac{\mathbb{E}\left((e^{S_1} + e^{S_2})\mathbf{1}_{\mathcal{E}}\right)}{e^{\frac{c_0}{2} r}} \leq \frac{2e^{c_1 r}}{e^{\frac{c_0}{2} r}} \leq e^{-Cr}$$

for some $C > 0$, since $S > c_0 r$ implies either S_1 or S_2 is at least $\frac{c_0 r}{2}$. □

Proof of Lemma 3.2. If there are at most $\mu n/4$ active particles after **Stabilization Step A** then at least $\mu n/4$ particles must have fallen asleep in this step. Thus either

(1) there were initially at least $\mu n/5$ active particles on $(0, r)$ in η and there were at least $\mu n/20$ sleepy particles on $(0, r)$ in $\widetilde{\eta}^A$ or

(2) there were initially at least at least $\mu n/5$ active particles on $(-r, 0)$ in η and there were at least $\mu n/20$ sleepy particles on $(-r, 0)$ in $\widetilde{\eta}^A$.

By Lemma 3.4 both of those events have exponentially small probability. Thus the lemma follows from an union bound over the two cases. □

For the proof of Lemma 3.3 we shall use the following lemma which is immediate from Lemma 3.4 by taking c_0 sufficiently small and we omit the proof.

Lemma 3.5. *For each $\delta_0 > 0$, the following holds for λ sufficiently small. Consider stabilizing any particle configuration η supported on $[-r, r]$ i.e. particles hitting $\{-r, r\}$ are ignored. Call the stabilized system η'. If η has A many active particles with $A \geq \delta_0 r$ then*

$$\mathbb{P}\left(\textit{the total number of particles supported on } \{-r, r\} \textit{ in } \eta' \textit{ is at least } .9A\right) \geq 1 - e^{-cr}.$$

Proof of Lemma 3.3. For this lemma we have to show the two events have exponentially small failure probability: (i) $\widetilde{\eta}^B$ has at least $0.9A$ active particles at $\mathbf{r}$, and (ii) all Y particles are active. The first part is immediate from Lemma 3.5. For (ii), observe the following.

Each X-particle, whenever it moves, follows an independent random walk trajectory that is stopped at hitting $\{-r, r\}$ (the number of steps in this trajectory that is realized has a complicated

dependent structure). By symmetry each of these trajectories are equally likely to end at $-r$ and r. Since $A \geq \mu n/8$ and using a standard Chernoff bound, it follows that with failure probability exponentially small in n, no more than $0.6A$ of these trajectories end at r (also at $-r$). Since by the first part, we know that at least $0.9A$ of these particles follows their trajectories to hit $\{-r, r\}$, this implies that except for exponentially small failure probability, both r and $-r$ are hit by at least $.3A$ many X-particles i.e., $\mathbf{r}$ is hit from both positive and negative side. This implies that every Y particle is hit by an X particle, and hence all Y particles are active in $\widetilde{\eta}^B$. □

We finish with a remark on lower bounding $T_n(\mu, \lambda)$.

Remark 3.6. *An exponential upper bound for $T_n(\mu, \lambda)$ is relatively easy to establish. Note that starting from any configuration, ignoring sleep instructions, one can get each particle to a different location, using only polynomial in n many instructions with probability at least $1 - e^{-cn}$, since for a random walk on $\mathcal{C}_n$, the hitting time for any point is a sub-exponential variable at scale n^2. Once the particles are all located at different sites, with probability at least $(\frac{\lambda}{1+\lambda})^n$, all of their next instructions are sleep instructions which causes the system to stabilize. Thus starting from any configuration, the probability of stabilizing in polynomially many steps is at least $(\frac{\lambda}{1+\lambda})^n$, which implies an exponential upper bound on the fixation time, by running independent trials of the above argument until one trial does succeed to stabilize the system.*

Part 3. Phase transition for Wishart matrices

The Wishart distribution is a fundamental object appearing in many domains, such as statistics, geometry, quantum physics, and wireless communications, among others. In statistics it arises as the distribution of the sample covariance matrix of a sample from a multivariate normal distribution. In geometry it is known as the Gram matrix of inner products of n points in $\mathbb{R}^d$, and it is also the starting point for canonical models of random geometric graphs [9, 6, 18].

It is well known that an $n \times n$ Wishart matrix with d degrees of freedom is close to the appropriately centered and scaled Gaussian Orthogonal Ensemble (GOE) if d is large enough (see, e.g., [9]). Recent work [6, 27] shows that the transition happens when $d = \Theta\left(n^3\right)$ and in this paper we study this critical window. In Theorem 3.8 below we explicitly compute the total variation distance between the Wishart and GOE matrices when $d/n^3 \to c \in (0, \infty)$, showing, in particular, that the phase transition from Wishart to GOE is smooth.

3.3. **Main result.** Let X be an $n \times d$ matrix where the entries are i.i.d. standard normal random variables, and let $W \equiv W(n, d) = XX^T$ be the corresponding $n \times n$ Wishart matrix with d degrees of freedom.[1] Let $M(n)$ be an $n \times n$ matrix drawn from the Gaussian Orthogonal Ensemble, i.e., a symmetric $n \times n$ random matrix where the diagonal entries are i.i.d. normal random variables with mean zero and variance 2, and the entries above the diagonal are i.i.d. standard normal random variables, with the entries on and above the diagonal all independent. In order to match the first moment and the scale of the Wishart matrix, we center and scale $M(n)$ appropriately: let $M(n, d) := \sqrt{d}M(n) + dI_n$, where I_n is the $n \times n$ identity matrix.

If d is large enough compared to n, then the Wishart matrix becomes approximately like the GOE. Recent work of Bubeck, Ding, Eldan, and Racz [6], and independently Jiang and Li [27], shows that the transition happens when $d = \Theta\left(n^3\right)$. Specifically, they proved the following theorem, where we write TV for total variation distance.

Theorem 3.7. *Define the random matrix ensembles $W(n, d)$ and $M(n, d)$ as above.*

(a) (Bubeck, Ding, Eldan, and Racz [6]) If $d/n^3 \to 0$ then

$$\mathrm{TV}\left(W(n, d), M(n, d)\right) \to 1.$$

[1] In statistics the number of samples is usually denoted by n and the number of parameters is usually denoted by p, resulting in a $p \times p$ Wishart matrix with n degrees of freedom. Here our notation is taken with the geometric perspective in mind, following [9, 6, 7].

(b) (Bubeck, Ding, Eldan, and Racz [6]; Jiang and Li [27]) If $d/n^3 \to \infty$ then

$$\mathrm{TV}\left(W(n,d), M(n,d)\right) \to 0.$$

Our focus is on the critical window and our main result is the explicit computation of the limiting total variation distance between $W(n,d)$ and $M(n,d)$ when $d/n^3 \to c \in (0,\infty)$.

Theorem 3.8. *Define the random matrix ensembles $W(n,d)$ and $M(n,d)$ as above and let $d = d(n)$ be such that $d/n^3 \to c \in (0,\infty)$. Then*

$$\lim_{n\to\infty} \mathrm{TV}\left(W(n,d), M(n,d)\right) = \mathrm{Erf}\left(\frac{1}{4\sqrt{3}\sqrt{c}}\right), \tag{3.1}$$

where recall that the error function is defined as

$$\mathrm{Erf}\,(x) = \frac{2}{\sqrt{\pi}} \int_0^x e^{-t^2} dt.$$

From this result we can immediately read off that, as $c \to 0$ and $c \to \infty$, the total variation distance goes to 1 and 0, respectively, recovering the previous results described in Theorem 3.7. Since $\mathrm{Erf}\,(x) = \frac{2}{\sqrt{\pi}} x\,(1 + o\,(1))$ as $x \to 0$, the limiting total variation distance decays as

$$\mathrm{Erf}\left(\frac{1}{4\sqrt{3}\sqrt{c}}\right) \sim \frac{1}{2\sqrt{3\pi}\sqrt{c}}$$

as $c \to \infty$. The behavior of the limit when c is small is plotted in Figure 3.

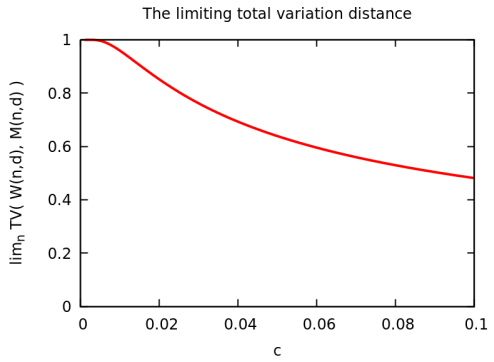

FIGURE 3. The limiting total variation distance as a function of c, when c is close to 0.

From the proof we shall see that the limit in (3.1) is the expected value of an explicit function of a two-dimensional Gaussian, which comes from the central limit theorem for the first and third moments of the empirical spectral distribution of a GOE matrix.

3.4. **Further related work and open problems.** Several recent works have explored extensions of Theorem 3.7, and Theorem 3.8 raises further questions.

Robustness. Bubeck and Ganguly [7] showed that the critical dimension is *universal* in the following sense: Theorem 3.7 holds (up to logarithmic factors) if the entries of X are i.i.d. from a sufficiently smooth distribution. What can be said about the transition in the critical regime? Are there other distributions for which the limiting total variation distance can be computed explicitly? If not, can one prove similar qualitative behavior?

Anisotropy. Eldan and Mikulincer [18] studied the effect of anisotropy on the power of detecting geometry in random geometric graphs. This is directly related to studying Wishart matrices where each row of X is a multivariate normal with a diagonal covariance matrix. The authors introduce new notions of dimensionality and prove a theorem similar to Theorem 3.7 with appropriate upper and lower bounds on the "effective critical dimension". While the primary open problem is to close the gap between these bounds, one may also ask about the nature of the transition at the effective critical dimension: can anisotropy cause qualitatively different behavior?

Other regimes. Theorems 3.7 and 3.8 state that as $d/n^3 \to \infty$, *all* statistics of the Wishart $W(n,d)$ and the GOE $M(n,d)$ have asymptotically the same distribution, but this is not the case if d/n^3 remains bounded. In the random matrix literature there has been lots of work showing that *particular* statistics of these ensembles have asymptotically the same distribution even when $d \ll n^3$. For instance, when $d = \Theta(n)$, then the limiting empirical spectral distribution of the Wishart is the Marchenko-Pastur law, which shows the difference between the Wishart and GOE, but the largest eigenvalue of the Wishart already behaves like that of the GOE [29, 16, 17]. This naturally raises the question of whether there are other regimes of d and n where there are interesting phase transitions.

4. Proof of Theorem 3.8

The main reason that allows for an explicit computation of the limiting total variation distance in Theorem 3.8 is that both $W(n,d)$ and $M(n,d)$ have explicit densities. The proof of Theorem 3.8

is similar to the case of $d/n^3 \to \infty$ presented in [6] and proceeds by a Taylor expansion of the ratio of the densities of the two random matrix ensembles. The difference compared to the case of $d/n^3 \to \infty$ is that here the Taylor expansion has to be done to one degree higher. As we shall see, taking the limit of the total variation distance as $d/n^3 \to c \in (0, \infty)$ then requires using the central limit theorem for the moments of the empirical spectral distribution of a GOE matrix.

Step 1: Writing out the total variation distance. Let $\mathcal{P} \subset \mathbb{R}^{\frac{n(n+1)}{2}}$ denote the cone of positive semidefinite matrices. It is well known (see, e.g., [62]) that when $d \geq n$, $W(n,d)$ has the following density with respect to the Lebesgue measure on $\mathcal{P}$:

$$f_{n,d}(A) := \frac{(\det(A))^{\frac{1}{2}(d-n-1)} \exp\left(-\frac{1}{2}\mathrm{Tr}(A)\right)}{2^{\frac{1}{2}dn} \pi^{\frac{1}{4}n(n-1)} \prod_{i=1}^{n} \Gamma\left(\frac{1}{2}(d+1-i)\right)},$$

where $\mathrm{Tr}(A)$ denotes the trace of the matrix A. The density of a GOE random matrix with respect to the Lebesgue measure on $\mathbb{R}^{\frac{n(n+1)}{2}}$ is $A \mapsto (2\pi)^{-\frac{1}{4}n(n+1)} 2^{-\frac{n}{2}} \exp\left(-\frac{1}{4}\mathrm{Tr}\left(A^2\right)\right)$ and so the density of $M(n,d)$ with respect to the Lebesgue measure on $\mathbb{R}^{\frac{n(n+1)}{2}}$ is

$$g_{n,d}(A) := \frac{\exp\left(-\frac{1}{4d}\mathrm{Tr}\left((A - dI_n)^2\right)\right)}{(2\pi d)^{\frac{1}{4}n(n+1)} 2^{\frac{n}{2}}}.$$

Denote the measure given by this density by $\mu_{n,d}$, let λ denote the Lebesgue measure on $\mathbb{R}^{\frac{n(n+1)}{2}}$ and write $A \succeq 0$ if A is positive semidefinite. We can then write

$$\begin{aligned} \mathrm{TV}(W(n,d), M(n,d)) &= \int_{\mathbb{R}^{\frac{n(n+1)}{2}}} \left(g_{n,d}(A) - f_{n,d}(A)\mathbf{1}_{\{A \succeq 0\}}\right)_+ d\lambda(A) \\ &= \int_{\mathbb{R}^{\frac{n(n+1)}{2}}} \left(1 - \frac{f_{n,d}(A)\mathbf{1}_{\{A \succeq 0\}}}{g_{n,d}(A)}\right)_+ d\mu_{n,d}(A), \end{aligned} \tag{4.1}$$

where $x_+ := \max\{x, 0\}$. Let $\mathcal{Q}$ denote the set of symmetric matrices for which all of the eigenvalues are in the interval $\left[d - 3\sqrt{dn}, d + 3\sqrt{dn}\right]$. Since $d/n^3 \to c > 0$, we have that $\mathcal{Q} \subset \mathcal{P}$ for all n large enough. It is known (see, e.g., [2]) that, with probability $1 - o(1)$, all the eigenvalues of $M(n)$ are in the interval $[-3\sqrt{n}, 3\sqrt{n}]$, which implies that $M(n,d) \in \mathcal{Q}$. Since the integrand in (4.1) is bounded, we can then write

$$\mathrm{TV}(W(n,d), M(n,d)) = \int_{\mathcal{Q}} \left(1 - \frac{f_{n,d}(A)}{g_{n,d}(A)}\right)_+ d\mu_{n,d}(A) + o(1) \tag{4.2}$$

and so we may restrict our attention to $\mathcal{Q}$.

Define $\alpha_{n,d}(A) := \log\left(f_{n,d}(A)/g_{n,d}(A)\right)$. Denote the eigenvalues of an $n \times n$ matrix A by $\lambda_1(A) \leq \cdots \leq \lambda_n(A)$; when the matrix is obvious from the context, we omit the dependence on A. Recall that $\det(A) = \prod_{i=1}^n \lambda_i$ and $\mathrm{Tr}(A) = \sum_{i=1}^n \lambda_i$. We then have that

$$\alpha_{n,d}(A) = \frac{1}{2}\sum_{i=1}^n \left\{(d-n-1)\log\lambda_i - \lambda_i + \frac{1}{2d}(\lambda_i - d)^2\right\} + \left\{\frac{n(n+3)}{4} - \frac{dn}{2}\right\}\log 2 + \frac{n}{2}\log\pi + \frac{n(n+1)}{4}\log d - \sum_{i=1}^n \log\Gamma\left(\frac{1}{2}(d+1-i)\right).$$

By Stirling's formula we know that $\log\Gamma(z) = \left(z-\frac{1}{2}\right)\log z - z + \frac{1}{2}\log(2\pi) + O\left(\frac{1}{z}\right)$ as $z \to \infty$, so

$$\alpha_{n,d}(A) = \frac{1}{2}\sum_{i=1}^n \left\{(d-n-1)\log\lambda_i - \lambda_i + \frac{1}{2d}(\lambda_i - d)^2\right\} + \frac{n(n+1)}{4}\log d - \frac{1}{2}\sum_{i=1}^n (d-i)\log(d+1-i) + \frac{1}{2}\sum_{i=1}^n (d+1-i) + O\left(\frac{n}{d}\right).$$

Now writing $\log(d+1-i) = \log d + \log\left(1-\frac{i-1}{d}\right) = \log d - \frac{i-1}{d} - \frac{(i-1)^2}{2d^2} + O\left(\frac{(i-1)^3}{d^3}\right)$ we get that

$$\alpha_{n,d}(A) = \frac{1}{2}\sum_{i=1}^n \left\{(d-n-1)\log\lambda_i - \lambda_i + \frac{1}{2d}(\lambda_i - d)^2\right\} - \frac{n}{2}\left\{(d-n-1)\log d - d\right\} - \frac{n^3}{12d} + o(1).$$

Defining $h(x) := \frac{1}{2}\left\{(d-n-1)\log(x/d) - (x-d) + \frac{1}{2d}(x-d)^2\right\}$, we have that

$$\alpha_{n,d}(A) = \sum_{i=1}^n h(\lambda_i) - \frac{n^3}{12d} + o(1). \tag{4.3}$$

Step 2: Taylor expansion and taking the limit. The derivatives of h at d are $h(d) = 0$, $h'(d) = -\frac{n+1}{2d}$, $h''(d) = \frac{n+1}{2d^2}$, $h^{(3)}(d) = \frac{d-n-1}{d^3}$, $h^{(4)}(d) = -\frac{3(d-n-1)}{d^4}$, and also $h^{(5)}(x) = \frac{12(d-n-1)}{x^5}$. Approximating h with its fourth order Taylor polynomial around d we get that

$$h(x) = -\frac{n+1}{2d}(x-d) + \frac{n+1}{4d^2}(x-d)^2 + \frac{d-n-1}{6d^3}(x-d)^3 - \frac{d-n-1}{8d^4}(x-d)^4 + \frac{d-n-1}{10\xi^5}(x-d)^5,$$

where ξ is some real number between x and d. From 4.3 we see that to compute $\alpha_{n,d}(A)$, we need to compute the sum over the eigenvalues $\{\lambda_i\}_{i=1}^n$ of each term in the expansion.

First, we argue that the contribution from the remainder term is negligible. Recall that $A \in \mathcal{Q}$, and hence $\lambda_i \in \left[d - 3\sqrt{dn}, d + 3\sqrt{dn}\right]$ for every $i \in [n]$. If $x \in \left[d - 3\sqrt{dn}, d + 3\sqrt{dn}\right]$, then

$$\left|\frac{d-n-1}{10\xi^5}(x-d)^5\right| \leq \frac{d-n-1}{10\left(d-3\sqrt{dn}\right)^5}\left(3\sqrt{dn}\right)^5 = O\left(\frac{1}{n^2}\right),$$

where we used that $d = \Theta\left(n^3\right)$. Summing n such terms gives a term of order $O(1/n)$, which is negligible in the limit. Turning to the four terms that matter, defining

$$S_1(n,d) := -\frac{n+1}{2d}\sum_{i=1}^{n}(\lambda_i - d), \qquad S_2(n,d) := \frac{n+1}{4d^2}\sum_{i=1}^{n}(\lambda_i - d)^2,$$
$$S_3(n,d) := \frac{d-n-1}{6d^3}\sum_{i=1}^{n}(\lambda_i - d)^3, \qquad S_4(n,d) := -\frac{d-n-1}{8d^4}\sum_{i=1}^{n}(\lambda_i - d)^4,$$

and also letting $S_0(n,d) := -n^3/(12d)$, we thus have that

$$\alpha_{n,d}(A) = S_0(n,d) + S_1(n,d) + S_2(n,d) + S_3(n,d) + S_4(n,d) + o(1). \tag{4.4}$$

For $i \in [n]$ define $\mu_i := \frac{1}{\sqrt{dn}}(\lambda_i - d)$. If $\{\lambda_i\}_{i=1}^n$ are the eigenvalues of $M(n,d)$, then $\{\mu_i\}_{i=1}^n$ are the eigenvalues of $\frac{1}{\sqrt{n}}M(n)$. Recall that the empirical spectral distribution $\frac{1}{n}\sum_{i=1}^n \delta_{\mu_i}$ converges weakly to the semicircle distribution with density $\rho_{\mathrm{sc}}(x) = \frac{1}{2\pi}\sqrt{4-x^2}\mathbf{1}_{\{|x|\leq 2\}}$ (see, e.g., [2]). With this notation we can rewrite the four quantities above as follows:

$$S_1(n,d) = -\frac{\sqrt{n}(n+1)}{2\sqrt{d}} \times \sum_{i=1}^{n}\mu_i, \qquad S_2(n,d) = \frac{n^2(n+1)}{4d} \times \frac{1}{n}\sum_{i=1}^{n}\mu_i^2,$$
$$S_3(n,d) = \frac{d-n-1}{6d} \times \sqrt{\frac{n^3}{d}} \times \sum_{i=1}^{n}\mu_i^3, \qquad S_4(n,d) = -\frac{d-n-1}{8d} \times \frac{n^3}{d} \times \frac{1}{n}\sum_{i=1}^{n}\mu_i^4.$$

Let U be a random variable distributed according to the semicircle law. We know that for any fixed $k \in \mathbb{N}$, the k^{th} moment of the empirical spectral distribution converges in probability to the k^{th} moment of the semicircle law (see [2, Lemmas 2.1.6 and 2.1.7]), i.e.,

$$\frac{1}{n}\sum_{i=1}^{n}\mu_i^k \to \mathbb{E}\left[U^k\right].$$

Since $\mathbb{E}\left[U^2\right] = 1$ and $\mathbb{E}\left[U^4\right] = 2$, we have that, as $d/n^3 \to c \in (0,\infty)$, $S_2(n,d) \to 1/(4c)$ and $S_4(n,d) \to -1/(4c)$, so put together we have that $S_2(n,d) + S_4(n,d) \to 0$.

The central limit theorem for the moments of the empirical spectral distribution of a GOE matrix (see [2, Theorem 2.1.31 and Exercise 2.1.35] and [3]) shows that

$$\left(\sum_{i=1}^{n}\mu_i,\sum_{i=1}^{n}\mu_i^3\right)\Longrightarrow(N_1,N_3)\,, \tag{4.5}$$

where (N_1,N_3) are jointly normal with mean zero and covariance matrix $C=\left(\begin{smallmatrix}2&6\\6&24\end{smallmatrix}\right)$. The entries of the covariance matrix C are special cases of the more general formulas found in [2, 3]. One can verify these numbers by using the identity

$$\sum_{i=1}^{n}\mu_i^k=\operatorname{Tr}\left(\left(\tfrac{1}{\sqrt{n}}M\left(n\right)\right)^k\right)=\sum_{i=1}^{n}\left(\left(\tfrac{1}{\sqrt{n}}M\left(n\right)\right)^k\right)_{i,i}$$

for $k=1$ and $k=3$, and computing appropriate moments of normal random variables. Using Chebyshev polynomials can simplify computations. Specifically, let T_k denote the Chebyshev polynomial of the first kind of degree k. That is, let $T_0\left(x\right)=1$, let $T_1\left(x\right)=x$, and for $n\geq 1$ let $T_{n+1}\left(x\right)=2xT_n\left(x\right)-T_{n-1}\left(x\right)$. Previous work [28, Corollary 2.8] shows that the random variables

$$\left\{\operatorname{Tr}\left(T_{2\ell+1}\left(\frac{1}{2\sqrt{n}}M\left(n\right)\right)\right)\right\}_{\ell=0}^{k}$$

converge weakly to independent normal random variables with mean zero and variances given by $\{(2\ell+1)/2\}_{\ell=0}^{k}$. The result in (4.5) then immediately follows from this result for $k=1$.

Putting everything together we see that, as $d/n^3\to c\in(0,\infty)$, we have that

$$\left(S_0,S_1,S_2,S_3,S_4\right)\Longrightarrow\left(-\frac{1}{12c},-\frac{1}{2\sqrt{c}}N_1,\frac{1}{4c},\frac{1}{6\sqrt{c}}N_3,-\frac{1}{4c}\right). \tag{4.6}$$

Therefore, since the function $(s_0,s_1,s_2,s_3,s_4)\mapsto\left(1-\exp\left(s_0+s_1+s_2+s_3+s_4\right)\right)_+$ is continuous and bounded, we have by (4.2), (4.4), and (4.6) that

$$\operatorname{TV}\left(W(n,d),M\left(n,d\right)\right)\to\mathbb{E}\left[\left(1-\exp\left(-\frac{1}{12c}-\frac{1}{2\sqrt{c}}N_1+\frac{1}{6\sqrt{c}}N_3\right)\right)_+\right]. \tag{4.7}$$

Step 3: Evaluating the limit. What remains is to evaluate the expectation on the right hand side of (4.7). Let Y and Z be independent normal random variables with mean zero and variances 2 and 6, respectively. Then (N_1,N_3) and $(Y,3Y+Z)$ have the same distribution, since both are

Gaussian with the same mean vector and covariance matrix. Notice that

$$-\frac{1}{2\sqrt{c}}Y + \frac{1}{6\sqrt{c}}(3Y + Z) = \frac{1}{6\sqrt{c}}Z$$

and hence the right hand side of (4.7) is equal to

$$\mathbb{E}\left[\left(1 - \exp\left(-\frac{1}{12c} + \frac{1}{6\sqrt{c}}Z\right)\right)_+\right].$$

Since $1 - \exp(-1/(12c) + z/(6\sqrt{c})) \geq 0$ if and only if $z \leq 1/(2\sqrt{c})$, we have that

$$\begin{aligned}
\mathbb{E}\left[\left(1 - \exp\left(-\frac{1}{12c} + \frac{1}{6\sqrt{c}}Z\right)\right)_+\right] &= \int_{-\infty}^{\frac{1}{2\sqrt{c}}} \left(1 - e^{-\frac{1}{12c} + \frac{1}{6\sqrt{c}}z}\right) \cdot \frac{1}{\sqrt{12\pi}} e^{-\frac{z^2}{12}} dz \\
&= \frac{1}{\sqrt{12\pi}} \int_{-\infty}^{\frac{1}{2\sqrt{c}}} e^{-\frac{z^2}{12}} dz - \frac{1}{\sqrt{12\pi}} \int_{-\infty}^{\frac{1}{2\sqrt{c}}} e^{-\frac{(z-1/\sqrt{c})^2}{12}} dz \\
&= \mathbb{P}\left(Z < \frac{1}{2\sqrt{c}}\right) - \mathbb{P}\left(Z < -\frac{1}{2\sqrt{c}}\right) = \mathrm{Erf}\left(\frac{1}{4\sqrt{3}\sqrt{c}}\right),
\end{aligned}$$

which concludes the proof.

Acknowledgements

We thank an anonymous reviewer for helpful suggestions.

Part 4. Intersections of random sets

The Boolean model is a geometric model for random sets in space: for example, bullets being fired at a tank, or antibodies attaching to a virus cell. One starts with a Poisson point process $\mathcal{X}$ of intensity λ on $\mathbb{R}^d$, and (for simplicity) some fixed set S. The Boolean model refers to the set

$$B_{\lambda,S} = \bigcup_{X \in \mathcal{X}} (X + S), \tag{4.8}$$

where, for $x \in \mathbb{R}^d$,

$$x + S = \{x + y : y \in S\}. \tag{4.9}$$

Conditioning on the (positive probability) event $\{0 \notin B_{\lambda,S}\}$, one then studies, among other things, the uncovered component of $\mathbb{R}^d$ containing 0, known as the *Crofton cell*.

The Boolean model was first defined and studied in the 1960s by E.N. Gilbert, who investigated both percolation [11] and coverage [12]. Gilbert's results (from both papers) were improved by Hall [14, 15], and Hall's result on coverage [14] was improved and generalized by Janson [18]. The books by Meester and Roy [22] and Hall [16] are standard references for the percolation and coverage processes respectively, and the more recent books by Haenggi [17] and Franceschetti and Meester [10] cover applications to wireless networks (the motivating example from [11]).

There are a number of well-studied cousins of the Boolean model. One such class of models is tessellations. For example, consider a hyperplane tessellation of intensity λ on $\mathbb{R}^d$. Namely, let $\mathcal{R} = \{R_n : n \in \mathbb{N}\}$ denote a Poisson point process with intensity λ – or, more generally, with intensity measure ν – on $\mathbb{R}$, and let $\theta_n, n \in \mathbb{N}$, be iid uniform over the $d-1$ dimensional unit sphere, independent of $\mathcal{R}$. The corresponding Poisson field $\mathcal{H}$ refers to the set of hyperplanes H_n given by

$$H_n = \{x \in \mathbb{R}^d : x \cdot \theta_n = R_n\}, \tag{4.10}$$

i.e., H_n is the hyperplane passing through the point $R_n\theta_n$, with normal vector parallel to θ_n. Note that, on average, 2λ hyperplanes intersect the unit sphere in this model. The analogous object in this context is the connected component of the tessellation containing 0, denoted D_0^λ.

Hyperplane tessellations have a history dating back to the 19th century. Crofton's formula (1868) expresses the length of a curve C in terms of the expected number of times C meets a random line, i.e., the expected number of times C intersects a random line tessellation. Generalizations of Crofton's formula led to the development of Integral Geometry [28]. Meanwhile, inspired by a question of Niels Bohr on cloud chamber tracks, Goudsmit in 1945 [13] computed the variance of the cell size in a random line tessellation, and Miles in 1964 [24, 25] initiated the systematic study of random line tessellations (with potential applications to papermaking in mind). We will make use of Goudsmit's result later. Calka's recent survey article [6] gives an excellent overview of the field.

We will also use a slightly different tessellation model: tessellation by spheres, rather than hyperplanes. Let $\mathcal{X}$ be a Poisson point process of intensity λ on $\mathbb{R}^d$, and let $\mathbb{S} = \partial\mathbb{B} = \{x \in \mathbb{R}^d : ||x||_2 = 1\}$ denote the boundary of the unit ball $\mathbb{B}$ in $\mathbb{R}^d$. Then the set

$$\bigcup_{X \in \mathcal{X}} (X + \mathbb{S}) \tag{4.11}$$

partitions $\mathbb{R}^d$ into a union of disjoint connected components. As before, it is common to study the connected component of this tessellation containing the origin, denoted E_0^λ.

A result due to Michel and Paroux [23] (see also [7]) gives a common scaling limit for these sets:

Theorem 4.1. *Let C_0^λ, D_0^λ and E_0^λ denote the Crofton cell in the boolean model (with $S = \mathbb{B}$), and the connected components in the hyperplane and sphere tessellation models, respectively. These three models have a common scaling limit in distribution:*

$$\lim_{\lambda\to\infty} S_d \lambda C_0^\lambda \sim \lim_{\lambda\to\infty} 2\lambda D_0^\lambda \sim \lim_{\lambda\to\infty} 2S_d \lambda E_0^\lambda \sim 2C, \tag{4.12}$$

where S_d is the Lebesgue measure of $\mathbb{S} = \partial\mathbb{B}$, C is the law of the normalized Crofton cell D_0^1, and $\sim$ denotes equality in distribution.

The scaling in this theorem is nontrivial and deserves some comment. Consider first the tessellation models. As $\lambda \to \infty$, the expected volume of the connected component containing the origin is inversely proportional to the expected number of connected components in $B_\varepsilon = \{x : ||x|| < \varepsilon\}$. This latter quantity is in turn proportional to the number of points of intersection (of spheres or hyperplanes) in B_ε. The number of such intersection points scales as λ^d, since each intersection

point is determined by d spheres (respectively hyperplanes), so the expected volume of the Crofton cell scales as λ^{-d}, leading to a linear scale factor of $1/\lambda$. Finally, the constants can be determined by computing the expected number of spheres (respectively hyperplanes) meeting B_ε in each of the three models: for C_0^λ, D_0^λ and E_0^λ these are asymptotically $S_d\lambda\varepsilon, 2\lambda\varepsilon$ and $2S_d\lambda\varepsilon$ respectively.

Our contribution is to introduce a new model to this group, which we term the *boolean intersection model*. Let $\mathbb{B}$ denote the closed unit ball in $\mathbb{R}^d$, and let $\mathcal{C}_\lambda$ be a Poisson point process with intensity λ on $\mathbb{B}$. (We will focus on the uniform intensity case, and discuss in Section 6 some ideas that apply for general intensity measures). Let

$$I^\lambda = \mathbb{B} \cap \left(\bigcap_{C \in \mathcal{C}_\lambda} (C + \mathbb{B}) \right) \tag{4.13}$$

be the intersection of copies of $\mathbb{B}$ shifted by $C \in \mathcal{C}_\lambda$. By definition, set $I^\lambda = \mathbb{B}$ if $\mathcal{C}_\lambda = \emptyset$. Note that for each λ, I^λ is a convex (connected) set contained in $\mathbb{B}$, containing 0. Our goal will be to show that I^λ shares the same limit as the Boolean and Poisson hyperplane tessellation processes, up to a constant.

Theorem 4.2. *Let C denote the law of the normalized Crofton cell D_0^1. The following distributional convergence holds:*

$$\lim_{\lambda \to \infty} S_d \lambda I^\lambda \sim 2C. \tag{4.14}$$

Write $|I|$ for the Lebesgue measure of a measurable set $I \subset \mathbb{R}^d$, and $\omega_d = \mathrm{vol}(\mathbb{B}) = \frac{1}{d} S_d$.

Proposition 4.3. *The limiting volume of the intersection is given by*

$$\lim_{\lambda \to \infty} \lambda^d \mathbb{E}|I^\lambda| = \frac{d! \omega_d}{\omega_{d-1}^d}. \tag{4.15}$$

For example, when $d = 2$, $\lim_{\lambda\to\infty} \lambda^2 \mathbb{E}|I^\lambda| = \frac{\pi}{2}$.

One proof of this fact is via (4.14), and an appeal to classical results on the statistics of the Crofton cell C [13]; we outline the details in Section 9. We give an alternative proof based on general results for the intersection model in Section 6. Similar formulas hold for a more general class of boolean intersection models, namely where the underlying point process is not uniform, or the balls are exchanged for other compact sets. For simplicity we focus on the case of balls of fixed

radius, and comment on generalizations in Section 6.2. Additionally, one can formulate all these results using 'fixed count' versions of these models: that is, instead of using an underlying Poisson process, for each n define I_n as the intersection of n iid copies of $\mathbb{B}$. This model also shares the Crofton cell D_0^1 as a scaling limit.

4.1. **Random variables in the space of closed sets.** Our main result, Theorem 4.2, refers to a convergence of random sets. The usual modes of convergence – in law, in probability, and in L^p – are trickier to define for random sets. We follow the approach taken in [7] and most of the existing literature, namely via the Hausdorff metric d_H on the space E of closed subsets of $\mathbb{R}^d$. In the most general setting, one defines convergence in law by convergence of capacity functionals. Suppose X is a random set taking values in E: the *capacity functional* of X is

$$T_X(K) = \mathbb{P}(X \cap K \neq \emptyset), \quad K \text{ a compact subset of } \mathbb{R}^d. \tag{4.16}$$

If X_n and X are random sets in E, *convergence in law* of X_n to X, written $X_n \to_d X$, refers to convergence of their capacity functionals, i.e., for any fixed compact $K \subset \mathbb{R}^d$,

$$T_{X_n}(K) \to T_X(K) \text{ as } n \to \infty. \tag{4.17}$$

A stronger notion, which is used in [7], and that we rely on in the proof of Theorem 4.2, is convergence in probability. If X_n and X are defined on the same probability space, we say $X_n \to X$ *in probability* if for every $\epsilon > 0$,

$$\mathbb{P}(d_H(X_n, X) > \epsilon) \to 0 \quad \text{as } n \to \infty. \tag{4.18}$$

The authors of [7] implicitly use the fact that convergence in probability for random sets implies the convergence in law defined above. Our proof of Theorem 4.2 gives an explicit coupling between the intersection model and the Crofton cell, under which (4.18) holds.

5. Overview of results

Although our main result is Theorem 4.2, we will present two different approaches to its corollary, Proposition 4.3. The first is direct, and appears in Section 6. The second is via Theorem 4.2, and occupies Sections 7, 8 and 9. Below, we summarize each approach in turn.

In Section 6, we first consider a single ball B, whose center lies inside the unit ball $\mathbb{B}$. A simple volume calculation lets us estimate (in Proposition 6.1) the probability that B contains the line segment $[0, r]$ on the positive x-axis. Next, we consider the full model, in which unit balls are centered at points of a Poisson process of intensity λ inside $\mathbb{B}$, forming an intersection I^λ. Write R^λ for the radius of I^λ in the positive x direction (for instance). Proposition 6.1, together with an approximation argument, allows us to show that the suitably scaled radius R^λ converges in distribution to an exponential random variable of mean one. Finally, Proposition 6.4 relates the expected volume of I^λ to the dth moment of R^λ, completing the calculation of $\mathbb{E}|I^\lambda|$ and proving Proposition 4.3.

As part of this analysis, we also prove a parallel series of results for a related hyperplane model K^λ, which approximates the ball model I^λ near the origin.

Section 7 contains some probabilistic and geometric lemmas that we will use in Section 8.

In Section 8, we prove Theorem 4.2. The main idea is to couple the intersection model with a sphere tessellation model. With I^λ as above, and J^λ defined as the cell containing the origin in an appropriately scaled sphere tessellation model, we show that, in our coupling, the scaled Hausdorff distance between I^λ and J^λ converges to 0 almost surely as $\lambda \to \infty$. To achieve this, we carry out the following steps:

(1) Show that only points of the Poisson process close to the boundary – namely, within distance $\varepsilon_\lambda = \frac{\log^2 \lambda}{\lambda}$ of $\partial\mathbb{B}$ – contribute to the shape of I^λ (asymptotically almost surely as $\lambda \to \infty$). We use a coupon-collector type process on $\partial\mathbb{B}$ as a test: if there are points of $\mathcal{C}_\lambda$ close to $\partial\mathbb{B}$ that are "spread out enough" (in terms of angle), then I^λ must be contained within a small ball at the origin.

(2) Match spheres close to $\partial\mathbb{B}$ from the intersection model with spheres close to $\partial\mathbb{B}$ from the tessellation model. Since some of the sphere centers in the tessellation model land outside $\mathbb{B}$, while the sphere centers in the intersection model are confined to $\mathbb{B}$, we must match them by shifting. We accordingly identify each point $R\theta$ of the underlying tessellation process (with $R \in (1, 1 + \varepsilon_\lambda)$ and $\theta \in \partial\mathbb{B}$) with the point $(R - 2)\theta$ in the intersection process. The spheres centered at these two points have almost the same effect on J^λ, except that one makes a 'concave' boundary and the other a 'convex' boundary.

(3) Show that the error in carrying out Step 2, in terms of the Hausdorff distance between the suitably scaled sets I^λ and J^λ, is negligible. This involves a careful coupling between the

underlying point processes: since we scale everything by a factor of λ, it is necessary to have an error of order $o(\lambda^{-1})$, not just $o(1)$.

Finally, in Section 9, we derive Proposition 4.3 from Theorem 4.2, using the d-dimensional version of Goudsmit's 1945 calculation [13] for the area of the Crofton cell. Although the relevant formulas appear in the work of Matheron [21] (Chapter 6), our treatment is short and self contained.

6. Statistics for the intersection model

To warm up, consider the following generic intersection process on $\mathbb{R}$. Let $\mathcal{C}_\lambda$ be a Poisson process with intensity λ on $[-1,1]$, and define

$$U = U_\lambda = [-1,1] \cap \left(\bigcap_{c \in C_\lambda} c + [-1,1] \right) \tag{6.1}$$

where $c + [-1,1] = [c-1, c+1]$ for $c \in \mathbb{R}$, with the convention that $U = [-1,1]$ if $\mathcal{C}_\lambda = \emptyset$. U is always an interval, so it is determined by $\sup U$ and $\inf U$. The distribution of the infimum can be determined as follows. We have that $\inf U < -u$ if and only if $\max \mathcal{C}_\lambda < 1-u$, which in turn holds if and only if each element of $\mathcal{C}_\lambda$ is less than $1-u$, i.e., if no point of $\mathcal{C}_\lambda$ lies in the interval $[1-u, 1]$. The latter event has probability $e^{-\lambda u}$, so $-\inf U \sim \mathrm{Exp}(\lambda^{-1})$.

Note that $\inf U$ is a function of $\mathcal{C}_\lambda \cap [0,1]$ and $\sup U$ is a function of $\mathcal{C}_\lambda \cap [-1,0]$; basic properties of Poisson processes imply that $\inf U$ and $\sup U$ are independent. Thus, as $\lambda \to \infty$, the left and right endpoints of U shrink to 0 independently, so we have

$$|U_\lambda| \sim \mathrm{Exp}(\lambda^{-1}) + \mathrm{Exp}(\lambda^{-1}) \sim \mathrm{Gamma}(2, \lambda^{-1}). \tag{6.2}$$

6.1. Ball and hyperplane intersection models.

We now explore some basic properties of two intersection models: the ball intersection model I^λ (defined as in 4.13), and an analogous intersection model with hyperplanes. Let $\widetilde{\mathcal{C}_\lambda}$ be a Poisson point process on $\mathbb{B}$ with intensity measure $\lambda(\nu \times \sigma)$, where σ is surface-area measure on $\mathbb{S}$ and ν is the measure supported on $[0,1]$ given by

$$\nu(0,r) = \frac{1}{d}\left(1 - (1-r)^d\right). \tag{6.3}$$

Define the hyperplane intersection model

$$K^\lambda = \mathbb{B} \cap \left(\bigcap_{\widetilde{C} \in \widetilde{\mathcal{C}_\lambda}} \mathbb{H}(\widetilde{C}) \right), \tag{6.4}$$

where $\mathbb{H}(\widetilde{C})$ is the half-space normal to the vector $\widetilde{C}$ and containing 0, i.e.,

$$\mathbb{H}(\widetilde{C}) = \widetilde{C} + \{x \in \mathbb{R}^d : x \cdot C < 0\}. \tag{6.5}$$

By definition, $K^\lambda = \mathbb{B}$ if $\widetilde{\mathcal{C}_\lambda} = \emptyset$. The choice of ν is special, because it makes K^λ asymptotically identical to the Boolean intersection model I^λ with copies of $\mathbb{B}$ defined earlier – the difference is that the copies of the unit disk have been exchanged for half spaces. Indeed, placing a single disk $\mathbb{B}$ with center $Z\Theta$ is like placing the half space $\mathbb{H}((Z-1)\Theta)$; the difference is asymptotically negligible as $\lambda \to \infty$. The error is quantified precisely in terms of the Hausdorff distance in Section 7. In this section we work with both K^λ and I^λ simultaneously: the same ideas can be used to analyze both models, with slightly different details.

For any $\theta \in \mathbb{S}$, define the 'radius in the θ direction:'

$$R^\lambda(\theta) = \sup\{t \in (0,1) : t\theta \in I^\lambda\}, \quad Q^\lambda(\theta) = \sup\{t \in (0,1) : t\theta \in K^\lambda\}. \tag{6.6}$$

The collections $\{R^\lambda(\theta) : \theta \in \mathbb{S}\}$ and $\{Q^\lambda(\theta) : \theta \in \mathbb{S}\}$ each consist of identically distributed but not independent variables: $R^\lambda(\theta)$ and $R^\lambda(\theta')$ are not independent for $\theta \neq \theta'$ (except for the special case $\theta' = -\theta$). We simply write $R = R^\lambda$ or $Q = Q^\lambda$ for the distribution of any one of the $R^\lambda(\theta)$ or $Q^\lambda(\theta)$, respectively. For $r \in (0,1)$, denote by $F(r)$ and $G(r)$ the probabilities

$$F(r) = \mathbb{P}(re_1 \notin B), \quad G(r) = \mathbb{P}(re_1 \notin H), \tag{6.7}$$

where B is an independent copy of a randomly placed ball $\mathbb{B} + C$ for $C \in \mathcal{C}_\lambda$, H is an independent copy of one of the random hyperplanes $\mathbb{H}(\widetilde{C}), \widetilde{C} \in \widetilde{\mathcal{C}_\lambda}$, and $\vec{e}_1 = (1, 0, \ldots, 0) \in \mathbb{R}^d$. The functions F and G are closely connected to the distributions of R and Q respectively, since for $r \in (0,1)$,

$$R > r \iff r\vec{e}_1 \in \mathbb{B} + C \text{ for every } C \in \mathcal{C}_\lambda, \tag{6.8}$$

and similarly for Q. Let ω_d denote the volume of the unit ball $\mathbb{B}$ in $\mathbb{R}^d$. We have the following formulas for F and G:

Proposition 6.1. *Consider the intersection boolean models I^λ and K^λ in dimension $d \geq 1$.*

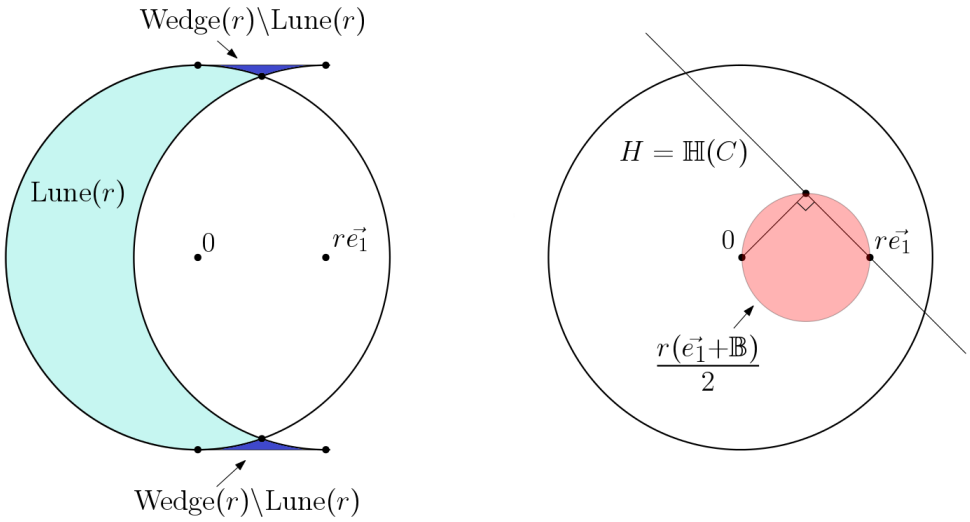

FIGURE 4. The left diagram shows $F(r)$ as the area of the teal set. Note that if any disk center lies in the lune, then I^λ does not contain the point $(r, 0)$. The error between the Lune and Wedge sets is shown in blue: its area is negligible, and this gives a quick approximation of the area of the lune. The analogous set for the hyperplane model is shown on the right: $G(r)$ is the mass placed on the red set by the probability measure $\frac{1}{S_d}\nu \times \sigma$. The fact that the red set is a circle follows from elementary geometry: the angle in a semicircle is a right angle.

i. *Let F be as in 6.7. For any $r \in (0, 1)$,*

$$F(r) = \frac{1}{\omega_d} |\mathbb{B} \setminus (r\vec{e_1} + \mathbb{B})| \tag{6.9}$$

$$= \frac{\omega_{d-1}}{\omega_d} r - O(r^3) \text{ as } r \to 0, \tag{6.10}$$

where $|\cdot|$ denotes the volume (Lebesgue measure) in $\mathbb{R}^d$.

ii. *Let G be as in 6.7. For any $r \in (0, 1)$,*

$$G(r) = \frac{1}{\omega_d} \int_{\mathbb{S}^+} \nu(0, r\langle \vec{e}_1, \theta \rangle)\, d\sigma(\theta) \tag{6.11}$$

$$= \nu \times \sigma \left(\frac{r(\vec{e}_1 + \mathbb{B})}{2} \right) \tag{6.12}$$

$$= \frac{(d-1)\omega_{d-1}}{d\omega_d} \sum_{k=1}^{d} (-1)^{1+k} \binom{d}{k} \frac{\Gamma(\frac{d-1}{2})\Gamma(\frac{k+1}{2})}{2\Gamma(\frac{k+d}{2})} r^k \tag{6.13}$$

$$= \frac{\omega_{d-1}}{\omega_d} r - O(r^2) \text{ as } r \to 0. \tag{6.14}$$

Note that F and G have the same linear approximation near 0: this is a reflection of the fact that the unit ball has smooth boundary, and hence locally is a hyperplane.

Proof. *i.* Write $B = C + \mathbb{B}$ where C is uniform over $\mathbb{B}$, and note that for $r \in (0,1)$,

$$r\vec{e_1} \notin B \iff \|C - r\vec{e_1}\| \geq 1 \iff C \in \mathbb{B} \setminus (r\vec{e_1} + \mathbb{B}). \tag{6.15}$$

The first equality follows immediately. The shape $\text{Lune}(r) = \mathbb{B} \setminus (r\vec{e_1} + \mathbb{B})$ is very close to the shape

$$\text{Wedge}(r) = \{\theta + t\vec{e_1} : \theta \in \mathbb{S}^-, t \in (0,r)\} \tag{6.16}$$

obtained by shifting half of $\mathbb{S}$ by r along the $\vec{e_1}$ axis, where $\mathbb{S}^- = \{\theta \in \mathbb{S} : \langle \theta, \vec{e_1} \rangle < 0\}$. The volume of $\text{Wedge}(r)$ is

$$|\text{Wedge}(r)| = \omega_{d-1} r. \tag{6.17}$$

Note that $\text{Lune}(r) \subset \text{Wedge}(r)$, and $\text{Lune}(r) = \text{Wedge}(r) \cap \mathbb{B}$. The error is contained a region with rectangular cross sections: in dimension $d = 2$, it has the form

$$\text{Wedge}(r) \setminus \text{Lune}(r) = \{(x^1, x^2) \in \mathbb{R}^2 : x^1 \in (0,r), x^2 \in (\sqrt{1 - (x^1)^2}, 1)\}. \tag{6.18}$$

In arbitrary dimension d, the error is contained in the region formed by rotating the same rectangle about the e_1 axis, (i.e. through the copy of the $(d-2)$-dimensional unit sphere lying in the hyperplane $x^1 = 0$). Using the expansion $\sqrt{1 - r^2} = 1 - \frac{r^2}{2} + O(r^4)$, it follows immediately that

$$|\text{Wedge}(r) \setminus \text{Lune}(r)| \leq \omega_{d-1} \frac{r^3}{4} + O(r^5), \tag{6.19}$$

as desired.

ii. Write $C = P\Theta$, where $P \in [0,1]$ is distributed according to ν, and $\Theta \in \mathbb{S}$ is distributed according to σ. The corresponding hyperplane, pinned at C, is given by

$$H = \mathbb{H}(C) = \{x : \langle x, \Theta \rangle \leq P\}, \tag{6.20}$$

and thus

$$\mathbb{P}(r\vec{e}_1 \notin H) = \mathbb{P}(P < \langle r\vec{e}_1, \Theta \rangle). \tag{6.21}$$

The first equality follows immediately by integrating. Moreover,

$$P < r\langle \vec{e}_1, \Theta \rangle \iff \left\| P\Theta - \frac{r}{2}\vec{e}_1 \right\| < \frac{r}{2} \iff C = P\Theta \in \frac{r(\vec{e}_1 + \mathbb{B})}{2}, \tag{6.22}$$

proving the second equality. To obtain the explicit sum formula, we can evaluate the integral directly by expanding the measure ν as

$$\nu(0, r) = \frac{1}{d}\left(1 - (1 - r)^d\right) = \frac{1}{d}\sum_{k=1}^{d}(-1)^{1+k}\binom{d}{k}r^k. \tag{6.23}$$

Thus for $d \geq 2$,

$$G(r) = \frac{1}{\omega_d}\int_{\mathbb{S}^+} \nu(0, r\langle \vec{e_1}, \theta \rangle)\, d\sigma(\theta) \tag{6.24}$$

$$= \frac{(d-1)\omega_{d-1}}{d\omega_d}\int_0^{\pi/2}\int_{\mathbb{S}^{d-1}}\sum_{k=1}^{d}(-1)^{1+k}\binom{d}{k}r^k \cos^k\alpha \sin^{d-2}\alpha\, d\phi\, d\alpha \tag{6.25}$$

$$= \frac{(d-1)\omega_{d-1}}{d\omega_d}\sum_{k=1}^{d}(-1)^{1+k}\binom{d}{k}\left(\int_0^{\pi/2}\cos^k\alpha\, \sin^{d-2}\alpha\, d\alpha\right) r^k. \tag{6.26}$$

(This integral isn't valid when $d = 1$: in that case, $G(r) = F(r) = 2r$.) The $d\alpha$ integral evaluates to

$$\int_0^{\pi/2}\cos^k\alpha\, \sin^{d-2}\alpha\, d\alpha = \frac{\Gamma(\frac{d-1}{2})\Gamma(\frac{k+1}{2})}{2\Gamma(\frac{k+d}{2})}, \tag{6.27}$$

and the coefficient of the linear term ($k = 1$) is $\frac{(d-1)\omega_{d-1}}{d\omega_d} \cdot d \cdot \frac{\Gamma(\frac{d-1}{2})}{2\Gamma(\frac{d+1}{2})} = \frac{\omega_{d-1}}{\omega_d}$.

□

For example, in dimension $d = 2$, an explicit computation – namely, for the area of intersection of two circles – yields

$$F(r) = 1 - \frac{1}{\pi}\left(2\arccos(r/2) - r\sqrt{1 - r^2/4}\right) = \frac{2r}{\pi} - \frac{r^3}{12\pi} + \cdots \tag{6.28}$$

Directly evaluating the integral (6.11) gives

$$G(r) = \frac{1}{\pi}\int_0^{\pi/2} (2r\cos\theta - r^2\cos^2\theta)\, d\theta = \frac{2r}{\pi} - \frac{r^2}{4}. \tag{6.29}$$

Recall that R and Q depend on d via the underlying dimension of the boolean intersection models I^λ and K^λ. The distributions of R^λ and Q^λ converge to exponential distributions as $\lambda \to \infty$:

Proposition 6.2. *For any $d \geq 1$, as $\lambda \to \infty$,*

$$\lambda\omega_d F(R^\lambda) \to \mathrm{Exp}(1), \tag{6.30}$$

and

$$\lambda\omega_d G(Q^\lambda) \to \mathrm{Exp}(1). \tag{6.31}$$

Proof. For any $r \in (0,1)$, since I consists of Poisson$(\lambda\omega_d)$ many copies of $\mathbb{B}$,

$$\mathbb{P}(R > r) = \mathbb{P}(r\vec{e}_1 \in I) = \exp(-\lambda\omega_d F(r)). \tag{6.32}$$

Similarly,

$$\mathbb{P}(Q > r) = \exp(-\lambda\omega_d G(r)). \tag{6.33}$$

Fix $z \in (0, \lambda\omega_d)$. Note that F and G are strictly increasing on $[0,1]$, and hence invertible. Thus we can write

$$\mathbb{P}(\lambda\omega_d F(R) > z) = \mathbb{P}(R > F^{-1}(z/\lambda\omega_d)) \tag{6.34}$$

$$= \exp(-\lambda\omega_d F(F^{-1}(z/\lambda\omega_d))) \tag{6.35}$$

$$= \exp(-z), \tag{6.36}$$

and similarly for $G(Q)$. Taking $\lambda \to \infty$ finishes the proof. □

Corollary 6.3. *The exact distributions of $\lambda\omega_d F(R)$ and $\lambda\omega_d G(Q)$ are given by*

$$\mathbb{P}(\lambda\omega_d F(R) > z) = \mathbb{P}(\lambda\omega_d G(Q) > z) = \begin{cases} e^{-z}, & 0 \le z \le \lambda\omega_d \\ 0, & z > \lambda\omega_d. \end{cases} \tag{6.37}$$

The collections $\{\lambda F(R)\}_\lambda$ *and* $\{\lambda G(Q)\}_\lambda$ *are uniformly integrable.*

Proposition 6.2 leads to a quick calculation for the expected area of I^λ and K^λ via the following proposition, which we state for general random sets. For a continuous function $f : \mathbb{S} \to [0, 1]$, let

$$U(f) = \{r\theta : r \in [0, f(\theta)], \theta \in \mathbb{S}\} \tag{6.38}$$

be the set with 'radius' $f(\theta)$ in the direction θ. Note that by definition, $I^\lambda = U(R^\lambda)$ and $K^\lambda = U(Q^\lambda)$, where R^λ and Q^λ are viewed as random functions on $\mathbb{S}$ as in (6.6). In general, if $A \subset \mathbb{R}^d$ is star-shaped, then the function $f_A : \mathbb{S} \to [0, 1]$ given by

$$f_A(\theta) = \sup\{t \in (0, 1) : t\theta \in A\} \tag{6.39}$$

satisfies $A = U(f_A)$.

A random closed set X is *rotationally invariant* if for any $\Phi \in \mathrm{SO}(d)$, X has the same distribution as $\Phi(X) = \{\Phi(x) : x \in X\}$.

Proposition 6.4. *Let* X *be any random closed set contained in* $\mathbb{B}$ *that is almost surely star-shaped and rotationally invariant. Let* $S : \mathbb{S} \to [0, 1]$ *be the random function, defined on the same probability space as* X*, satisfying* $X = U(S)$*. Then*

$$\mathbb{E}|X| = \omega_d \mathbb{E}\left[S(\vec{e_1})^d\right]. \tag{6.40}$$

Proof. The volume of any closed, star-shaped set A with $A = U(f)$, for a continuous function $f : \mathbb{S} \to [0, 1]$, is given by

$$|A| = \frac{1}{d} \int_{\mathbb{S}} f(\theta)^d \, d\sigma(\theta). \tag{6.41}$$

See Appendix 11.2 for a proof. Since X is rotationally invariant, $\mathbb{E}\left[S(\theta)^d\right]$ does not depend on θ. Thus,

$$\mathbb{E}|X| = \mathbb{E}\left[\frac{1}{d}\int_{\mathbb{S}} S(\theta)^d \, d\sigma(\theta)\right] \tag{6.42}$$

$$= \frac{1}{d}\int_{\mathbb{S}} \mathbb{E}\left[S(\theta)^d\right] \, d\sigma(\theta) \tag{6.43}$$

$$= \frac{1}{d}\int_{\mathbb{S}} \mathbb{E}\left[S(\vec{e_1})^d\right] \, d\sigma(\theta) \tag{6.44}$$

$$= \frac{1}{d}\mathbb{E}\left[S(\vec{e_1})^d\right] \int_{\mathbb{S}} 1 \, d\sigma(\theta) \tag{6.45}$$

$$= \omega_d \mathbb{E}\left[S(\vec{e_1})^d\right]. \tag{6.46}$$

Since $X \subset \mathbb{B}$, the expression inside the expectation is almost surely bounded by ω_d, and hence the interchange of limit and expectation is valid by the dominated convergence theorem. □

Applying this proposition to I^λ and K^λ gives:

Corollary 6.5. *For any $d \geq 2$ and $\lambda > 0$,*

$$\mathbb{E}\left|I^\lambda\right| = \omega_d \mathbb{E}(R^\lambda)^d, \quad \mathbb{E}\left|K^\lambda\right| = \omega_d \mathbb{E}(Q^\lambda)^d. \tag{6.47}$$

We are now ready to compute $\mathbb{E}|I^\lambda|$.

Proposition 6.6. $\lim_{\lambda\to\infty} \lambda^d \mathbb{E}|I^\lambda| = \lim_{\lambda\to\infty} \lambda^d \mathbb{E}|K^\lambda| = \frac{d!\omega_d}{\omega_{d-1}^d}$.

Proof. Here we carry out the details only for I; the analysis for K is similar. Since $R^\lambda \to 0$ almost surely as $\lambda \to \infty$, $F(R)$ is approximately equal to its linear term for λ large. It will suffice to show that, for any $c > 0$,

$$|F(R^\lambda) - \frac{\omega_{d-1}}{\omega_d} R^\lambda| < c\lambda^{-1} \text{ a.s. for } \lambda \text{ sufficiently large.} \tag{6.48}$$

Assuming (6.48) holds, (and since almost sure convergence implies convergence in distribution), Proposition 6.2 gives us that

$$\lambda\omega_d \frac{\omega_{d-1}}{\omega_d} R^\lambda \to_d \text{Exp}(1) \text{ as } \lambda \to \infty. \tag{6.49}$$

By Corollary 6.3, the collection $\{\lambda F(R^\lambda)\}_{\lambda>0}$ is uniformly integrable. By taking expectations in (6.48), we have that

$$\mathbb{E}\left|\lambda F(R^\lambda) - \frac{\omega_{d-1}}{\omega_d}\cdot \lambda R^\lambda\right| \to 0 \text{ a.s. as } \lambda \to \infty. \tag{6.50}$$

It follows that the collection $\{\lambda R^\lambda\}_{\lambda>0}$ is also uniformly integrable. Together, convergence in distribution and uniform integrability imply convergence of moments (see Theorem 25.12 of [3], for example). Thus, as $\lambda \to \infty$,

$$\lambda^d \mathbb{E}(R^\lambda)^d \to \left(\omega_d \cdot \frac{\omega_{d-1}}{\omega_d}\right)^{-d} \mathbb{E}[\mathrm{Exp}(1)^d] = \frac{d!}{\omega_{d-1}^d}. \tag{6.51}$$

Combining this with Proposition 6.4 yields the result. So it remains to prove (6.48). It is enough to show that, for any $c' > 0$,

$$R^\lambda < c'\lambda^{-1/2} \text{ a.s. for } \lambda \text{ sufficiently large,} \tag{6.52}$$

since by Proposition 6.1 this implies that for some constant $C > 0$,

$$|F(R^\lambda) - c_d R^\lambda| \le C(R^\lambda)^3 < C\cdot(c')^3\lambda^{-3/2} \text{ a.s. for } \lambda \text{ sufficiently large.} \tag{6.53}$$

By Proposition 6.2 and the definition of F,

$$\begin{aligned}
\mathbb{P}(R^\lambda > c'\lambda^{-1/2}) &= \mathbb{P}(c'\lambda^{-1/2}\vec{e}_1 \in I^\lambda) && (6.54)\\
&= \exp(-\lambda\omega_d F(c'\lambda^{-1/2})) && (6.55)\\
&\le \exp\left(-\lambda\omega_d(c_d c'\lambda^{-1/2} - O(\lambda^{-3/2}))\right) && (6.56)\\
&= \exp(-O(\sqrt{\lambda})). && (6.57)
\end{aligned}$$

To finish, we will apply the Borel Cantelli lemma to the process $\lambda^{1/2}R^\lambda$. To that end, for $n \in \mathbb{N}$, let A_n denote the event

$$A_n = \{\lambda^{1/2}R^\lambda \ge c' \text{ for some } \lambda \in [n, n+1)\}. \tag{6.58}$$

We may assume that the underlying point sets $\{\mathcal{C}_\lambda\}_{\lambda>0}$ are nested, i.e. $\mathcal{C}_\lambda \subset \mathcal{C}_{\lambda'}$ if $\lambda < \lambda'$, so that

$$N_\lambda = |\mathcal{C}_\lambda| \tag{6.59}$$

is a Poisson waiting-time process of intensity ω_d on $\mathbb{R}^+$. Let B_n denote the event

$$B_n = \{N_\lambda = N_{\lambda'} \text{ for all } \lambda, \lambda' \in [n, n+1), |\lambda - \lambda'| < n^{-2}\}. \tag{6.60}$$

For any $z, \delta > 0$, the bound $e^{-\delta} \geq 1 - \delta$ implies

$$\mathbb{P}(N_{z+\delta} - N_z \geq 2) = \mathbb{P}(\mathrm{Poi}(\omega_d \delta) \geq 2) \leq 1 - (1 - \omega_d \delta)(1 + \omega_d \delta) = \omega_d^2 \delta^2. \tag{6.61}$$

Taking $\delta = n^{-2}$, a union bound over the intervals $[n + jn^{-2}, n + (j+1)n^{-2}], j = 0, 1, \ldots, n^2 - 1$ gives

$$\mathbb{P}(B_n^c) \leq n^2 \cdot \omega_d^2 n^{-4} = \omega_d^2 n^{-2}. \tag{6.62}$$

On the event B_n, A_n does not occur if and only if $\lambda^{1/2} R^\lambda < c'$ at each of the points $\lambda = n + jn^{-2}$, $j = 0, 1, \ldots, n^2 - 1$. Thus

$$\mathbb{P}(A_n) \leq \mathbb{P}(B_n^c) + \mathbb{P}(A_n \cap B_n) \leq \frac{\omega_d^2}{2} n^{-2} + n^2 \exp(-O(\sqrt{n})). \tag{6.63}$$

Note that these probabilities are summable over n. By the Borel Cantelli lemma, A_n occurs finitely often almost surely, proving 6.52.

□

6.2. **Formulas for general intensity measures.** We now give a generalization of these ideas for a wider class of intersection models, where the underlying Poisson process has arbitrary intensity measure, and the sets comprising the intersection are arbitrary. There are many possible ways to generalize this model: we chose a way that yields examples with the same flavor as I^λ and K^λ, but with potentially different asymptotic behavior.

Consider a general Poisson point process $\mathcal{C}_{\mu,\lambda}$ on $\mathbb{B} \cong [0,1] \times \mathbb{S}$ with intensity measure $\lambda(\mu \times \sigma)$, where $\lambda > 0$, σ is surface-area measure on $\mathbb{S}$, and μ is a probability measure on $[0,1]$. For each $x \in \mathbb{B}, x \neq 0$, let $\mathrm{SO}_x(d)$ denote the subgroup of $\mathrm{SO}(d)$ given by

$$\mathrm{SO}_x(d) = \left\{ \Phi \in \mathrm{SO}(d) : \Phi(\vec{e_1}) = \frac{x}{\|x\|} \right\}. \tag{6.64}$$

Let $A \subset \mathbb{R}^d$ be a fixed closed set such that for any $x \in \mathbb{B} \setminus \{0\}$, and $\Phi \in \mathrm{SO}_x(d)$,

$$0 \in \Phi(A) + x. \tag{6.65}$$

This assumption ensures that the intersection model is non-empty almost surely for every $\lambda > 0$.

Note that $\mathrm{SO}_x(d)$ is a compact group for each fixed x, and hence it has a unique Haar probability measure κ_x. For each $C \in \mathcal{C}_{\mu,\lambda}$, sample a random element $\Phi_C \in \mathrm{SO}_C(d)$ from κ_C. The generalized intersection model $I_A^{\mu,\lambda}$ is:

$$I_A^{\mu,\lambda} = \mathbb{B} \cap \left(\bigcap_{C \in \mathcal{C}_{\mu,\lambda}} \Phi_C(A) + C \right), \tag{6.66}$$

In words, $\Phi_C(A)$ is a copy of A that we give a random spin and pin at a random point; and $I_A^{\mu,\lambda}$ is the intersection of a Poisson number of such independent copies. Clearly $I_A^{\mu,\lambda}$ is rotationally invariant in distribution, and if 0 lies on the boundary of A, then the intersection shrinks to the origin in Hausdorff distance almost surely as $\lambda \to \infty$.

Let ρ and $\widehat{\nu}$ denote the probability measures $\rho(0,r) = r^d$ and $\widehat{\nu}(0,r) = 1 - (1-r)^d$ for $r \in (0,1)$. The boolean intersection models I^λ and K^λ are special cases of the general intersection model with respect to these measures, i.e.,

$$I^\lambda = I_{\mathbb{B}}^{\rho,\lambda}, \quad K^\lambda = I_{\mathbb{H}}^{\widehat{\nu},\lambda}, \tag{6.67}$$

where $\mathbb{H} = \{x \in \mathbb{R}^d : x \cdot \vec{e_1} < 0\}$. Define the auxiliary function F_A^μ analogous to F in (6.7): let $A^\mu = \Phi_C(A) + C$ be one of the randomly rotated and shifted copies of A comprising the intersection model $I_A^{\mu,\lambda}$ where C is drawn from the probability measure $\frac{1}{d\omega_d}\mu \times \sigma$, and let

$$F_A^\mu(r) = \mathbb{P}(r\vec{e}_1 \notin A^\mu). \tag{6.68}$$

There is a simple generic formula in terms of F_A^μ for the expected volume of the intersection.

Fact 6.7. *For any $\lambda > 0$,*

$$\mathbb{E}\left|I_A^{\mu,\lambda}\right| = d\omega_d \int_0^1 r^{d-1} \exp(-\lambda \omega_d F_A^\mu(r))\, dr. \tag{6.69}$$

The proof of Fact 6.7 is a straightforward consequence of a well known formula for the volume of a random set (see for example [26]).

Proof. Write $I = I_A^{\mu,\lambda}$. By Tonelli's theorem,

$$\mathbb{E}|I| = \mathbb{E}\int_{\mathbb{B}} 1\{x \in I\}\, dx \tag{6.70}$$

$$= \int_{\mathbb{B}} \mathbb{P}(x \in I)\, dx \tag{6.71}$$

$$= \int_{\mathbb{B}} \exp(-\lambda\omega_d F_A^{\mu}(||x||))\, dx \tag{6.72}$$

$$= \int_0^1 \int_{\mathbb{S}} \exp(-\lambda\omega_d F_A^{\mu}(r)) r^{d-1}\, dr\, d\sigma(\theta) \tag{6.73}$$

$$= d\omega_d \int_0^1 r^{d-1} \exp(-\lambda\omega_d F_A^{\mu}(r))\, dr, \tag{6.74}$$

as desired. □

For example, in dimension 2, using the exact equality (6.28) and Fact 6.7 gives the exact formula

$$\mathbb{E}|I^{\lambda}| = 2\pi \int_0^1 r \exp\left(-\lambda + \frac{\lambda}{\pi}\left(2\arccos\left(\frac{r}{2}\right) - r\sqrt{1-\frac{r^2}{4}}\right)\right) dr. \tag{6.75}$$

Unfortunately, this integral doesn't admit a simple asymptotic expansion in λ. The methods of Proposition 6.4, on the other hand, do allow an easy and explicit calculation.

Continuing with the ideas of the previous section, define the radius of the intersection as in (6.6):

$$R_A^{\mu,\lambda} = \sup\{t \in (0,1) : t\theta \in I^{\mu,\lambda}\}. \tag{6.76}$$

The analog of Proposition 6.2 holds in general:

Proposition 6.8. *Let μ be any probability measure on $[0,1]$. As $\lambda \to \infty$,*

$$\lambda\omega_d \cdot F_A^{\mu}(R_A^{\mu,\lambda}) \to_d \mathrm{Exp}(1). \tag{6.77}$$

The proof is identical to that of Proposition 6.2. Combining Propositions 6.4 and 6.8 and mimicking the ideas of Proposition 6.6 gives a general program to compute the asymptotic scaling of the volume of $I_A^{\mu,\lambda}$. Below are three examples of intersection models that can be analyzed using this program. **Example 1** Consider $I_{\mathbb{H}}^{\rho,\lambda}$ in dimension $d = 2$, i.e., the hyperplane intersection model K^{λ}, but where the underlying Poisson point process is uniform. In this case,

$$F_{\mathbb{H}}^{\rho}(r) = \int_0^{\pi/2} r^2 \cos^2\theta\, d\theta = \frac{\pi r^2}{4}. \tag{6.78}$$

By Proposition 6.8,

$$\frac{\pi^2}{4}\lambda \cdot (R_{\mathbb{H}}^{\rho,\lambda})^2 \to \text{Exp}(1). \tag{6.79}$$

Thus, by Proposition 6.4,

$$\lambda \mathbb{E}|I_{\mathbb{H}}^{\rho,\lambda}| = \pi\lambda \mathbb{E}(Q_{\mathbb{H}}^{\rho,\lambda})^2 \to \pi \cdot \frac{4}{\pi^2} = \frac{4}{\pi}. \tag{6.80}$$

Note the difference in scale: $R_{\mathbb{H}}^{\rho,\lambda}$ is roughly $\lambda^{-1/2}$, while $Q^{\lambda} = R_{\mathbb{H}}^{\widehat{\nu},\lambda}$ is roughly λ^{-1}. This limit scaling reflects the behavior of the densities of ρ and $\widehat{\nu}$ near 0.

Example 2 Fix $\beta \in (0, \pi)$, and define the cone set

$$\text{Cone}(\vec{e_1}, \beta) = \left\{ x \in \mathbb{R}^d : \arccos\left(\frac{\langle x, \vec{e_1}\rangle}{\|x\|}\right) < \beta \right\}. \tag{6.81}$$

In dimension $d = 2$, one can show that

$$F^{\rho}_{\text{Cone}(\vec{e_1},\beta)}(r) \approx C(\beta) r \text{ as } r \to 0 \tag{6.82}$$

for some constant $C(\beta)$, and thus Propositions 6.8 and 6.4 suggest

$$\mathbb{E}|I^{\rho,\lambda}_{\text{Cone}(\vec{e_1},\beta)}| \approx \frac{2}{\pi C(\beta)^2}\lambda^{-2}. \tag{6.83}$$

Unlike the ball and hyperplane models, however, the cone model does not have the Crofton cell D_0^1 as a scaling limit – see Section 10 for further discussion.

Example 3 Consider the L^1 ball in dimension d, scaled by a factor of $\sqrt{d}$:

$$\sqrt{d}B_1^d = \{(x^1, x^2, \ldots, x^d) \in \mathbb{R}^d : |x^1| + \cdots + |x^d| = \sqrt{d}\}. \tag{6.84}$$

This scaling ensures that $0 \in \Phi_x(\sqrt{d}B_1^d) + x$ for any $x \in \mathbb{B}$, and that the intersection model $I^{\mu,\lambda}_{\sqrt{d}B_1^d}$ almost surely converges to 0 as $\lambda \to \infty$.

7. Some geometric and probabilistic lemmas

In this section, we state some basic lemmas needed to prove Theorem 4.2 via the coupling outlined in Section 5. We begin with some notation. For any $\theta \in \mathbb{S}$, let $\text{Cone}(\theta, \delta)$ denote the cone set

$$\text{Cone}(\theta, \delta) = \left\{ x \in \mathbb{R}^d : \arccos\left(\frac{\langle x, \theta\rangle}{\|x\|}\right) < \delta \right\}. \tag{7.1}$$

Consider the spherical and planar 'caps'

$$\mathrm{Cap}(\theta, \delta) = \mathrm{Cone}(\theta, \delta) \cap \partial\mathbb{B} \tag{7.2}$$

and

$$\mathrm{Hyp}(\theta, \delta) = \mathrm{Cone}(\theta, \delta) \cap \{x : x \cdot \theta = 1\}. \tag{7.3}$$

Write d_H for Hausdorff distance, defined by

$$d_H(X, Y) = \max\left\{\sup_{x\in X}\inf_{y\in Y}||x-y||, \sup_{y\in Y}\inf_{x\in X}||x-y||\right\}. \tag{7.4}$$

Our first fact is a simple consequence of the convexity of the unit ball $\mathbb{B}$.

Fact 7.1. *For δ sufficiently small,*

$$d_H(\mathrm{Cap}(\theta, \delta), \mathrm{Hyp}(\theta, \delta)) = 1 - \cos\delta \leq \delta^2. \tag{7.5}$$

Write $\mathrm{Sh}^-(\varepsilon)$ for the (inner) spherical shell

$$\mathrm{Sh}^-(\varepsilon) = \{x \in \mathbb{R}^d : ||x|| \in (1-\varepsilon, 1)\}. \tag{7.6}$$

Similarly, write $\mathrm{Sh}^+(\varepsilon)$ for the outer spherical shell

$$\mathrm{Sh}^-(\varepsilon) = \{x \in \mathbb{R}^d : ||x|| \in (1, 1+\varepsilon)\}, \tag{7.7}$$

and set $\mathrm{Sh}(\varepsilon) = \mathrm{Sh}^-(\varepsilon) \cup \partial\mathbb{B} \cup \mathrm{Sh}^+(\varepsilon)$.

Fact 7.2. *For any $\varepsilon > 0$, there is a partition of $\mathrm{Sh}^-(\varepsilon)$ into $K = K(d)$ sets $A_i = A_i(\varepsilon)$, $i = 1, \ldots, K$, such that for any K points $x_i \in A_i$, $i = 1, \ldots, K$, the component of the origin in the Boolean tessellation generated by copies of $\partial\mathbb{B}$ centered at the points x_i is contained in $\mathbb{B}_{2\varepsilon} = \{x : ||x|| < 2\varepsilon\}$, where K does not depend on ε.*

For instance, when $d = 2$, we may take $K(2) = 6$, and make the A_i consecutive thickened arcs of length $\pi/3$. To see this, assume for simplicity that all the points x_i lie on the inner boundary of $\mathrm{Sh}^-(\varepsilon)$, i.e., that $||x_i|| = 1 - \varepsilon$. Then, with $K(2) = 6$, the angle between two consecutive x_i, x_j is at most $2\pi/3$, so that the circles $C_i = x_i + \partial\mathbb{B}$ and $C_j = x_j + \partial\mathbb{B}$ are both tangent to $C_\varepsilon = \partial\mathbb{B}_\varepsilon = \{x : ||x|| = \varepsilon\}$ at points p_i, p_j on C_ε separated by an angle of less than $2\pi/3$. Replacing C_i, C_j by lines l_i, l_j tangent to C_ε at p_i, p_j, we see that l_i and l_j make an angle of at least $\pi/3$

enclosing C_ε, so that their intersection lies in $\mathbb{B}_{2\varepsilon}$; the same applies to the intersection of C_i and C_j.

In higher dimensions, a similar argument applies. Once again, we may assume that the points x_i all satisfy $||x_i|| = 1-\varepsilon$. The A_i will be thickened cap-like sets partitioning $\mathrm{Sh}^-(\varepsilon)$ in such a way that the angle x_iOx_i' formed by two points $x_i, x_i' \in A_i$ and the origin O is small. Consequently, the corresponding angle formed by points x_i, x_j in adjacent caps A_i, A_j is also small. The spheres $S_i = x_i + \partial\mathbb{B}$ and $S_j = x_j + \partial\mathbb{B}$ are tangent to $S_\varepsilon = \partial\mathbb{B}_\varepsilon = \{x : ||x|| = \varepsilon\}$ at points p_i, p_j as before; we replace S_i, S_j by hyperplanes Π_i, Π_j, tangent to S_ε at p_i, p_j, whose unit normal vectors n_i, n_j are such that $n_i \cdot n_j$ is small. This applies to points in every pair of adjacent caps A_i, A_j, so that the vertices of the polytope formed from the hyperplanes Π_i all lie inside $\mathbb{B}_{2\varepsilon}$.

Upper bounds on $K(d)$ can be obtained from classical results on covering the surface of a high-dimensional unit ball with small spherical caps; see, for instance, Theorem 6.3.1 of [4].

We will also need three standard statistical estimates: one regarding the coupon collector process, and two related to Poisson random variables. The 'coupon collector' refers to the following discrete time process. Given a finite collection of coupons, say $\{1, 2, \ldots, K\} = [K]$, we generate an iid sequence $(X_t)_{t\leq T}$ of $[K]$-valued random variables from any discrete distribution (not necessarily uniform). The process concludes at the stopping time T when every coupon has been collected at least once:

$$T = \inf\{t \in \mathbb{N} : [K] \subset \{X_1, X_2, \ldots, X_t\}\}. \tag{7.8}$$

Fact 7.3. *Consider any coupon collector process on K coupons, for $K = K(d)$ as in Fact 7.2. Let T denote the time it takes to collect all K coupons, and let a_* denote the minimum probability of selecting any of the coupons. Then for any $\lambda > 0$,*

$$\mathbb{P}(T > \log\lambda) < K\lambda^{\log(1-a_*)}. \tag{7.9}$$

Note that, since the sets A_i appearing in Fact 7.2 do not necessarily have equal volume, the coupon collector process considered in Fact 7.3 is not necessarily uniform. In any case, we can construct the A_i so that $a_* > 0$, and thus the probability in (7.9) goes to 0 as $\lambda \to \infty$.

Proof of Fact 7.3. Let $a_1, a_2, \ldots, a_K$ denote the probabilities of selecting the K coupons respectively, and

$$a_* = \min\{a_1, a_2, \ldots, a_K\}. \tag{7.10}$$

Let $V_i(t)$ denote the indicator random variable of the event that coupon i has not been collected by time t, i.e.,

$$V_i(t) = \{i \notin \{X_1, X_2, \ldots, X_t\}\}. \tag{7.11}$$

Note that

$$\mathbb{E}V_i(t) = (1 - a_i)^t. \tag{7.12}$$

By Markov's inequality,

$$\mathbb{P}(T > t) = \mathbb{P}\left(\sum_{i=1}^{K} V_i(t) \geq 1\right) \leq \sum_{i=1}^{K} \mathbb{E}V_i(t) = \sum_{i=1}^{K} (1 - a_i)^t \leq K(1 - a_*)^t.$$

Setting $t = \log \lambda$ yields the result.

□

Proposition 7.4. *Fix any $\mu, \delta > 0$, and let $N \sim \mathrm{Poi}(\mu)$, $N' \sim \mathrm{Poi}(\mu + \delta)$. Then*

$$\mathrm{TV}(N, N') \leq \delta, \tag{7.13}$$

where TV *denotes total variation distance between probability distributions.*

See for instance [1].

Fact 7.5. *Let $Y \sim \mathrm{Poi}(V_\varepsilon \lambda)$, where V_ε is the volume of $\mathrm{Sh}(\varepsilon_\lambda)$, and $\varepsilon_\lambda = \lambda^{-1} \log^2 \lambda$. Then*

$$\mathbb{P}(Y < \log \lambda) < \lambda^{-1}, \tag{7.14}$$

for sufficiently large λ.

See [9], for example.

8. Coupling the intersection and tessellation models

The goal of this section is to prove our main convergence result, Theorem 4.2. We carry out the argument for the intersection model with balls, by coupling it to the tessellation model with

spheres. Under this coupling, the Hausdorff distance between the two models tends to 0 as $\lambda \to \infty$, even after re-scaling both sets by λ.

The coupling works as follows. Let $\mathcal{X} = \mathcal{X}_\lambda$ be a Poisson point process in $\mathbb{R}^d$ of intensity $\frac{\lambda}{2}$, and consider the set

$$\bigcup_{x \in \mathcal{X}} (x + \partial\mathbb{B}). \tag{8.1}$$

Let J^λ be the connected component of the origin in the resulting tessellation. Also, let I^λ denote the ball intersection model on $\mathbb{B}$, that is,

$$I^\lambda = \bigcap_{C \in \mathcal{C}_\lambda} (C + \mathbb{B}), \tag{8.2}$$

where $\mathcal{C}_\lambda$ is a Poisson point process on $\mathbb{B}$ of intensity λ. The reason that I comes from a point process of intensity twice that of J is that only points inside $\mathbb{B}$ contribute to I, while points both inside and outside $\mathbb{B}$ will contribute to the shape of J. Recalling notation from the previous section, define

$$\mathcal{X}^\varepsilon = \mathcal{X} \cap \mathrm{Sh}(\varepsilon), \tag{8.3}$$

and consider the 'restricted' model J^λ_ε, the connected component of the origin in the tessellation induced by

$$\bigcup_{x \in \mathcal{X}^\varepsilon} (x + \partial\mathbb{B}). \tag{8.4}$$

Also, let $\mathcal{C}^\varepsilon_\lambda = C_\lambda \cap \mathrm{Sh}(\varepsilon) = C_\lambda \cap \mathrm{Sh}^-(\varepsilon) = \{C \in \mathcal{C}_\lambda : ||C|| \in (1-\varepsilon, 1)\}$, and define

$$I^\lambda_\varepsilon = \bigcap_{C \in \mathcal{C}^\varepsilon_\lambda} (C_i + \mathbb{B}). \tag{8.5}$$

For ε chosen appropriately, the restricted models are not far from the original models. Precisely:

Proposition 8.1. *Set $\varepsilon = \varepsilon_\lambda = \frac{\log^2 \lambda}{\lambda}$. As $\lambda \to \infty$,*

$$\mathbb{P}(J^\lambda_{2\varepsilon} = J^\lambda) \to 1 \text{ and } \mathbb{P}(I^\lambda_{2\varepsilon} = I^\lambda) \to 1. \tag{8.6}$$

Moreover, on the event $J^\lambda_{2\varepsilon} = J^\lambda$, we have that $J^\lambda \subset \mathbb{B}_{2\varepsilon}$; and when $I^\lambda_{2\varepsilon} = I^\lambda$, $I^\lambda \subset \mathbb{B}_{2\varepsilon}$.

This is essentially the statement that only points near $\partial\mathbb{B}$ contribute to the component of the origin.

Proof. We will prove the assertion for J^λ; the proof for I^λ is similar. The main ingredients are Fact 7.2 and Fact 7.3. Fix any $\lambda > 0$, and let $\{A_i(\varepsilon_\lambda)\}_{i=1}^K$ denote the sets given by Fact 7.2. Consider the stopping time

$$\lambda^{\text{cov}} = \min\{\eta : \mathcal{X}_\eta \cap A_i(\varepsilon_\lambda) \neq \emptyset, \text{ for } i = 1, 2, \ldots, K\}. \tag{8.7}$$

We regard the Poisson point processes $\mathcal{X} = \mathcal{X}_\eta$ as nested, i.e., they are coupled so as to form a non-decreasing sequence of sets as η increases. This makes λ^{cov} is a well-defined stopping time.

Fix $\eta > \lambda^{\text{cov}}$. By Fact 7.2, $J^\eta \subset \mathbb{B}_{2\varepsilon_\lambda}$. It follows that any point $y \in \mathcal{X}_\eta \cap \text{Sh}(2\varepsilon_\lambda)^c$ does not contribute to J^η, i.e., $y + \partial\mathbb{B}$ does not lie on the boundary of J^η. Thus $J^\eta_{2\varepsilon_\lambda} = J^\eta$ in this case.

To finish the proof, it suffices to show that

$$\mathbb{P}(\lambda^{\text{cov}} < \lambda) \to 1 \text{ as } \lambda \to \infty. \tag{8.8}$$

For the above event to occur, the point process $\mathcal{X}_\lambda$ must have at least one point in each set $A_i(\varepsilon_\lambda)$. It is enough to have $\log \lambda$ points of $\mathcal{X}_\lambda$ in $\mathcal{X}^\varepsilon_\lambda$ – then by Fact 7.3, each A_i will have at least one point with high probability. The number of such points is Poisson with mean $V_\varepsilon \cdot \lambda$. By Fact 7.5 and a union bound,

$$\mathbb{P}(\lambda^{\text{cov}} \geq \lambda) \leq K\lambda^{\log(1-a_*)} + \lambda^{-1} \to 0 \text{ as } \lambda \to \infty. \tag{8.9}$$

□

Additionally, the two restricted models are close to each other.

Proposition 8.2. *As $\lambda \to \infty$, with $\varepsilon = \varepsilon_\lambda/2 = \frac{\log^2 \lambda}{2\lambda}$ as in Proposition 8.1,*

$$\mathbb{P}(d_H(\lambda I^\lambda_\varepsilon, \lambda J^\lambda_\varepsilon) \leq C\lambda\varepsilon^2) \to 1, \tag{8.10}$$

for some global constant $C > 0$.

Proof. We will give an explicit coupling of the intersection and tessellation models on the same probability space where the two models agree with high probability. The coupling works as follows. We will build the intersection model from the Poisson point process $\mathcal{X}$: so the random sets J^λ and J^λ_ε are defined above (see (8.4)). Fix any $\lambda > 0$, and partition $\mathcal{X}^\varepsilon = \mathcal{X}^\varepsilon_\lambda$ into two sets

$$\mathcal{X}^\varepsilon = \{x \in \mathcal{X}^\varepsilon : ||x|| > 1\} \cup \{x \in \mathcal{X}^\varepsilon : ||x|| < 1\} := \mathcal{X}^{\varepsilon,+} \cup \mathcal{X}^{\varepsilon,-}. \tag{8.11}$$

Enumerate these sets as

$$\mathcal{X}^{\varepsilon,+} = \{X_1, X_2, \ldots, X_{N'}\}, \mathcal{X}^{\varepsilon,-} = \{X_{N'+1}, \ldots, X_N\}. \tag{8.12}$$

Write $X_i = S_i\Theta_i$ for $i = 1, 2, \ldots, N'$, where $S_i \in [0,1]$ and $\Theta_i \in \mathbb{S}$, and set

$$C_i' = (S_i - 2)\Theta_i \text{ for } i = 1, 2, \ldots, N', \tag{8.13}$$

while $C_i' = X_i$ for $i = N'+1, \ldots, N$. Generate further points $C_i', i = N+1, \ldots, Z$ from a Poisson process of intensity λ in $\{x \in \mathbb{B} : ||x|| < 1 - \varepsilon\}$. Then we set

$$(I^\lambda)' = \bigcap_{i=1}^{Z}(C_i' + \mathbb{B}) \text{ and } (I_\varepsilon^\lambda)' = \bigcap_{i=1}^{N}(C_i' + \mathbb{B}). \tag{8.14}$$

Note that the set $(I_\varepsilon^\lambda)'$ doesn't have exactly the same distribution as I_ε^λ: because $\mathrm{Sh}^+(\varepsilon)$ has more volume than $\mathrm{Sh}^-(\varepsilon)$, $(I_\varepsilon^\lambda)'$ has slightly more points than I_ε^λ. Also, since the shift map $s\theta \to (s-2)\theta$ is not an isometry, those points are no longer uniformly distributed over the inner shell. It remains to show that error between these two point processes is small. The two distributions in question can be described as follows:

(1) I_ε^λ is formed by sampling a Poisson variable N with mean $\mu = \lambda\omega_d(1 - (1-\varepsilon)^d)$, and placing N points on $\mathrm{Sh}^-(\varepsilon)$ with iid uniform angles in $\mathbb{S}$ and iid radii R distributed as

$$\mathbb{P}(R = 1 - w) = h(w) = (d+1)\frac{(1-w)^d}{1-(1-\varepsilon)^d}, w \in (0, \varepsilon). \tag{8.15}$$

(2) $(I_\varepsilon^\lambda)'$ is formed by sampling a Poisson variable N' with mean $\mu' = \lambda\omega_d((1+\varepsilon)^d - 1)$, and placing N' points on $\mathrm{Sh}^+(\varepsilon)$ with iid uniform angles in $\mathbb{S}$ and iid radii R' distributed as

$$\mathbb{P}(R' = 1 - w) = h'(w) = (d+1)\frac{(1+w)^d}{(1+\varepsilon)^d - 1}, w \in (0, \varepsilon). \tag{8.16}$$

The difference between the means is

$$\mu' - \mu = \lambda\omega_d((1+\varepsilon)^d + (1-\varepsilon)^d - 2) = \lambda\omega_d d(d-1)\varepsilon^2 + O(\varepsilon^3). \tag{8.17}$$

By Proposition 7.4, $\mathrm{TV}(N, N') \leq c\lambda\varepsilon^2$ for some $c > 0$. To couple the points of I_ε^λ and $(I_\varepsilon^\lambda)'$, first note that the random angles can be coupled directly, so it suffices to couple the radii. We rely on an idea from optimal transport, namely the optimal coupling for the Wasserstein-1 distance,

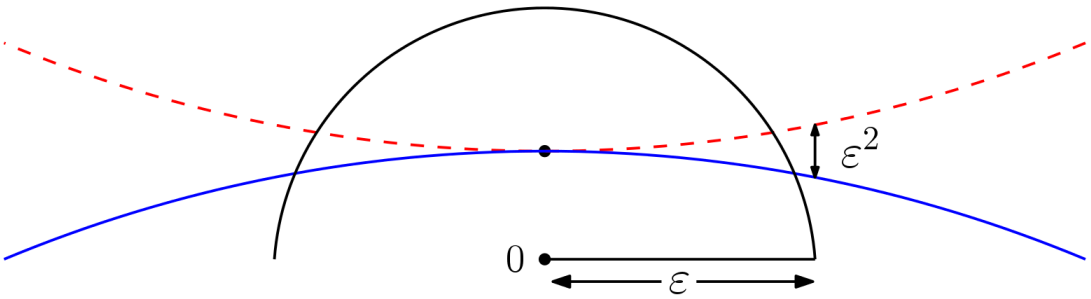

FIGURE 5. On the event that the intersection model is contained in $\mathbb{B}_\varepsilon$, the difference between $(I^\lambda)'$ and J^λ is that some of the copies of $\mathbb{B}$ in the former comprise a concave piece of the boundary (red/dashed), while those in the latter form a convex boundary piece (blue/solid). The difference is small in Hausdorff distance, because the boundary of the ball is differentiable.

rather than total variation. Let H and H' denote the CDFs of R and R', respectively. The optimal coupling with respect to the L^1 distance is given by the transport map $H' \circ H^{-1}$: that is, given R, the random variable $H'(H^{-1}(R))$ on the same probability space is distributed as R', and the minimum expected L^1 distance between R and R' is minimized for this coupling; see for instance Section 2.1 of [27]. A straightforward computation shows that for $u \in (0, \varepsilon)$,

$$u - H' \circ H^{-1}(u) = \frac{d(d-1)\varepsilon}{d + O(\varepsilon)} u + O(\varepsilon^3). \tag{8.18}$$

Since $u - H' \circ H^{-1}(u) = O(\varepsilon^2) \ll \lambda^{-3/2}$ for $u \in (0, \varepsilon)$, for λ sufficiently large there exists a coupling between R and R' such that

$$|R - R'| \leq \lambda^{-3/2} \text{ a.s. as } \lambda \to \infty. \tag{8.19}$$

Thus, we see that I_ε^λ and $(I_\varepsilon^\lambda)'$ can be coupled so that

$$\mathbb{P}(d_H(\lambda I_\varepsilon^\lambda, \lambda (I_\varepsilon^\lambda)') > \lambda^{-1/2}) < c\lambda\varepsilon^2 \to 0 \text{ as } \lambda \to \infty. \tag{8.20}$$

By Proposition 8.1, $(I_\varepsilon^\lambda)' = I^\lambda$ and $J_\varepsilon^\lambda = J^\lambda$ with high probability. The difference between $(I_\varepsilon^\lambda)'$ and J_ε^λ is that the boundary of J_ε^λ may be concave, on the boundary of $X_i + \mathbb{B}$ for $1 \leq i \leq N'$, while the corresponding parts of the boundary of $(I_\varepsilon^\lambda)'$, i.e., points on the boundary of $C_i' + \mathbb{B}$ for $1 \leq i \leq N'$, are convex. Note that these two sets meet at the point $(R_i - 1)\theta_i$, and on the event

$J_\varepsilon^\lambda = J^\lambda$, $R_i - 1 \in (0, \varepsilon)$. Applying Fact 7.1 twice – comparing both the concave and convex parts with the hyperplane between them – shows that

$$\mathbb{P}(d_H(\lambda(I_\varepsilon^\lambda)', \lambda J_\varepsilon^\lambda) > 18\lambda\varepsilon^2) \to 0. \tag{8.21}$$

Combining the above results with the triangle inequality and a union bound yields the result. □

The final ingredient is a union bound.

Proof of Theorem 4.2. Combining Propositions 8.1 and 8.2 gives

$$\mathbb{P}(d_H(\lambda J^\lambda, \lambda I^\lambda) > C\lambda\varepsilon^2) \le \mathbb{P}(J_{2\varepsilon}^\lambda \neq J^\lambda) + \mathbb{P}(I_{2\varepsilon}^\lambda \neq I^\lambda) + \mathbb{P}(d_H(\lambda J_\varepsilon^\lambda, \lambda I_\varepsilon^\lambda) > C\lambda\varepsilon^2) \to 0. \tag{8.22}$$

□

This method could likely be applied to a wider class of intersection models: namely, the ball $\mathbb{B}$ could be replaced by another set satisfying some curvature condition. The difficulty in such a generalization would lie in finding a canonical way to construct a coupling between the intersection model and another model known to have the Crofton cell of a tessellation model as a scaling limit.

9. The expected volume of I^λ

We first sketch Goudsmit's classical calculation for the second moment of the area A of a typical cell in a Poisson line tessellation T, when $d = 2$.

First we recall some basic facts about T, which can be defined as follows. Let $\mathcal{P}$ be a unit intensity Poisson process on $[0, 2\pi) \times \mathbb{R}^+$. We associate the point $(\theta, \rho) \in \mathcal{P}$ with the line $x\cos\theta + y\sin\theta = \rho$. This yields a translation and rotation invariant measure on families of lines in the plane; T is a random instance of this measure. It is not hard to show that the intersections of T and another random line form a Poisson process of rate 2, and also that T has π intersections, and thus π cells, per unit area.

Goudsmit in 1945 [13] considered tessellations on the surface of a sphere, but we can rephrase his argument in terms of a realization of T over a large circular region R of area N. We choose two points $x, y \in R$ uniformly at random and ask for the probability q_N that they lie in the same cell

of T. If $f(t)$ denotes the density function for the area A of a typical cell, then, as $N \to \infty$,

$$Nq_N \to \frac{\int_0^\infty t^2 f(t)\,dt}{\int_0^\infty t f(t)\,dt} = \frac{\mathbb{E}(A^2)}{\mathbb{E}(A)},$$

since $tf(t)$ is the density function for the area of a cell containing a given point. On the other hand, x and y lie in the same cell of T if and only if the line segment l_{xy} joining them does not intersect T. As noted above, the number of intersections between l_{xy} and T is Poisson with rate 2, so there are no such intersections with probability e^{-2l}. Consequently,

$$Nq_N \to \int_0^\infty 2\pi l e^{-2l}\,dl = \frac{\pi}{2}.$$

Combining these two expressions yields the formula $\mathbb{E}(A^2) = \frac{\pi}{2}\mathbb{E}(A) = \frac{1}{2}$, which we may rewrite as

$$\frac{\mathbb{E}(A^2)}{\mathbb{E}(A)^2} = \frac{\pi^2}{2}.$$

Goudsmit's argument generalizes to higher dimensions. Write V_d for the volume of a typical cell in a Poisson hyperplane tessellation T_d in $\mathbb{R}^d$. This time we will choose a different normalization for the measure μ_{d-1} on the space $A(d, d-1)$ of affine hyperplanes in R^d, in which the measure of hyperplanes meeting the unit ball is 2, i.e., the diameter of the unit ball. Consequently, in the corresponding tessellation T_d, the expected number of hyperplanes H meeting the unit ball is 2. With N now representing the volume of a large spherical region R, and q_N as before, we once again have

$$Nq_N \to \frac{\int_0^\infty t^2 f(t)\,dt}{\int_0^\infty t f(t)\,dt} = \frac{\mathbb{E}(V_d^2)}{\mathbb{E}(V_d)}$$

as $N \to \infty$. The second part of the calculation requires a slight modification; we now wish to estimate the number I_d of intersections of a line L of length l with T_d. Once again, I_d has a Poisson distribution, with mean c_d given by Crofton's formula [29] (page 172), namely

$$\frac{1}{l}\int_{A(d,d-1)} |L \cap H| \mu_{d-1}(dH) = \frac{2\omega_{d-1}}{d\omega_d} := c_d,$$

where

$$\omega_d = \frac{\pi^{d/2}}{\Gamma(d/2+1)}$$

is the volume of the unit ball. Continuing the argument as before, and recalling that $S_d = d\omega_d$ is the surface area of the unit ball, we have

$$Nq_N \to \int_0^\infty S_d l^{d-1} e^{-c_d l}\, dl = \frac{d!}{c_d^d}\omega_d.$$

As before, this yields

$$\frac{\mathbb{E}(V_d^2)}{\mathbb{E}(V_d)} = \frac{d!}{c_d^d}\omega_d,$$

and, since (with this normalization) we have

$$\mathbb{E}(V_d) = \left(\frac{2}{c_d}\right)^d \frac{1}{\omega_d}$$

(see [21], pages 156 and 179), we conclude that

$$\frac{\mathbb{E}(V_d^2)}{\mathbb{E}(V_d)^2} = \frac{d!}{2^d}\omega_d^2,$$

in agreement with [21] (page 179).

9.1. **Intersection model.** In this section, we apply the above results to give an alternative proof of Proposition 4.3. This is essentially contained in Theorem 4.2 and the formulas above; Theorem 4.2 relates the volumes of I^λ and D_0^1, and the above analysis applies to D_0^1. The scaling in Theorem 4.2 relies on the scaling in Theorem 4.1, which was briefly sketched in the introduction. For completeness, we now explain the scaling in more detail, in the context of Theorem 4.2.

Suppose then that we know that the intersection $I^\lambda = I_d^\lambda$ converges to the Crofton cell of a suitably-scaled Poisson hyperplane process, and we wish to determine the scaling.

First, consider the Poisson hyperplane model normalized, as above, so that the expected number of hyperplanes meeting the unit ball is 2. Write $B_\varepsilon = \{x : ||x|| < \varepsilon\}$, so that the expected number of hyperplanes meeting B_ε is 2ε. For this process, the expected volume $\mathbb{E}(V_d^0)$ of the Crofton cell V_d^0 is related to the volume of the typical cell V_d as follows:

$$\mathbb{E}(V_d^0) = \frac{\mathbb{E}(V_d^2)}{\mathbb{E}(V_d)} = \frac{d!}{c_d^d}\omega_d = \frac{d! d^d \omega_d^{d+1}}{2^d \omega_{d-1}^d}.$$

Second, let us choose $\varepsilon = \varepsilon(\lambda) \to 0$ so that the expected number of spheres in the intersection model that meet B_ε tends to infinity. Then the intersection model inside B_ε is well-approximated by a Poisson hyperplane tessellation. The number of intersecting spheres meeting B_ε is the number of points of the underlying Poisson process in the shell $\mathrm{Sh}^-(\varepsilon) = \{x \in \mathbb{R}^d : ||x|| \in (1-\varepsilon, 1)\}$. This

number is asymptotically $\varepsilon\lambda d\omega_d$, i.e., $\lambda d\omega_d/2$ times the "normalized" value above. Consequently, as $\lambda \to \infty$,

$$\mathbb{E}(|I_d^\lambda|) = (1+o(1))\mathbb{E}(V_d^0)\left(\frac{2}{\lambda d\omega_d}\right)^d = (1+o(1))\frac{d!\omega_d}{\lambda^d \omega_{d-1}^d},$$

so that

$$\lim_{\lambda\to\infty} \lambda^d \mathbb{E}(|I_d^\lambda|) \to \frac{d!\omega_d}{\omega_{d-1}^d},$$

in agreement with Proposition 4.3.

10. Further questions

We close with some questions related to intersection processes that arose in the course of our research.

Question 10.1. *What class of intersection models has the Crofton cell of the hyperplane tessellation model D_0^1 as a scaling limit?*

Some kind of curvature condition is likely necessary: for example, consider the cone intersection model $I^{\rho,\lambda}_{\mathrm{Cone}(\vec{e_1},\beta)}$. Just like the hyperplane model, the cone model is a polyhedron for any β, with vertices formed by intersections of pairs of cones. However, when $\beta \neq \frac{\pi}{2}$, each cone whose apex lies inside the intersection will contribute an additional vertex to the intersection. We conjecture that these vertices remain with positive probability in the limit $\lambda \to \infty$, which strongly suggests that the cone model does not have D_0^1 as a scaling limit.

The cone model fails because it has non-smooth boundary points. It seems likely that this is the only obstruction: that is, any intersection model with underlying sets having differentiable boundary should share the same scaling limit as the ball and hyperplane models.

Question 10.2. *Fix a closed set A and consider the intersection model $I_A^{\mu,\lambda}$. Proposition 6.8 shows that the radius $R_A^{\mu,\lambda}$ converges to an exponential distribution under some rescaling. How does the rescaling relate to the geometry of A? How does it relate to the behavior of μ?*

This statistical question is a natural first step for general intersection models with distributional rotational invariance.

Question 10.3. *Let S_λ denote the number of faces of the intersection model I^λ. Fact 7.2 suggests that S_λ is uniformly tight – i.e. that for any $\delta > 0$ and any $\lambda > 0$, there exists $t > 0$ such that*

$\mathbb{P}(S_\lambda > t) < \delta$ – *and thus there is a limiting stationary distribution. Can the limiting distribution and transition probabilities for the stochastic process* $(S_\lambda)_{\lambda>0}$ *be computed or approximated?*

A similar question has been answered for the typical Poisson-Voronoi cell and for the Crofton cell of a hyperplane tessellation, in a different limiting context [5, 8]. The intersection construction of the Crofton cell D_0^1 seems ideal to study this question, because it has a natural renewal quality as λ increases.

11. Appendix

11.1. **Appendix A.** In this appendix we recall the definition and some basic properties of Poisson point processes, which are used throughout this article.

Definition 11.1. *Let $\Omega \subset \mathbb{R}^d$ be a Borel set, and μ a finite Borel measure on Ω. The **Poisson point process (PPP)** on Ω with intensity μ, denoted $\mathcal{X}$, is the finite set consisting of Poisson$(\mu(\Omega))$ many independent points sampled from the probability measure $\frac{1}{\mu(\Omega)}\mu$.*

This is a natural, intuitive definition; for a proper introduction to the theory of Poisson point processes, see [20].

Fact 11.2. *Suppose $\mathcal{X}$ is a PPP on a Borel set $\Omega \subset \mathbb{R}^d$ with intensity meausre μ.*

a. *Let $A \subset \Omega$ be any Borel set. Then*

$$|A \cap \mathcal{X}| \sim \text{Poisson}(\mu(A)). \tag{11.1}$$

b. *If $A, B \subset \Omega$ are disjoint Borel sets, then $\mathcal{X} \cap A$ and $\mathcal{X} \cap B$ are independent.*

An important special case of Fact 8.2a is that the probability that a given region A contains no points of $\mathcal{X}$ is given by:

$$\mathbb{P}(A \cap \mathcal{X} = \emptyset) = \exp(-\mu(A)). \tag{11.2}$$

11.2. **Appendix B.** In this appendix we prove a formula for finding the volume of a star-shaped domain in $\mathbb{R}^m$ by doing an integration over the $(m-1)$ dimensional sphere.

Theorem 11.3. *Suppose $f : \mathbb{S}^{m-1} \to \mathbb{R}^+$ is continuous, and let $A \subset \mathbb{R}^m$ be the star-shaped open set defined by*

$$A = \{x \in \mathbb{R}^m : |x| < f(x/|x|)\}.$$

Then Vol$(A) = \frac{1}{m}\int_{\mathbb{S}^{m-1}} f^m \, dS$, where dS is the $(m-1)$-dimensional surface area form on $\mathbb{S}^{m-1}$.

The following proof was generously provided by Jack Lee.

Proof. Since f is continuous, it can be approximated uniformly by a sequence of smooth functions $f_i \to f$. Let $A_i = \{x \in \mathbb{R}^m : |x| < f_i(x/|x|)\}$. It follows from the dominated convergence theorem that $\mathrm{Vol}(A_i) \to \mathrm{Vol}(A)$, so it suffices to prove the theorem under the assumption that f is smooth.

Now assuming f is smooth, extend it to a function on all of $\mathbb{R}^m \setminus \{0\}$, still denoted by f, by declaring it to be constant on rays from the origin. Define a map $F : \mathbb{B}^m \to A$ by $F(x) = f(x)x$ for $x \neq 0$ and $F(0) = 0$. Then F is a homeomorphism with inverse $F^{-1}(y) = y/f(y)$ for $y \neq 0$, and F is smooth away from the origin. It follows that

$$\mathrm{Vol}(A) = \int_{\mathbb{B}^m} F^* dV,$$

where $dV = dx^1 \wedge \cdots \wedge dx^m$ is the Euclidean volume form of $\mathbb{R}^d$. We compute (ignoring the origin, which has measure zero),

$$F^*dV = d(f(x)x^1) \wedge \cdots \wedge d(f(x)x^m) = (f(x)dx^1 + x^1 df) \wedge \cdots \wedge (f(x)dx^m + x^m df).$$

When expanded, this gives 2^m terms. But note that if df appears in two or more of those terms, the result is zero because $df \wedge df = 0$. Thus the expression reduces to

$$F^*dV = f(x)^m dx^1 \wedge \cdots \wedge dx^m + \sum_{i=1}^m dx^1 \wedge \cdots \wedge (x^i df) \wedge \cdots \wedge dx^m.$$

In the ith term in the sum, when we expand $df = \sum_j (\partial f/\partial x^j) dx^j$, only the term with $j = i$ survives; the others vanish because $dx^j \wedge dx^j = 0$. Thus

$$F^*dV = f(x)^m dx^1 \wedge \cdots \wedge dx^m + \left(\sum_{i=1}^m x^i (\partial f/\partial x^i)\right) dx^1 \wedge \cdots \wedge dx^m.$$

Because f is constant on rays and the vector field $x^i \partial/\partial x^i$ points radially outward everywhere, it follows that $x^i \partial f/\partial x^i \equiv 0$, so the sum in parentheses above is identically zero. Thus $F^* dV = f(x)^m dV$.

Finally, in spherical coordinates, $dV = \rho^{m-1} d\rho\, dS$, where ρ is the distance from the origin. Thus because f is constant on radii,

$$\mathrm{Vol}(A) = \int_{\mathbb{B}^m} f^m dV = \int_{\mathbb{S}^{m-1}} \int_0^1 f^m \rho^{m-1}\, d\rho\, dS = \int_{\mathbb{S}^{m-1}} f^m \left(\int_0^1 \rho^{m-1}\, d\rho \right) dS = \frac{1}{m} \int_{\mathbb{S}^{m-1}} f^m dS,$$

which was to be proved. □

References

[1] Adell, J.A., Jodrá, P., Exact Kolmogorov and total variation distances between some familiar discrete distributions, Journal of Inequalities and Applications 2006, 64307.

[2] G. Ambrus, P. Kevei and V. Vigh, The diminishing segment process, *Statistics and Probability Letters* **82** (2012), 191–195.

[3] P. Billingsley, Probability and Measure, Third Edition, Wiley Series in Probability and Mathematical Statistics, 1995.

[4] K. Böröczky, Finite Packing and Covering, Cambridge University Press, 2004.

[5] P. Calka, An explicit expression for the distribution of the number of sides of the typical Poisson-Voronoi cell, *Advances in Applied Probability* **35.4** (2003), 863–870.

[6] P. Calka, Some classical problems in random geometry, in: Stochastic Geometry, Lecture Notes in Mathematics **2237**, Springer, 1–43, 2019.

[7] P. Calka, J. Michel and K. Paroux, Refined convergence for the Boolean model, *Advances in Applied Probability* **41** (2009), 940–957.

[8] P. Calka and T. Schreiber, Limit theorems for the typical Poisson-Voronoi cell and the Crofton cell with a large inradius, *The Annals of Probability* **33** (2005), 1625–1642.

[9] C. Cannone, A short note on Poisson tail bounds, available at
`http://www.cs.columbia.edu/∼ccanonne/files/misc/2017-poissonconcentration.pdf`

[10] M. Franceschetti and R. Meester, Random Networks for Communication, Cambridge University Press, 2007.

[11] E. Gilbert, Random plane networks, *J. Soc. Indust. Appl. Math.* **9** (1961), 533–543.

[12] E. Gilbert, The probability of covering a sphere with N circular caps, *Biometrika* **56** (1965), 323–330.

[13] S. Goudsmit, Random distribution of lines in a plane, *Rev. Mod. Phys.* **17** (1945), 321–322.

[14] P. Hall, On the coverage of k-dimensional space by k-dimensional spheres, *Annals of Probability* **13** (1985), 991–1002.

[15] P. Hall, On continuum percolation, *Annals of Probability* **13** (1985), 1250–1266.

[16] P. Hall, Introduction to the Theory of Coverage Processes, Wiley, New York, 1988.

[17] M. Haenggi, Stochastic Geometry for Wireless Networks, Cambridge University Press, 2013.

[18] S. Janson, Random coverings in several dimensions, *Acta Mathematica* **156** (1986), 83–118.

[19] P. Kevei and V. Vigh, On the diminishing process of Bálint Tóth, *Trans. Amer. Math. Soc.* **368** (2016), 8823–8848.

[20] J. F. C. Kingman, Poisson Processes, Clarendon Press, 1992.

[21] G. Matheron, Random Sets and Integral Geometry, Wiley, 1975.

[22] R. Meester and R. Roy, Continuum Percolation, Cambridge University Press, 1996.

[23] J. Michel and K. Paroux, Local convergence of the Boolean shell model towards the thick Poisson hyperplane process in the Euclidean space, *Advances in Applied Probability* **35** (2003), 354–361.

[24] R. Miles, Random polygons determined by random lines in a plane I, *Proc. Nat. Acad. Sci. USA* **52** (1964), 901-907.

[25] R. Miles, Random polygons determined by random lines in a plane II, *Proc. Nat. Acad. Sci. USA* **52** (1964), 1157–1160.

[26] H. E. Robbins, On the Measure of a Random Set, *The Annals of Mathematical Statistics* **15** (1944), 70–74.

[27] F. Santambrogio, Optimal Transport for Applied Mathematicians, Birkhauser, 2015.

[28] L. Santaló, Integral Geometry and Geometric Probability, Addison Wesley, 1976.

[29] R. Schneider and W. Weil, Stochastic and Integral Geometry, Springer, 2008.

Part 5. Rumor source obfuscation

Detecting the source of information diffusion on a network is an important problem in network science, with applications such as finding the source of a virus epidemic or finding the source of a rumor on Twitter. A prototypical graph on which source detection is studied is the infinite d-regular tree $\mathbb{T}_d$ (with $d \geq 3$), which is our focus in this paper as well.

Rumor source detection. Perhaps the simplest and most natural model of information diffusion on a network is the susceptible-infected (SI) model, where the rumor is spread along each edge of the network at a constant rate, and once a node is infected it remains infected forever. Shah and Zaman studied detecting the source in this model [44, 45]. Formally, at time $t = 0$ a vertex $v^* \in \mathbb{T}_d$ is "infected" and the information propagates on the network according to the SI model; one then observes the subset V_t of infected vertices at time t, which consists of $N_t := |V_t|$ vertices. We assume that the underlying graph (in this case $\mathbb{T}_d$) is known and hence the subgraph G_t induced by the vertices in V_t is also known. The goal is to find the rumor source v^*.

The maximum likelihood estimator (MLE) $\widehat{v}_{\mathrm{ML}} := \arg\max_{v \in V_t} \mathbb{P}\left(G_t \,|\, v^* = v\right)$ has particularly nice properties in this setting [44, 45]. In particular, Shah and Zaman showed that it is computable in linear time and that it detects the source with constant probability. More precisely, they show (in [46]) that there exists a universal constant $\alpha_d > 0$ such that $\lim_{t\to\infty} \mathbb{P}\left(\widehat{v}_{\mathrm{ML}} = v^*\right) = \alpha_d$ (when $d \geq 3$). Many results extend to more general settings such as random trees [46].

Wang et al. [60] studied rumor source detection in the same setting but now with multiple independent observations; that is, observing the infected nodes $V_t^{(1)}, \ldots, V_t^{(k)}$ of k independent diffusions started from the same source v^*. They show that the detection probability increases with k and that it goes to 1 exponentially as $k \to \infty$.

Rumor source obfuscation. The results above show that if information propagates according to the SI model, then the source can be found efficiently and with good probability (that is, with at least constant probability). In certain applications, such as anonymous messaging apps[2], this is undesirable. Motivated by these applications, Fanti et al. [23] asked whether it is possible to devise messaging protocols that can *obfuscate* the rumor source, while at the same time still spreading information widely and quickly.

They devised a family of messaging protocols, termed *adaptive diffusions*, for this purpose; see Section 11.3 for a detailed description. Their main result shows that a specific messaging protocol

[2]Examples include Whisper [61], Blind [5], and the now-defunct Yik Yak [63] and Secret [43].

within this family achieves *perfect obfuscation*: under this spreading model a "snapshot adversary" can do no better than randomly guessing the source node:

$$\mathbb{P}\left(\widehat{v}_{\mathrm{ML}} = v^* \,|\, N_t = n\right) = \frac{1 + o\left(1\right)}{n}. \tag{11.3}$$

Many results extend to more general settings such as irregular trees [21, 22].

Our results. We study the source obfuscation guarantees that adaptive diffusion protocols can provide, in a couple of settings. First, we do this in the context of the adversary having multiple independent observations. We show that when an adversary has access to two independent observations then a weak form of obfuscation is still possible. However, when it has access to three or more independent snapshots, then source detection with constant probability is always possible, regardless of the adaptive diffusion protocol.

We also do this in the context of spreading information *locally* around the source. We introduce a natural quantitative measure of local spreading, and characterize the tradeoff between local spreading and source obfuscation for adaptive diffusion protocols (under a single snapshot).

Put together, these results raise questions about the robustness of possible anonymity guarantees when spreading information in social networks. In order to precisely state our results, we first describe in Section 11.3 the setting of information diffusion processes in general and adaptive diffusions in particular. We then state our results in Sections 11.4 and 11.5.

11.3. **Information diffusion and adaptive diffusion.** We define a (discrete time) information diffusion process on a graph $G = (V, E)$ as a (potentially random) increasing sequence of subgraphs $G_0 \subseteq G_1 \subseteq G_2 \subseteq \ldots$, where $G_t = (V_t, E_t)$ is the subgraph induced by the vertices V_t who have the information at time t. Throughout the paper we assume that G_0 consists of a single vertex $v^* \in G$, which we term the *source*. We also assume that the information spreads along the edges of the graph and hence $V_{t+1} \subseteq V_t \cup \partial G_t$, where $\partial G_t := \{v \in V : v \notin V_t, \exists w \in V_t : (v, w) \in E\}$ denotes the (outer) vertex boundary of G_t, consisting of vertices that are not in G_t but which are connected to a vertex in G_t.

A simple example is when every vertex who obtains the information spreads it to all its neighbors in the next time step. In this case $G_t = B_t\left(v^*\right)$ for every $t \geq 0$, where $B_r\left(v\right) := \{u \in V : \delta_G\left(u, v\right) \leq r\}$ denotes the (closed) ball of radius r around vertex $v \in V$ (here δ_G denotes graph distance in G).

The SI model mentioned above[3] can be defined inductively as follows: given G_t, let v_{t+1} be a uniformly randomly chosen vertex from ∂G_t and let $V_{t+1} := V_t \cup \{v_{t+1}\}$.

The *source detection* problem is the following: given the underlying graph G, the distribution of the sequence $\{G_t\}_{t\geq 0}$, and a single observation G_t at some time $t > 0$, the goal is to estimate the source v^*. This is also known as the "snapshot adversary" model, since we get to observe G_t, a single snapshot in time.

Adaptive diffusion, introduced by Fanti et al. [23], is a family of information diffusion processes designed with *source obfuscation* in mind. We now introduce and define adaptive diffusion on $\mathbb{T}_d =: G$; we refer the reader to [22] for a comprehensive introduction more generally.

Adaptive diffusion is defined via an auxiliary process, the path $\{vs_t\}_{t\geq 0}$ of a so-called *virtual source*. This is a time-inhomogeneous Markov chain, which we now define. Initially, the virtual source is the same as the true source: $vs_0 := v^*$. Next, it moves to a uniformly random neighbor of v^*:

$$\mathbb{P}\left(vs_1 = w\right) = \frac{1}{d}\mathbf{1}_{\{(w,v^*)\in E\}}.$$

For the remainder of the path, assuming that vs_t is given, vs_{t+1} is defined as follows. If t is odd, then $vs_{t+1} = vs_t$; that is, the virtual source stays put. If t is even, then the virtual source either stays put or it moves to one of its $d-1$ neighbors that it has not visited before; in the latter case, it chooses the neighbor to move to uniformly at random. Note that if the virtual source moves then it moves *away* from the source v^*. The probability of choosing one action or the other is a function of time t and also the distance of vs_t from v^* (hence the name *adaptive*). Specifically, let $h_t := \delta_G(vs_t, v^*)$ denote the graph distance between vs_t and v^*. Then

- with probability $\alpha(t, h_t)$ we have that $vs_{t+1} = vs_t$, that is, the virtual source stays put;
- and with probability $1 - \alpha(t, h_t)$ the virtual source moves to one of its $d-1$ neighbors that it has not visited before, chosen uniformly at random.

The probabilities $\alpha(t, h) \in [0, 1]$, with $t \in \{2, 4, 6, \ldots\}$ and $h \in \{1, 2, 3, \ldots, t/2\}$, are parameters that fully describe the distribution of the path $\{vs_t\}_{t\geq 0}$ of the virtual source. Each choice of parameters defines a particular Markov chain and thus a particular adaptive diffusion protocol.

[3]Note that the SI model is often defined in continuous time. Viewing this continuous-time process at the times when a new vertex obtains the information, we obtain the described discrete time information diffusion process.

Having defined the path of the virtual source, we are now ready to define the associated adaptive diffusion protocol, given $\{vs_t\}_{t\geq 0}$. When t is even, the set of infected nodes is defined as

$$V_t := \{v \in V : \delta_G(v, vs_t) \leq t/2\}.$$

That is, V_t is a ball of radius $t/2$—equivalently, a balanced tree of depth $t/2$—around the virtual source vs_t. For t odd, the set of infected nodes V_t is chosen so that $\{G_t\}_{t\geq 0}$ satisfies $V_{t+1} \subseteq V_t \cup \partial G_t$.[4] The resulting information diffusion process is called an *adaptive diffusion*; see Figure 6 for an illustration. Note that by construction adaptive diffusion spreads the information to $N_t \asymp (d-1)^{t/2}$ nodes at time t, which is only a factor of two slower than the fastest possible spread.

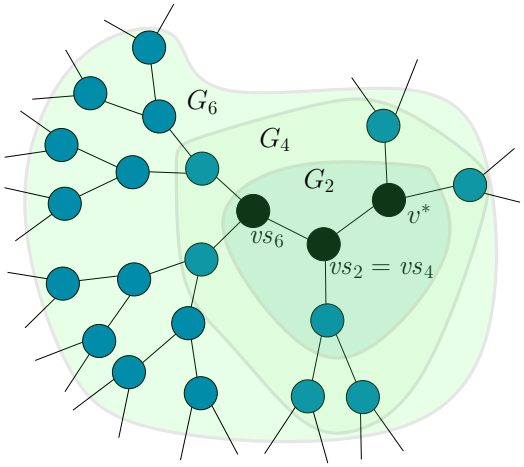

FIGURE 6. An example of an adaptive diffusion spreading on the infinite 3-regular tree $\mathbb{T}_3$. Here the virtual source moves to a uniformly randomly chosen neighbor of the source v^* at time 1, then it stays put for several time steps, and moves again at time 5. The shaded regions show the infected subgraphs G_t for $t \in \{2, 4, 6\}$; note that they are all balanced trees of depth $t/2$, centered at the virtual source vs_t.

Fanti et al. [23] show that a particular adaptive diffusion protocol—specifically, the process with $\alpha(t, h) := ((d-1)^{t/2-h+1} - 1)/((d-1)^{t/2+1} - 1)$—perfectly obfuscates the source from an adversary who sees a snapshot of a single diffusion. The key property of this construction is that, for t even, all vertices in $V_t \setminus \{vs_t\}$ are equally likely to be the original source v^* and hence an adversary can do no better than randomly guess among them. A similar statement holds also for t odd, showing that the MLE satisfies (11.3).

11.4. **Results: adaptive diffusion with multiple independent observations.** In many applications it is common for individuals to send not just one but multiple messages over time, each one spreading over the same underlying network. If an adversary has access to a snapshot of each

[4]Specifically, we have the following. First, $V_1 := \{vs_0, vs_1\}$. Next, for $t \geq 3$ such that t is odd, we distinguish two cases. If $vs_t = vs_{t-1}$, then $V_t := V_{t-1}$; that is, if the virtual source stays put (instead of moving), then the set of infected nodes is unchanged. If $vs_t \neq vs_{t-1}$, then $V_t := V_{t-1} \cup \{w \in \partial G_{t-1} : \delta_G(w, vs_t) = (t-1)/2\}$; in other words, if the virtual source moves, then the information is spread in the same direction.

such diffusion, then they are in a much better position to find the source. Is it still possible to obfuscate the source with some form of information diffusion? We investigate this question in the context of adaptive diffusion protocols.

We show that when an adversary has access to two independent observations, a weak form of obfuscation is still possible with adaptive diffusion. However, when three or more independent observations are available, detection with constant probability is always possible, regardless of which adaptive diffusion protocol is used. This is the content of Theorems 11.4 and 11.5.

Theorem 11.4 (Two independent observations)**.** *Suppose that information is spread according to an adaptive diffusion protocol on $\mathbb{T}_d$, $d \geq 3$, and that an adversary has two independent observations of infected subgraphs, $G_{t_1}^1$ and $G_{t_2}^2$, started from a fixed source v^*.*

(a) There exists a computationally efficient estimator $\widehat{v}$, which is agnostic to the adaptive diffusion protocol, such that if $t_1, t_2 \geq 2$ then

$$\mathbb{P}\left(\widehat{v} = v^*\right) \geq \frac{d-1}{d} \cdot \frac{2}{\min\left\{t_1, t_2\right\}}.$$

(b) There exists an adaptive diffusion protocol such that the maximum likelihood estimator $\widehat{v}_{\mathrm{ML}}$ satisfies for all $t_1, t_2 \geq 1$ that

$$\mathbb{P}\left(\widehat{v}_{\mathrm{ML}} = v^*\right) \leq \frac{d-1}{d} \cdot \frac{7}{\min\left\{t_1, t_2\right\}}. \tag{11.4}$$

A few comments are in order. First, the bounds in parts (a) and (b) above match up to a small constant factor, hence this is best possible within the family of adaptive diffusions. Next, the detection probability in (11.4) still vanishes as $t = \min\left\{t_1, t_2\right\} \to \infty$, but only very slowly—exponentially more slowly than in the case of one observation (see (11.3) and recall that $N_t \asymp (d-1)^{t/2}$ is exponential in t). We also note that the adaptive diffusion protocol in part (b) is different from the one used by Fanti et al. [23] to achieve perfect obfuscation in the case of a single observation; in fact, if this latter adaptive diffusion protocol is used to independently spread two diffusions, then the estimator $\widehat{v}$ in part (a) succeeds at finding the source with constant probability. Finally, we mention that the estimator in part (a) is essentially the same as the MLE in part (b) when t_1 and t_2 are both even—see Section 13 for details.

Once the adversary has three independent observations, not even weak obfuscation is possible with adaptive diffusion. In fact, the detection probability converges to one exponentially quickly

in the number of observations (see (11.5) below), extending the results of Wang et al. [60] for the SI model to the family of adaptive diffusions.

Theorem 11.5 (Three or more independent observations)**.** *Suppose that information is spread according to an adaptive diffusion protocol on $\mathbb{T}_d$, $d \geq 3$, and that an adversary has $k \geq 3$ independent observations of infected subgraphs, $G_{t_i}^i$ for $i \in \{1, \ldots, k\}$, started from a fixed source v^*.*

When $k = 3$, there is a computationally efficient estimator $\widehat{v}$, which is agnostic to the adaptive diffusion protocol, satisfying

$$\mathbb{P}\left(\widehat{v} = v^*\right) \geq \frac{(d-1)(d-2)}{d^2}.$$

More generally, there exists a computationally efficient estimator $\widehat{w} = \widehat{w}(k)$, which is agnostic to the adaptive diffusion protocol, such that

$$\mathbb{P}\left(\widehat{w} = v^*\right) \geq 1 - d \times \exp\left(-\tfrac{(d-2)^2}{2d^2}k\right). \tag{11.5}$$

This result follows from basic symmetry properties of adaptive diffusion (see Section 12).

11.5. **Results: local spreading vs. source obfuscation.** It is often desirable to not only spread information widely and quickly, but also to spread it *locally* around the source. Indeed, the local neighborhood of the source typically consists of nodes that are closely related to the source, and the information that the source is spreading is often most relevant to this local neighborhood. In particular, this is true for scenarios where source obfuscation is relevant and important, for instance, spreading information about a local protest. At the same time, local spreading is at odds with source obfuscation. Here we introduce a natural way to quantify local spreading, and characterize the tradeoff between local spreading and source obfuscation for adaptive diffusion protocols (under a single snapshot).

Formally, define for an adaptive diffusion the quantity

$$R_t := \max\left\{r \geq 0 : B_r\left(v^*\right) \subseteq G_t\right\}.$$

In words, R_t is the radius of the largest ball of infected nodes centered at the rumor source at time t. Since R_t is (in general) a random quantity, we may use $\mathbb{E}\left[R_t\right]$ as a deterministic measure of local spreading of an adaptive diffusion protocol. Observe that $0 \leq R_t \leq t/2$ and hence also $0 \leq \mathbb{E}\left[R_t\right] \leq t/2$.

Ideally for local spreading we would like $\mathbb{E}[R_t]$ to grow linearly with t; at the very least, local spreading requires $\mathbb{E}[R_t] \to \infty$ as $t \to \infty$. However, the adaptive diffusion protocol that achieves perfect source obfuscation (see the end of Section 11.3) does not have local spreading: in fact, $\mathbb{E}[R_t] \leq 1$ for all t and, moreover, $\sup_t R_t$ is finite almost surely.

This shows that source obfuscation guarantees have to be relaxed in order to have local spreading. It turns out that it is still possible to have reasonable source obfuscation guarantees—we refer to this as "polynomial obfuscation", see (11.6) below—and local spreading at the same time. The following theorem characterizes this tradeoff for adaptive diffusion protocols (under a single snapshot). For simplicity, we focus here on even times t.

Theorem 11.6 (Tradeoff between local spreading and source obfuscation)**.** *Suppose that information is spread according to an adaptive diffusion protocol on $\mathbb{T}_d$, $d \geq 3$, and that an adversary observes, at an even time t, an infected subgraph, G_t, started from a fixed source v^*.*

(a) Suppose that the adaptive diffusion protocol achieves "polynomial obfuscation", that is, the following holds:

$$\mathbb{P}(\widehat{v}_{\mathrm{ML}} = v^*) \leq \frac{C}{N_t^{\gamma}} \tag{11.6}$$

for some $\gamma \in (0,1)$ and $C < \infty$, where recall that

$$N_t = |V_t| = \tfrac{d}{d-2}\left((d-1)^{t/2} - 1\right) + 1 \asymp (d-1)^{t/2}.$$

Then

$$\mathbb{E}[R_t] \leq (1-\gamma)\frac{t}{2} + \frac{\log(Ct)}{\log(d-1)} + 2.$$

(b) For every $\gamma \in (0,1)$ there exists an adaptive diffusion protocol that satisfies (11.6) with $C = 2(d-1)$ and also

$$\mathbb{E}[R_t] \geq (1-\gamma)\frac{t}{2}$$

for all even $t > 2/\gamma$ (and for all even $t \leq 2/\gamma$ we have $\mathbb{E}[R_t] = t/2 - 1$).

In particular, we see from Theorem 11.6 that the power γ in polynomial obfuscation (see (11.6)) and the speed $(1-\gamma)/2$ of local spreading are directly related. This precisely quantifies the tradeoff between local spreading and source obfuscation guarantees: the faster local spreading is—that is, the smaller γ is—the weaker the source obfuscation guarantee.

11.6. **Organization.** The rest of the paper is organized as follows. We first prove Theorem 11.5 in Section 12, since the proof relies only on a simple symmetry property of adaptive diffusion protocols on $\mathbb{T}_d$ and provides good intuition for the subsequent proofs. We then prove Theorem 11.4 in Section 13; the proof of part (a) is similar to the proof of Theorem 11.5 in Section 12, while the proof of part (b) requires understanding the maximum likelihood estimator in the case of two observations. (Some cases in the proof of part (b) of Theorem 11.4 are deferred to Appendix A.) In Section 14 we turn to studying local spreading and prove Theorem 11.6. Finally, we conclude in Section 15 by discussing some implications and limitations of our results, how they relate to other works, as well as further questions for future research.

12. Adaptive diffusion with $k \geq 3$ independent observations

In this section we prove Theorem 11.5. The main idea is simple and relies on a symmetry property of adaptive diffusion protocols on $\mathbb{T}_d$: that they send the virtual source in a uniformly random direction. First, note that if we remove the source v^* from the tree $\mathbb{T}_d$ then it breaks into d subtrees. The main observation is that the virtual source of an adaptive diffusion is equally likely to be in each subtree. This symmetry property alone guarantees a constant probability of detection when there are at least three independent observations, as we now explain.

Assume for now that $t_1, \dots, t_k$ are even; the proof is cleaner in this case, though not much changes in the general case. Recall that for an adaptive diffusion protocol the infected tree G_t is a ball with center vs_t when t is even. Hence from the infected tree G_t we may determine the virtual source vs_t. We may thus assume that the adversary is given k independent virtual sources $vs^1, vs^2, \dots, vs^k$ (the time stamps of the virtual sources are not relevant for what follows). The main observation is that if vs^1, vs^2, and vs^3 are in different subtrees, then v^* is the unique vertex at the intersection of the three shortest paths connecting vs^1 and vs^2, vs^1 and vs^3, and vs^2 and vs^3; see Figure 7 for an illustration.

This immediately leads to a source detection algorithm: if the three shortest paths connecting vs^1 and vs^2, vs^1 and vs^3, and vs^2 and vs^3 intersect at a single vertex, the algorithm outputs this vertex; if not, pick a vertex from the intersection uniformly at random. Since each virtual source is equally likely to be in each subtree, there is a constant probability that vs^1, vs^2, and vs^3 are in different subtrees and therefore the algorithm successfully detects the source.

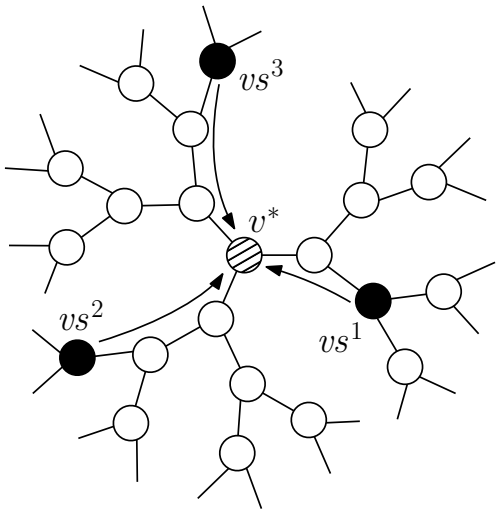

FIGURE 7. **Detecting the source from three observations.** If the three virtual sources are in different subtrees, then the paths connecting them intersect in a single node: the source v^*.

The proof that follows makes this formal and also presents an improved algorithm when the number of observations k is large, in order to show that the detection probability goes to 1 as $k \to \infty$.

Proof of Theorem 11.5. We start with some notational preliminaries. For distinct nodes $x, y \in \mathbb{T}_d$, let T_x^y denote the subtree of $\mathbb{T}_d$ away from y in the direction of x. In other words, if y were removed from $\mathbb{T}_d$ then the tree would break into a forest of d trees and T_x^y is the tree that contains x. Formally, if n_x^y is the neighbor of y that is closest to x, then

$$T_x^y := \{z \in \mathbb{T}_d : \delta(z, n_x^y) < \delta(z, y)\}.$$

We first assume, for simplicity, that $t_1, \ldots, t_k$ are all even; this simplifies the proof and we explain at the end what changes if some of these times are odd. Then for every $i \in \{1, \ldots, k\}$ we have that $G_{t_i}^i$ is a ball (of radius $t_i/2$) with center $vs_{t_i}^i$, the virtual source at time t_i. Thus we may assume that the adversary observes $k \geq 3$ independent virtual sources $vs^1, \ldots, vs^k \in \mathbb{T}_d$; as the time indices do not play a role in what follows, we drop them for notational convenience. We first define an estimator $\widehat{v}$ using only the first three samples (vs^1, vs^2, and vs^3) and show that it detects the source with constant probability. For $i, j \in \{1, 2, 3\}$ let P_{ij} denote the set of vertices in the unique path in $\mathbb{T}_d$ between vs^i and vs^j. If the three paths P_{12}, P_{13}, and P_{23} intersect in a single vertex, let $\widehat{v}$ be this vertex. If the intersection of P_{12}, P_{13}, and P_{23} contains more than one vertex, let $\widehat{v}$ pick a vertex from this intersection uniformly at random.

Consider the event A where the three virtual sources take different first steps away from the source. By the construction of adaptive diffusion, this is the same as the virtual sources being in different subtrees for all positive times; that is,

$$A = \left\{T^{v^*}_{vs^1} \cap T^{v^*}_{vs^2} = \emptyset\right\} \cap \left\{T^{v^*}_{vs^1} \cap T^{v^*}_{vs^3} = \emptyset\right\} \cap \left\{T^{v^*}_{vs^2} \cap T^{v^*}_{vs^3} = \emptyset\right\}.$$

On the event A we have that $P_{12} \cap P_{13} \cap P_{23} = \{v^*\}$ and, hence, $\widehat{v} = v^*$. That is, on the event A, the estimator correctly detects the source of the diffusion. Since the direction of the first step of a virtual source is uniformly random among the d choices and the different samples are independent, we have that $\mathbb{P}(A) = \frac{(d-1)(d-2)}{d^2}$, which concludes this part of the proof.

We now explain how more samples can be used to achieve a detection probability that converges to 1 exponentially in k as $k \to \infty$. For any vertex $v \in \mathbb{T}_d$ and w a neighbor of v, define

$$N_w(v) := \#\left\{j \in [k] : vs^j \in T^v_w\right\}.$$

That is, $N_w(v)$ counts the number of virtual sources in the subtree of $\mathbb{T}_d$ away from v in the direction of w. Using these quantities we define the following estimator:

$$\widehat{w} := \arg\min_{v \in \mathbb{T}_d} \max_{w:(w,v)\in E} N_w(v), \tag{12.1}$$

provided that this is well-defined (i.e., the minimum is attained at a single vertex); if this is not well-defined, let $\widehat{w}$ be an arbitrary vertex. Let $w_1, \ldots, w_d$ denote the neighbors of v^* in $\mathbb{T}_d$ and let $Y := (N_{w_1}(v^*), \ldots, N_{w_d}(v^*))$. We now argue that if $\|Y\|_\infty < k/2$, then $\widehat{w} = v^*$, that is, the estimator correctly detects the source of the diffusion.

First, observe that $\max_{w:(w,v^*)\in E} N_w(v^*) = \|Y\|_\infty$, which is less than $k/2$ under the assumption. Second, if $v \neq v^*$, then there must exist w' a neighbor of v and $i \in [d]$ such that

$$T^v_{w'} \supseteq \bigcup_{j \in [d]\setminus\{i\}} T^{v^*}_{w_j}.$$

This implies that

$$N_{w'}(v) \geq \sum_{j\in[d]\setminus\{i\}} N_{w_j}(v^*) = k - N_{w_i}(v^*) \geq k - \|Y\|_\infty > k/2,$$

where we used that $\|Y\|_1 = k$, as well as the assumption that $\|Y\|_\infty < k/2$. Consequently, $\max_{w:(w,v)\in E} N_w(v) \geq N_{w'}(v) > k/2$ and, hence, $\widehat{w} \neq v$. We have thus shown that $\|Y\|_\infty < k/2$ implies that $\widehat{w} = v^*$.

To conclude, we estimate from below the probability that $\|Y\|_\infty < k/2$, or rather, we estimate from above the complimentary event that $\|Y\|_\infty \geq k/2$. First, by a union bound and symmetry we have that $\mathbb{P}(\|Y\|_\infty \geq k/2) \leq d \times \mathbb{P}(N_{w_1}(v^*) \geq k/2)$. Now since $N_{w_1}(v^*) \sim \mathrm{Bin}(k, 1/d)$, we have by a Chernoff bound that

$$\mathbb{P}(N_{w_1}(v^*) \geq k/2) = \mathbb{P}\left(N_{w_1}(v^*) - \mathbb{E}[N_{w_1}(v^*)] \geq \tfrac{d-2}{2d}k\right) \leq \exp\left(-\tfrac{(d-2)^2}{2d^2}k\right).$$

Finally, we return to our simplifying assumption that the observation times $t_1, \ldots, t_k$ are all even. If t_i is odd, then there are two cases. If $G^i_{t_i}$ is a ball, then it is a ball with center $vs^i_{t_i}$, so the adversary can again determine the virtual source at time t_i and everything is unchanged. If $G^i_{t_i}$ is not a ball, then it is symmetric about the edge connecting $vs^i_{t_i-1}$ and $vs^i_{t_i}$. Thus the adversary can determine the set $\left\{vs^i_{t_i-1}, vs^i_{t_i}\right\}$. Picking either element of the set as the virtual source, the remainder of the proof goes through unchanged. □

At first glance, it may appear that computing the estimator $\widehat{w}$ requires solving a minimization problem over the entire infinite tree $\mathbb{T}_d$, but this is not the case. For every vertex v that is not on a shortest path between two virtual sources we have that $\max_{w:(w,v)\in E} N_w(v) = k$ and therefore $\widehat{w}$ must lie on a shortest path between two virtual sources. Moreover, the distance between any two virtual sources is at most $2\max_{i\in[k]} t_i$. Thus the minimization problem in (12.1) is over a set of size $O(k^2 \max_{i\in[k]} t_i)$ and can be solved efficiently.

13. Adaptive diffusion with two independent observations

In this section we prove Theorem 11.4. We start with the proof of part (a) in Section 13.1, which builds on similar ideas as the proof of Theorem 11.5 in Section 12. Then, in order to prove part (b) of Theorem 11.4, we need to understand the maximum likelihood estimator—this is done in Section 13.2. Due to the nature of adaptive diffusion, we have to deal with even and odd times separately. To focus on the key insights and computations, we first prove Theorem 11.4(b) when t_1 and t_2 are both even—this is in Section 13.3. The cases when one or both of t_1 and t_2 are odd are similar but more complicated, while not adding anything conceptually—hence we defer the proof in these cases to Appendix A.

13.1. **Source detection.** The proof of Theorem 11.4(a) builds on similar ideas as the proof of Theorem 11.5 in Section 12. Recall the notation that we introduced in Section 12, which we use here.

Proof of Theorem 11.4(a). Assume first that t_1 and t_2 are even; this simplifies the proof and we explain at the end what changes if either time is odd. Then for $i \in \{1, 2\}$ we have that $G^i_{t_i}$ is a ball of radius $t_i/2$ with center $vs^i_{t_i}$. The adversary can thus determine the two virtual sources $vs^1 \equiv vs^1_{t_1}$ and $vs^2 \equiv vs^2_{t_2}$.

By definition we always have that $v^* \in V^1_{t_1} \cap V^2_{t_2}$, that is, the source v^* is contained in both sets of infected nodes. Let P_{12} denote the set of vertices that are on the path in $\mathbb{T}_d$ between vs^1 and vs^2, excluding vs^1 and vs^2. Furthermore, define the set $S := P_{12} \cap V^1_{t_1} \cap V^2_{t_2}$. Let A_{12} denote the event that vs^1 and vs^2 are in different subtrees away from v^*; that is,

$$A_{12} := \left\{ T^{v^*}_{vs^1} \cap T^{v^*}_{vs^2} = \emptyset \right\}. \tag{13.1}$$

Since the two diffusions are independent and the first step of the virtual source is to a uniformly random neighbor of v^*, we have that $\mathbb{P}(A_{12}) = (d-1)/d$. The main observation is that, on the event A_{12}, we have that $v^* \in P_{12}$; see Figure 8 for an illustration.[5] Consequently, on the event A_{12} we also have that $v^* \in S$.

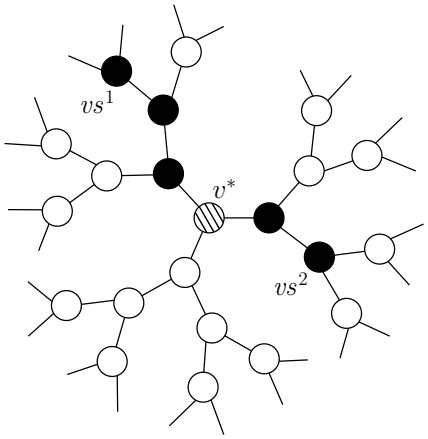

FIGURE 8. **Detecting the source from two observations.** If the two virtual sources are in different subtrees, then the path connecting them contains the source v^*.

[5]The two virtual sources can indeed be excluded from P_{12} and we still have that $v^* \in P_{12}$ on the event A_{12}. This is because the virtual source can never be the true source, by construction. This assumes that $t_1, t_2 \geq 1$—which holds, since we assume in the proof that $t_1, t_2 \geq 2$. In any case, if $\min\{t_1, t_2\} < 2$, then one of the observed snapshots contains at most two vertices, so a random guess succeeds in identifying the source with probability at least $1/2$.

This suggests a natural estimator: if $S \neq \emptyset$, let $\widehat{v}$ be a uniformly randomly chosen node from S (note that S is a measurable function of $G^1_{t_1}$ and $G^2_{t_2}$); if $S = \emptyset$ (this occurs when $\delta(vs^1, vs^2) \leq 1$), let $\widehat{v}$ be an arbitrary node. Then, given A_{12} and S, the conditional probability that $\widehat{v} = v^*$ is $1/|S|$ (note that A_{12} implies that $|S| \geq 1$, as we argued above). We have thus shown that

$$\mathbb{P}\left(\widehat{v} = v^*\right) \geq \mathbb{P}\left(\widehat{v} = v^* \,|\, A_{12}\right) \mathbb{P}\left(A_{12}\right) = \mathbb{E}\left[1/|S| \,|\, A_{12}\right] \frac{d-1}{d}.$$

To conclude, it suffices to show that $|S| \leq \min\{t_1/2, t_2/2\}$ whenever A_{12} holds. To see this, note that the intersection $P_{12} \cap V^1_{t_1}$ contains at most $t_1/2$ nodes, since $G^1_{t_1}$ is a (closed) ball of radius $t_1/2$ centered at vs^1, the path P_{12} starts at the virtual source vs^1, and vs^1 is not included in P_{12}. Thus $|S| \leq \left|P_{12} \cap V^1_{t_1}\right| \leq t_1/2$. Similarly, $P_{12} \cap V^2_{t_2}$ contains at most $t_2/2$ nodes, and the claim follows.

Finally, we explain what changes when t_i is odd for $i = 1$ and/or $i = 2$. If $G^i_{t_i}$ is a ball, then its center is $vs^i_{t_i}$, so the adversary can again determine the virtual source at time t_i and everything is unchanged. If $G^i_{t_i}$ is not a ball, then it is symmetric about the edge connecting vs_{t_i-1} and vs_{t_i}. Thus the adversary can determine the set $\{vs_{t_i-1}, vs_{t_i}\}$. Connecting *both* of these virtual sources with the other virtual source(s), we again obtain a path, where now at both ends of the path we have either one or two virtual sources. In any case, we can define P_{12} analogously, where again the known virtual sources are not considered as part of P_{12}. The rest of the proof is unchanged. □

13.2. **Maximum likelihood source estimation.** In order to prove Theorem 11.4(b), we need to understand maximum likelihood source estimation. Here we discuss this for adaptive diffusions in general. Recall that an adaptive diffusion protocol is given by the probabilities $\alpha(t,h) \in [0,1]$, with $t \in \{2,4,6,\ldots\}$ and $h \in \{1,2,3,\ldots,t/2\}$, which determine the distribution of the path of the virtual source $\{vs_t\}_{t\geq 0}$. Let $h_t := \delta\left(vs_t, v^*\right)$ denote the graph distance between vs_t and v^*, and let $p(t,h) := \mathbb{P}\left(h_t = h\right)$ denote the distribution of h_t.

When determining the likelihood function $L(v) = \mathbb{P}\left(G_t \,|\, v^* = v\right)$ we have to specify whether the value of t is known or not (since it is not always possible to infer the value of t from the observation G_t). We assume in the following that t is *known*. Note that knowing t can only help the adversary and hence any upper bounds on the success probability of the MLE under this assumption still hold without this assumption. Furthermore, the rumor source detection results (Theorem 11.4(a) and Theorem 11.5) hold regardless of whether we assume this or not. Finally, note that this assumption is also what is used in previous works [23, 21, 22].

We now determine the likelihood function $L(v) = \mathbb{P}(G_t \,|\, v^* = v)$ for even t; it is similar for odd t, but we leave this for later. First, we always have that $v^* \in V_t \setminus \{vs_t\}$, so $L(v) = 0$ if $v \notin V_t \setminus \{vs_t\}$. Next, since G_t is a ball of radius $t/2$ with center vs_t, it is fully determined by the position of the virtual source, together with the time t. It is important to note a key symmetry property of adaptive diffusion: all nodes at a particular distance from the virtual source are equally likely to have been the source. This is because the virtual source always moves to a uniformly randomly chosen neighbor away from the source. Thus the distribution of the virtual source is completely determined by the distribution of h_t. Altogether, since there are $d(d-1)^{h-1}$ nodes at distance $h \geq 1$ from a particular vertex, we obtain that

$$L(v) = \frac{1}{d(d-1)^{\delta(v,vs_t)-1}} p\left(t, \delta\left(v, vs_t\right)\right) \mathbf{1}_{\{v \in V_t \setminus \{vs_t\}\}}. \tag{13.2}$$

Now assume that we have k independent observations of infected subgraphs, $G_{t_i}^i = \left(V_{t_i}^i, E_{t_i}^i\right)$ for $i \in \{1, \ldots, k\}$, started from a fixed source v^*. Assume also, for now, that all the times $t_1, \ldots, t_k$ are even. Then, by independence, the likelihood function is

$$L(v) = \left(\frac{d-1}{d}\right)^k \prod_{i=1}^k p\left(t_i, X_i(v)\right) \cdot (d-1)^{-X_i(v)} \mathbf{1}_{\left\{v \in \bigcap_{i=1}^k \left(V_{t_i}^i \setminus \left\{vs_{t_i}^i\right\}\right)\right\}},$$

where we have introduced

$$X_i(v) := \delta\left(v, vs_{t_i}^i\right) \tag{13.3}$$

for convenience (and recall that we can determine $vs_{t_i}^i$, and thus also $X_i(v)$, from $G_{t_i}^i$). By taking logarithms, we obtain that the MLE satisfies

$$\widehat{v}_{\mathrm{ML}} \in \underset{v \in \bigcap_{i=1}^k \left(V_{t_i}^i \setminus \left\{vs_{t_i}^i\right\}\right)}{\arg\max} \sum_{i=1}^k \left\{\log p\left(t_i, X_i(v)\right) - X_i(v) \log(d-1)\right\}. \tag{13.4}$$

We now turn to determining the likelihood function $L(v) = \mathbb{P}(G_t \,|\, v^* = v)$ for odd t. This is similar to the case of even t, but there are slight differences. Specifically, there are two cases to distinguish: when t is odd, the observed graph G_t is either a ball or it is not (in which case it consists of two balanced rooted trees of depth $(t-1)/2$, whose roots are connected by an edge).

The former case occurs when the virtual source does not move at time $t-1$, that is, when $vs_{t-1} = vs_t$. In this case, we know that $G_{t-1} = G_t$, we know the likelihood of G_{t-1} (which is given by (13.2) with t replaced by $t-1$), and in order to obtain the likelihood of G_t we have to multiply this by the probability that $vs_{t-1} = vs_t$, which is $\alpha(t-1, X(v))$, where $X(v) = \delta(v, vs_{t-1}) = \delta(v, vs_t)$.

In the latter case, when G_t is not a ball, we know that the virtual source moved at time $t-1$. Furthermore, we can determine the set $\{vs_{t-1}, vs_t\}$, as these two vertices are connected by the central edge of G_t. In this case, we define $X(v) := \min\{\delta(v, vs_{t-1}), \delta(v, vs_t)\}$ (note that $X(v)$ can be determined from G_t). In order to obtain the likelihood of G_t we have to multiply the expression in (13.2) (with t replaced by $t-1$ and $\delta(v, vs_t)$ replaced with $\min\{\delta(v, vs_{t-1}), \delta(v, vs_t)\}$) with the probability that $vs_{t-1} \neq vs_t$, which is $1 - \alpha(t-1, X(v))$.

Altogether, when t is odd we have that the likelihood function is

$$L(v) = \begin{cases} \frac{1}{d(d-1)^{X(v)-1}} p\left(t-1, X(v)\right) \alpha(t-1, X(v)) \mathbf{1}_{\{v \in V_t \setminus \{vs_t\}\}} & \text{if } G_t \text{ is a ball,} \\ \frac{1}{d(d-1)^{X(v)-1}} p\left(t-1, X(v)\right) \{1 - \alpha(t-1, X(v))\} \mathbf{1}_{\{v \in V_t \setminus \{vs_{t-1}, vs_t\}\}} & \text{otherwise,} \end{cases} \tag{13.5}$$

where $X(v) := \min\{\delta(v, vs_{t-1}), \delta(v, vs_t)\}$ (note that this definition of $X(v)$ works for both cases; when G_t is a ball then $vs_{t-1} = vs_t$ and hence $X(v) = \delta(v, vs_{t-1}) = \delta(v, vs_t)$).

13.3. **Source obfuscation — even times.** We are now ready to prove Theorem 11.4(b). We first prove this when both t_1 and t_2 are even. This is done in order to highlight the key insights and computations. The remaining cases (when one or both of t_1 and t_2 are odd) are similar but more complicated and hence are deferred to Appendix A.

Proof of Theorem 11.4(b) when t_1 and t_2 are both even. We may assume in the following that $t_1, t_2 \geq 4$, since when $\min\{t_1, t_2\} = 2$ then the right hand side of (11.4) is greater than 1 and thus the statement is vacuously true.

Consider the adaptive diffusion protocol—which we term the *uniform protocol* $\mathcal{U}$ for reasons to become clear—given by the probabilities

$$\alpha_{\mathcal{U}}(t, h) := \frac{t - 2h + 2}{t + 2} \tag{13.6}$$

for $t \in \{2, 4, 6, \ldots\}$ and $h \in \{1, 2, \ldots, t/2\}$. This is the same protocol introduced by Fanti et al. [23] to achieve perfect obfuscation from a single snapshot on $\mathbb{Z}$—the difference is that here we use this protocol regardless of the degree d. The important property of this protocol is that the distance $h_t := \delta\left(vs_t, v^*\right)$ between the virtual source vs_t and the true source v^* is *uniformly distributed* over the set of possible values $\{1, 2, \ldots, t/2\}$, for all even t. That is, for all even t we have that

$$p_{\mathcal{U}}(t, h) = \frac{2}{t} \mathbf{1}_{\{h \in \{1, 2, \ldots, t/2\}\}}. \tag{13.7}$$

This can be shown by induction; we leave the details to the reader.

We now turn to analyzing the maximum likelihood estimator of the source, $\widehat{v}_{\mathrm{ML}}$, given two independent snapshots $G^1_{t_1}$ and $G^2_{t_2}$. Recall that we assume now that t_1 and t_2 are both even. The adversary can thus determine the two virtual sources $vs^1 \equiv vs^1_{t_1}$ and $vs^2 \equiv vs^2_{t_2}$. By plugging in (13.7) into (13.4), we obtain that the MLE satisfies

$$\widehat{v}_{\mathrm{ML}} \in \operatorname*{arg\,min}_{v \in V^1_{t_1} \cap V^2_{t_2} \setminus \{vs^1, vs^2\}} \left(X_1(v) + X_2(v)\right),$$

where recall from (13.3) that $X_i(v) = \delta(v, vs^i)$ for $i \in \{1, 2\}$. In words, the maximum likelihood estimator minimizes the sum of the distances to the two virtual sources, over all nodes that were infected in both diffusions, excluding the two virtual sources.

To understand the MLE better we distinguish three cases, the last one being the most important:

(1) If $vs^1 = vs^2$, then $\widehat{v}_{\mathrm{ML}}$ chooses a neighbor of $vs^1 = vs^2$ uniformly at random.

(2) If $\delta(vs^1, vs^2) = 1$, then $\widehat{v}_{\mathrm{ML}}$ chooses a neighbor of the set $\{vs^1, vs^2\}$ uniformly at random.[6]

(3) If $\delta(vs^1, vs^2) \geq 2$, then $X_1(v) + X_2(v)$ is minimized when v is on the shortest path between vs^1 and vs^2. Let P_{12} denote the set of vertices that are on the shortest path between vs^1 and vs^2, excluding vs^1 and vs^2. Furthermore, define the set $S := P_{12} \cap V^1_{t_1} \cap V^2_{t_2}$ and note that when $\delta(vs^1, vs^2) \geq 2$, then S is nonempty, because the vertex in P_{12} that is closest to v^* is always in S. We have thus argued that the likelihood function is maximized at the nodes in S and thus the maximum likelihood estimator $\widehat{v}_{\mathrm{ML}}$ chooses a node from S uniformly at random.

Note that $\widehat{v}_{\mathrm{ML}}$ is (essentially) the same as the estimator $\widehat{v}$ introduced in the proof of part (a) of Theorem 11.4.

Let A_{12} denote the event that vs^1 and vs^2 are in different subtrees away from v^* (see (13.1)), and note that $\mathbb{P}(A_{12}) = (d-1)/d$. Observe that if the event A_{12} holds, then necessarily $\delta(vs^1, vs^2) \geq 2$, and hence the first two cases above imply that A_{12} does not hold. To compute the probability that the MLE $\widehat{v}_{\mathrm{ML}}$ is correct, we may condition on whether or not A_{12} holds:

$$\begin{aligned}
\mathbb{P}\left(\widehat{v}_{\mathrm{ML}} = v^*\right) &= \mathbb{P}\left(\widehat{v}_{\mathrm{ML}} = v^* \,|\, A_{12}\right) \mathbb{P}\left(A_{12}\right) + \mathbb{P}\left(\widehat{v}_{\mathrm{ML}} = v^* \,\middle|\, A^C_{12}\right) \mathbb{P}\left(A^C_{12}\right) \\
&= \mathbb{P}\left(\widehat{v}_{\mathrm{ML}} = v^* \,|\, A_{12}\right) \cdot \frac{d-1}{d} + \mathbb{P}\left(\widehat{v}_{\mathrm{ML}} = v^* \,\middle|\, A^C_{12}\right) \cdot \frac{1}{d}. \qquad (13.8)
\end{aligned}$$

[6] Here we use that $t_1, t_2 \geq 4$, to ensure that all neighbors of the set $\{vs^1, vs^2\}$ are in $V^1_{t_1} \cap V^2_{t_2}$.

Let us now turn to computing $\mathbb{P}\left(\widehat{v}_{\mathrm{ML}} = v^* \,\middle|\, A_{12}^C\right)$. There are two cases when the MLE can be correct, given that A_{12} does not hold. First, corresponding to Case (1) above: if $vs^1 = vs^2$ and $\delta(v^*, vs^1) = \delta(v^*, vs^2) = 1$, then the MLE is correct with probability $1/d$. Second, corresponding to Case (2) above: if $\delta(v^*, vs^1) = \delta(vs^1, vs^2) = 1$ or if $\delta(v^*, vs^2) = \delta(vs^1, vs^2) = 1$, then the MLE is correct with probability $1/(2d-2)$. If $\delta(vs^1, vs^2) \geq 2$ and A_{12} does not hold, then $\widehat{v}_{\mathrm{ML}} \neq v^*$. Putting these together and using (13.7) we obtain that

$$\mathbb{P}\left(\widehat{v}_{\mathrm{ML}} = v^* \,\middle|\, A_{12}^C\right) = \frac{2}{t_1} \cdot \frac{2}{t_2} \cdot \frac{1}{d} + 2 \cdot \frac{2}{t_1} \cdot \frac{2}{t_2} \cdot \frac{1}{2d-2} = \frac{4}{t_1 t_2}\left(\frac{1}{d} + \frac{1}{d-1}\right). \tag{13.9}$$

We now turn to computing $\mathbb{P}\left(\widehat{v}_{\mathrm{ML}} = v^* \,|\, A_{12}\right)$. Given A_{12} and S, the conditional probability that $\widehat{v}_{\mathrm{ML}} = v^*$ is $1/|S|$. We thus have that

$$\mathbb{P}\left(\widehat{v}_{\mathrm{ML}} = v^* \,|\, A_{12}\right) = \mathbb{E}\left[1/|S| \,|\, A_{12}\right]. \tag{13.10}$$

On the event A_{12}, we can express $|S|$ as a function of $X_1(v^*)$ and $X_2(v^*)$ as follows. First, the set S always contains v^* when A_{12} holds. Next, there are $X_1(v^*) - 1$ nodes on the path P_{12} between v^* and vs^1. However, only the $t_2/2 - X_2(v^*)$ nodes of these that are closest to v^* are in $V_{t_2}^2$ as well. Similarly, there are $X_2(v^*) - 1$ nodes on the path P_{12} between v^* and vs^2, but only the $t_1/2 - X_1(v^*)$ nodes of these that are closest to v^* are in $V_{t_1}^1$ as well. Altogether, on the event A_{12} we have that

$$|S| = 1 + \min\left\{X_1(v^*) - 1, t_2/2 - X_2(v^*)\right\} + \min\left\{X_2(v^*) - 1, t_1/2 - X_1(v^*)\right\}. \tag{13.11}$$

Recall from (13.7) that $X_i(v^*)$ is uniformly distributed on $\{1, 2, \ldots, t_i/2\}$, for $i \in \{1, 2\}$. Moreover, $X_1(v^*)$ and $X_2(v^*)$ are independent. Both of these statements hold conditioned on A_{12}. Therefore, plugging in (13.11) into (13.10) and writing out the expectation we obtain that

$$\mathbb{P}\left(\widehat{v}_{\mathrm{ML}} = v^* \,|\, A_{12}\right) = \frac{1}{st} \sum_{j=1}^{s} \sum_{\ell=1}^{t} \frac{1}{1 + \min\left\{j-1, t-\ell\right\} + \min\left\{\ell - 1, s - j\right\}}, \tag{13.12}$$

where we have introduced $s := \min\left\{t_1, t_2\right\}/2$ and $t := \max\left\{t_1, t_2\right\}/2$ in order to abbreviate notation. With this notation, we can write $|S|$ from (13.11) more succintly by breaking things into three cases, as follows:

- If $X_1(v^*) + X_2(v^*) \leq s + 1$, then $|S| = X_1(v^*) + X_2(v^*) - 1$.
- If $s + 1 < X_1(v^*) + X_2(v^*) \leq t + 1$, then $|S| = s$.
- If $t + 1 < X_1(v^*) + X_2(v^*)$, then $|S| = 1 + s + t - (X_1(v^*) + X_2(v^*))$.

Accordingly, we can break the sum in (13.12) into three parts. Let $\mathcal{I} := \{(j,\ell) : 1 \le j \le s, 1 \le \ell \le t\}$ denote the index set over which we take the sum in (13.12). We can write it as the disjoint union $\mathcal{I} = \mathcal{I}_1 \cup \mathcal{I}_2 \cup \mathcal{I}_3$, where $\mathcal{I}_1 := \{(j,\ell) \in \mathcal{I} : j + \ell \le s + 1\}$, $\mathcal{I}_2 := \{(j,\ell) \in \mathcal{I} : s + 1 < j + \ell \le t + 1\}$, and $\mathcal{I}_3 := \{(j,\ell) \in \mathcal{I} : t + 1 < j + \ell\}$. We now consider the index sets $\mathcal{I}_1$, $\mathcal{I}_2$, and $\mathcal{I}_3$ separately.

First, suppose that $m \in \{2, 3, \dots, s+1\}$. There are $m - 1$ pairs of indices $(j,\ell) \in \mathcal{I}_1$ such that $j + \ell = m$. For each such index pair, the fraction in (13.12) is equal to $1/(m-1)$. Since there are s different values of m, the sum over the index set $\mathcal{I}_1$ is equal to s.

Next, observe that $|\mathcal{I}_2| = s(t-s)$. For every $(j,\ell) \in \mathcal{I}_2$, the fraction in (13.12) is $1/s$. Therefore the sum over the index set $\mathcal{I}_2$ is equal to $s(t-s)/s = t - s$.

Finally, suppose that $m \in \{t+2, \dots, t+s\}$. There are $1 + s + t - m$ pairs of indices $(j,\ell) \in \mathcal{I}_3$ such that $j + \ell = m$. For each such index pair, the fraction in (13.12) is equal to $1/(1+s+t-m)$. Since there are $s - 1$ different values of m, the sum over the index set $\mathcal{I}_3$ is equal to $s - 1$.

Putting together the previous three paragraphs, we thus have that

$$\sum_{j=1}^{s} \sum_{\ell=1}^{t} \frac{1}{1 + \min\{j-1, t-\ell\} + \min\{\ell-1, s-j\}} = s + t - 1.$$

Plugging this back into (13.12), and returning to the notation of t_1 and t_2, we obtain that

$$\mathbb{P}\left(\widehat{v}_{\mathrm{ML}} = v^* \,|\, A_{12}\right) = \frac{s+t-1}{st} = \frac{2t_1 + 2t_2 - 4}{t_1 t_2}. \tag{13.13}$$

Putting together (13.8), (13.9), and (13.13), we have obtained that

$$\mathbb{P}\left(\widehat{v}_{\mathrm{ML}} = v^*\right) = \frac{d-1}{d} \cdot \frac{2t_1 + 2t_2 - 4}{t_1 t_2} + \frac{1}{d} \cdot \frac{4}{t_1 t_2} \left(\frac{1}{d} + \frac{1}{d-1}\right) < \frac{d-1}{d} \cdot \frac{2t_1 + 2t_2}{t_1 t_2},$$

where we used that $1/d + 1/(d-1) < 1$. Using that $2t_1 + 2t_2 \le 4\max\{t_1, t_2\}$, we obtain the bound in (11.4), when t_1 and t_2 are both even. □

14. Local spreading vs. source obfuscation

In this section we prove Theorem 11.6. Recall the notation we introduced in previous sections, which we use here as well. In particular, $h_t := \delta(vs_t, v^*)$ denotes the graph distance between vs_t and v^* and $p(t,h) := \mathbb{P}(h_t = h)$. We will also use the elementary inequalities

$$(d-1)^{t/2} \le N_t \le \frac{d}{d-2}(d-1)^{t/2}. \tag{14.1}$$

Proof of Theorem 11.6. Our starting observation is that, due to the definition of adaptive diffusion protocols, we have that

$$R_t = \frac{t}{2} - h_t. \tag{14.2}$$

Thus in order to understand R_t it is equivalent to understand h_t.

We first turn to part (a) of the theorem. We described the likelihood function in Section 13.2, see (13.2) in particular, from which it follows that

$$\mathbb{P}\left(\widehat{v}_{\mathrm{ML}} = v^*\right) = \max_{1 \le h \le t/2} \frac{p(t,h)}{d\,(d-1)^{h-1}}. \tag{14.3}$$

The assumption (11.6) thus implies that

$$p(t,h) \le \frac{Cd\,(d-1)^{h-1}}{N_t^{\gamma}} \le Cd\,(d-1)^{h-\gamma t/2-1} \tag{14.4}$$

for all $1 \le h \le t/2$, where in the second inequality we used (14.1). Now define

$$m_t := \frac{\gamma t}{2} - \frac{\log(Ct)}{\log(d-1)} - 1.$$

We then have that

$$\begin{aligned}\mathbb{P}\left(h_t \le m_t\right) &\le \sum_{h=1}^{\lfloor m_t \rfloor} Cd\,(d-1)^{h-\gamma t/2-1} = Cd\,(d-1)^{-\gamma t/2}\,\frac{(d-1)^{\lfloor m_t \rfloor} - 1}{d-2} \\ &\le Cd\,(d-1)^{m_t - \gamma t/2} = \frac{d}{d-1} \cdot \frac{1}{t} \le \frac{2}{t}.\end{aligned}$$

In particular, we thus have that $\mathbb{P}\left(h_t > m_t\right) \ge 1 - 2/t$. Therefore

$$\mathbb{E}\left[h_t\right] \ge m_t \mathbb{P}\left(h_t > m_t\right) \ge m_t \left(1 - \frac{2}{t}\right) \ge \frac{\gamma t}{2} - \frac{\log(Ct)}{\log(d-1)} - 1 - \gamma.$$

Now using (14.2) we have that

$$\mathbb{E}\left[R_t\right] = \frac{t}{2} - \mathbb{E}\left[h_t\right] \le (1-\gamma)\,\frac{t}{2} + \frac{\log(Ct)}{\log(d-1)} + 1 + \gamma,$$

which concludes the proof of part (a) of the theorem.

We now turn to part (b) of the theorem. Consider the adaptive diffusion protocol defined as follows:

- For $t \le 2/\gamma$, let $\alpha(t,h) = 1$ for all $1 \le h \le t/2$.
- For $t > 2/\gamma$, let $\alpha(t,h) = 1$ if $\lfloor \gamma t/2 \rfloor = \lfloor \gamma\,(t/2+1) \rfloor$ and let $\alpha(t,h) = 0$ otherwise.

This construction guarantees that for all even t we have that $h_t = 1$ if $t \leq 2/\gamma$, while for even $t > 2/\gamma$ we have that

$$h_t = \lfloor \gamma t/2 \rfloor$$

deterministically. Thus by (14.2) we have, for all even t satisfying $t > 2/\gamma$, that

$$R_t = t/2 - h_t = t/2 - \lfloor \gamma t/2 \rfloor \geq (1-\gamma)\, t/2.$$

On the other hand, by (14.3) we have, for all even t satisfying $t > 2/\gamma$, that

$$\mathbb{P}\left(\widehat{v}_{\mathrm{ML}} = v^*\right) = \frac{1}{d\,(d-1)^{\lfloor \gamma t/2 \rfloor - 1}} \leq \frac{1}{d\,(d-1)^{\gamma t/2 - 2}}.$$

From (14.1) it follows that $(d-1)^{-t/2} \leq \left(d/\left(d-2\right)\right)/N_t$ and so

$$\mathbb{P}\left(\widehat{v}_{\mathrm{ML}} = v^*\right) \leq \frac{(d-1)^2}{d}\left(\frac{d}{d-2}\right)^{\gamma} \frac{1}{N_t^{\gamma}} \leq \frac{(d-1)^2}{d-2} \cdot \frac{1}{N_t^{\gamma}} \leq \frac{2\,(d-1)}{N_t^{\gamma}},$$

where in the second inequality we used that $\gamma \leq 1$ and in the third inequality we used that $d \geq 3$. □

15. Discussion

The main message of this work is that while adaptive diffusion protocols can hide the source from a snapshot adversary, they are ineffective when the adversary has access to multiple independent snapshots. The main question raised by our work is whether there exist other diffusion protocols that can obfuscate the source against such an adversary.

We make several simplifying assumptions in this work, which are important to discuss and study further. First, we assume throughout that the underlying graph is the infinite d-regular tree $\mathbb{T}_d$ (with $d \geq 3$), which is not a realistic model of real-world (social) networks. It is therefore important to study the questions we consider here on other underlying graphs, for instance, on more realistic models as well as on real-world social networks. We conjecture that our qualitative conclusions will carry over to more realistic settings, which motivates studying such a simplified setting.

We also assume that the adversary observes multiple *independent* snapshots. Previous work has considered multiple *sequential* snapshots (in time): Wang et al. [60] show that additional sequential snapshots cannot improve detectability under the SI model, while Fanti et al. [22] show that they can improve the detection probability at most logarithmically for adaptive diffusions. On the other hand, Cai et al. [8] show that multiple sequential snapshots can help detection when the

spreading rates are heterogeneous, both theoretically and on Twitter data. As mentioned before, Wang et al. [60] show that multiple independent snapshots help significantly with detection under the SI model, and our results extend this to the family of adaptive diffusions. An interesting question is what happens in between, when the adversary observes multiple correlated snapshots (that are not necessarily sequential observations of the same diffusion). In particular, can spreading protocols take advantage of correlation in order to obfuscate the source against an adversary who observes multiple snapshots?

This question is related to local spreading as follows. An adversary who observes multiple snapshots can always use the following simple source estimator: pick a node uniformly at random among those which are infected in each snapshot. The probability of success of this estimator is the inverse of the size of the set of nodes which are infected in each snapshot. To minimize this, a spreading protocol should aim to maximize the size of this set. This can be done by having highly correlated snapshots, or by having a large amount of local spreading (which we have discussed in Sections 11.5 and 14). In any case, we conjecture that if there is a reasonable amount of independence among the observed snapshots, then the results will be qualitatively similar to those which we have obtained.

There are also many natural variations on what information the adversary has access to. For instance, Fanti et al. [20, 22] consider a spy-based model, where a fraction of nodes are corrupted and continuously monitor metadata such as message timestamps; they also consider a mixed model using both spies and a snapshot. Other information models include having a snapshot and additional relative information about the infection times of a fraction of node pairs [35], having partial infection timestamps [56], and having a noisy time series of observations [52, 51]. Understanding how our results change under these different information models of adversaries is a natural question for future work.

Further avenues to explore related to our work include game-theoretic formulations [39], optimal sensor/spy placement [50], confidence sets for the source [34], and multiple rumor sources [49].

In conclusion, most results in this space—including ours in this work—are positive in terms of rumor source detection, and thus highlight major difficulties with guaranteeing anonymity for the source of a message in a social network. As surveillance techniques grow ever more prominent in society, this emphasizes the need for further research, with the hope of ultimately providing robust anonymity guarantees.

Appendix A. Proof of Theorem 11.4(b) when one or both of t_1 and t_2 are odd

Here we prove Theorem 11.4(b) when one or both of t_1 and t_2 are odd. This is similar to the proof presented in Section 13.3 when both t_1 and t_2 are even, but there are more cases to consider (especially when both t_1 and t_2 are odd). To keep things clear, we also separate below the proof when one of t_1 and t_2 is even and the other is odd, from the proof when both t_1 and t_2 are odd.

A.1. When one of t_1 and t_2 is even and the other is odd.

Proof of Theorem 11.4(b) when one of t_1 and t_2 is even and the other is odd. W.l.o.g. suppose that t_1 is even and t_2 is odd. We may (and will) assume that $t_1 \geq 4$ and that $t_2 \geq 5$, since if $\min\{t_1, t_2\} \leq 3$, then the right hand side of (11.4) is greater than 1 and thus the statement is vacuously true.

Recall that we are analyzing the MLE for the *uniform protocol* given by the probabilities in (13.6) and for which we have that (13.7) holds. We start with a few observations. First, $G^1_{t_1}$ is a ball of radius $t_1/2$ around $vs^1 \equiv vs^1_{t_1}$ and hence we can determine vs^1. We may thus define $X_1(v) := \delta\left(v, vs^1\right)$. Next, the observation $G^2_{t_2}$ is either a ball or it is not. If $G^2_{t_2}$ is a ball, then it is a ball of radius $(t_2-1)/2$ around $vs^2_{t_2-1} = vs^2_{t_2}$ and hence we can determine $vs^2_{t_2-1} = vs^2_{t_2}$. If $G^2_{t_2}$ is not a ball, then its central edge is $\left\{vs^2_{t_2-1}, vs^2_{t_2}\right\}$ and hence we can determine the set $\left\{vs^2_{t_2-1}, vs^2_{t_2}\right\}$. In any case, we may thus define $X_2(v) := \min\left\{\delta\left(v, vs^2_{t_2-1}\right), \delta\left(v, vs^2_{t_2}\right)\right\}$ and note that the function $X_2 : V \mapsto \mathbb{R}$ is determined by the observation $G^2_{t_2}$.

With this notation, using the expressions (13.2) and (13.5), the independence of the two observations, and substituting the expressions in (13.6) and (13.7), we obtain that the likelihood function is the following:

$$L(v) = \begin{cases} \left(\frac{d-1}{d}\right)^2 \cdot \frac{2}{t_1} \cdot \frac{2}{t_2-1} \cdot (d-1)^{-(X_1(v)+X_2(v))} \cdot \frac{t_2+1-2X_2(v)}{t_2+1} \cdot \mathbf{1}_{\left\{v \in V^1_{t_1} \cap V^2_{t_2} \setminus \left\{vs^1_{t_1}, vs^2_{t_2}\right\}\right\}} & \text{if } G^2_{t_2} \text{ is a ball,} \\ \left(\frac{d-1}{d}\right)^2 \cdot \frac{2}{t_1} \cdot \frac{2}{t_2-1} \cdot (d-1)^{-(X_1(v)+X_2(v))} \cdot \frac{2X_2(v)}{t_2+1} \cdot \mathbf{1}_{\left\{v \in V^1_{t_1} \cap V^2_{t_2} \setminus \left\{vs^1_{t_1}, vs^2_{t_2}, vs^2_{t_2-1}\right\}\right\}} & \text{otherwise.} \end{cases}$$

The first three factors in the expressions above do not depend on v and hence do not matter for the MLE. By taking logarithms and pulling out a minus sign, we obtain that the MLE satisfies the

following:

$$\widehat{v}_{\mathrm{ML}} \in \begin{cases} \underset{v \in V^1_{t_1} \cap V^2_{t_2} \setminus \left\{vs^1_{t_1}, vs^2_{t_2}\right\}}{\arg\min} \left[(X_1(v) + X_2(v)) \log(d-1) - \log\left(t_2 + 1 - 2X_2(v)\right)\right] & \text{if } G^2_{t_2} \text{ is a ball,} \\ \underset{v \in V^1_{t_1} \cap V^2_{t_2} \setminus \left\{vs^1_{t_1}, vs^2_{t_2}, vs^2_{t_2-1}\right\}}{\arg\min} \left[(X_1(v) + X_2(v)) \log(d-1) - \log X_2(v)\right] & \text{otherwise.} \end{cases} \tag{A.1}$$

To understand the MLE in (A.1) better, we distinguish six cases. These are based on whether $X_2(vs^1)$ is 0, 1, or at least 2, and whether or not $G^2_{t_2}$ is a ball. Compared to the case when both t_1 and t_2 are even (see Section 13.3) we have twice as many cases to consider because $G^2_{t_2}$ can be a ball or not. In all of the six cases there is a simple description of the MLE:

(1) *$G^2_{t_2}$ is a ball and $X_2(vs^1) = 0$.* In this case $vs^1 = vs^2_{t_2} = vs^2_{t_2-1}$ and both terms in (A.1) ($(X_1(v) + X_2(v)) \log(d-1)$ and $-\log\left(t_2 + 1 - 2X_2(v)\right)$) are minimized by the neighbors of vs^1. Therefore $\widehat{v}_{\mathrm{ML}}$ chooses a neighbor of vs^1 uniformly at random.

(2) *$G^2_{t_2}$ is not a ball and $X_2(vs^1) = 0$.* In this case $vs^2_{t_2-1}$ and $vs^2_{t_2}$ are neighbors and $vs^1 \in \left\{vs^2_{t_2-1}, vs^2_{t_2}\right\}$. The function $(X_1(v) + X_2(v)) \log(d-1)$ is minimized (among vertices not in $\left\{vs^1_{t_1}, vs^2_{t_2}, vs^2_{t_2-1}\right\}$) by the neighbors of vs^1 that are not in $\left\{vs^2_{t_2}, vs^2_{t_2-1}\right\}$. The expression in (A.1) also contains another term, $-\log X_2(v)$, which is not minimized among the neighbors of vs^1. However, this is a lower order term compared to the first term and it can be seen that the full expression in (A.1) is minimized by the neighbors of vs^1 that are not in $\left\{vs^2_{t_2}, vs^2_{t_2-1}\right\}$. Therefore $\widehat{v}_{\mathrm{ML}}$ chooses a neighbor of vs^1 that is not in $\left\{vs^2_{t_2}, vs^2_{t_2-1}\right\}$ uniformly at random.

(3) *$G^2_{t_2}$ is a ball and $X_2(vs^1) = 1$.* In this case $vs^2_{t_2-1} = vs^2_{t_2} \equiv vs^2$, and vs^1 and vs^2 are neighbors. The first term in (A.1) ($(X_1(v) + X_2(v)) \log(d-1)$) is minimized by the neighbors of the set $\left\{vs^1, vs^2\right\}$. The second term in (A.1) ($-\log\left(t_2 + 1 - 2X_2(v)\right)$) is minimized by the neighbors of vs^2 that are not vs^1. Thus the whole expression is minimized by the neighbors of vs^2 that are not vs^1. Therefore $\widehat{v}_{\mathrm{ML}}$ chooses one of the $d-1$ neighbors of vs^2 that is not vs^1, uniformly at random.[7]

(4) *$G^2_{t_2}$ is not a ball and $X_2(vs^1) = 1$.* This is similar to Case (2) above and we omit the details for brevity. The MLE is the same: $\widehat{v}_{\mathrm{ML}}$ chooses one of the $d-1$ neighbors of vs^1 that is not in $\left\{vs^2_{t_2}, vs^2_{t_2-1}\right\}$, uniformly at random.

[7]Here we use that $t_1 \geq 4$, to ensure that all neighbors of vs^2 are in $V^1_{t_1}$.

(5) $G^2_{t_2}$ *is a ball and* $X_2(vs^1) \geq 2$. In this case $vs^2_{t_2-1} = vs^2_{t_2} \equiv vs^2$. The expression in (A.1) contains two terms. The first term $((X_1(v) + X_2(v)) \log(d-1))$ is minimized on the shortest path between vs^1 and vs^2. The second term $(-\log(t_2 + 1 - 2X_2(v)))$ is minimized when $X_2(v)$ is minimized. We also have the constraint that $v \in V^1_{t_1} \cap V^2_{t_2} \setminus \{vs^1, vs^2\}$. Let P_{12} denote the set of vertices that are on the shortest path between vs^1 and vs^2, excluding vs^1 and vs^2. Define v' to be the vertex in $P_{12} \cap V^1_{t_1} \cap V^2_{t_2}$ that is closest to vs^2 (note that $P_{12} \cap V^1_{t_1} \cap V^2_{t_2}$ is nonempty, due to the assumption that $X_2(vs^1) \geq 2$). Given the constraints, v' is the unique vertex that minimizes both terms in the expression in (A.1). Therefore $\widehat{v}_{\mathrm{ML}} = v'$.

(6) $G^2_{t_2}$ *is not a ball and* $X_2(vs^1) \geq 2$. This is similar to Case (5) above, so we omit the details for brevity and just state the conclusion. Let v'' be the vertex in $P_{12} \cap V^1_{t_1} \cap V^2_{t_2}$ that is closest to vs^1 (note again that $P_{12} \cap V^1_{t_1} \cap V^2_{t_2}$ is nonempty, due to the assumption that $X_2(vs^1) \geq 2$). Then $\widehat{v}_{\mathrm{ML}} = v''$.

Now that we understand the MLE, we can compute the probability that it is correct. We may again condition on whether or not A_{12} holds (see (13.8)) to obtain that

$$\mathbb{P}(\widehat{v}_{\mathrm{ML}} = v^*) = \mathbb{P}(\widehat{v}_{\mathrm{ML}} = v^* \mid A_{12}) \cdot \frac{d-1}{d} + \mathbb{P}\left(\widehat{v}_{\mathrm{ML}} = v^* \,\middle|\, A^C_{12}\right) \cdot \frac{1}{d}. \tag{A.2}$$

Note that if A_{12} holds then we must be in Case (5) or in Case (6). Consequently, Cases (1), (2), (3), and (4) imply that A_{12} does not hold.

Let us start by computing $\mathbb{P}\left(\widehat{v}_{\mathrm{ML}} = v^* \,\middle|\, A^C_{12}\right)$. Recall from Cases (5) and (6) above that if $X_2(vs^1) \geq 2$ then $\widehat{v}_{\mathrm{ML}} \in P_{12}$, so if A^C_{12} also holds then $\widehat{v}_{\mathrm{ML}} \neq v^*$. Thus only Cases (1), (2), (3), and (4) contribute to the probability $\mathbb{P}\left(\widehat{v}_{\mathrm{ML}} = v^* \,\middle|\, A^C_{12}\right)$. In the following computations we use the expressions (13.6) and (13.7).

First, corresponding to Case (1) above: if $\delta\left(v^*, vs^1_{t_1}\right) = \delta\left(v^*, vs^2_{t_2-1}\right) = 1$ and $vs^2_{t_2-1} = vs^2_{t_2}$, then the MLE is correct with probability $1/d$. This gives a contribution of $\frac{2}{t_1} \cdot \frac{2}{t_2-1} \cdot \frac{t_2-1}{t_2+1} \cdot \frac{1}{d} = \frac{4}{t_1(t_2+1)} \cdot \frac{1}{d}$.

Second, corresponding to Case (2) above: if $\delta\left(v^*, vs^1_{t_1}\right) = \delta\left(v^*, vs^2_{t_2-1}\right) = 1$ and $\delta\left(v^*, vs^2_{t_2}\right) = 2$, then the MLE is correct with probability $1/(d-1)$. This gives a contribution of $\frac{2}{t_1} \cdot \frac{2}{t_2-1} \cdot \frac{2}{t_2+1} \cdot \frac{1}{d-1} = \frac{4}{t_1(t_2+1)} \cdot \frac{2}{t_2-1} \cdot \frac{1}{d-1}$.

Next, corresponding to Case (3) above: if $\delta\left(v^*, vs^2_{t_2-1}\right) = 1$, $\delta\left(vs^2_{t_2-1}, vs^1_{t_1}\right) = 1$, and $vs^2_{t_2-1} = vs^2_{t_2}$, then the MLE is correct with probability $1/(d-1)$. This gives a contribution of $\frac{2}{t_1} \cdot \frac{2}{t_2-1} \cdot \frac{t_2-1}{t_2+1} \cdot \frac{1}{d-1} = \frac{4}{t_1(t_2+1)} \cdot \frac{1}{d-1}$.

Finally, corresponding to Case (4) above: if $\delta\left(v^*, vs^1_{t_1}\right) = 1$, $\delta\left(v^*, vs^2_{t_2-1}\right) = 2$, $\delta\left(v^*, vs^2_{t_2}\right) = 3$, then the MLE is correct with probability $1/(d-1)$. This gives a contribution of $\frac{2}{t_1} \cdot \frac{2}{t_2-1} \cdot \frac{4}{t_2+1} \cdot \frac{1}{d-1} = \frac{4}{t_1(t_2+1)} \cdot \frac{4}{t_2-1} \cdot \frac{1}{d-1}$.

Putting together these four contributions, we obtain that

$$\mathbb{P}\left(\widehat{v}_{\mathrm{ML}} = v^* \,\middle|\, A_{12}^C\right) = \frac{4}{t_1\left(t_2+1\right)}\left(\frac{1}{d} + \frac{1}{d-1} + \frac{6}{t_2-1} \cdot \frac{1}{d-1}\right). \tag{A.3}$$

We now turn to computing $\mathbb{P}\left(\widehat{v}_{\mathrm{ML}} = v^* \,|\, A_{12}\right)$. As mentioned before, if A_{12} holds, then we must be in Case (5) or in Case (6) above. Accordingly, we have contributions to the probability $\mathbb{P}\left(\widehat{v}_{\mathrm{ML}} = v^* \,|\, A_{12}\right)$ from these two cases and we can break this probability into two terms:

$$\mathbb{P}\left(\widehat{v}_{\mathrm{ML}} = v^* \,|\, A_{12}\right) = \mathbb{P}\left(\widehat{v}_{\mathrm{ML}} = v^*, vs^2_{t_2-1} = vs^2_{t_2} \,\middle|\, A_{12}\right) + \mathbb{P}\left(\widehat{v}_{\mathrm{ML}} = v^*, vs^2_{t_2-1} \neq vs^2_{t_2} \,\middle|\, A_{12}\right) \tag{A.4}$$

Here the first term corresponds to Case (5) and the second corresponds to Case (6).

Recall that in Case (5) we have that $\widehat{v}_{\mathrm{ML}} = v'$, where v' is the vertex in $P_{12} \cap V^1_{t_1} \cap V^2_{t_2}$ that is closest to vs^2. Given that A_{12} holds, we have that $v^* = v'$ in exactly two situations: if $\delta\left(v^*, vs^2\right) = 1$ or if $\delta\left(v^*, vs^1\right) = t_1/2$. In addition, to be in Case (5) we have to have $vs^2_{t_2-1} = vs^2_{t_2}$ (the other condition, $X_2(vs^1) \geq 2$, is guaranteed given A_{12}). By separating into these cases we can write:

$$\begin{aligned}
&\mathbb{P}\left(\widehat{v}_{\mathrm{ML}} = v^*, vs^2_{t_2-1} = vs^2_{t_2} \,\middle|\, A_{12}\right) \\
&\qquad = \mathbb{P}\left(\left(\left\{\delta\left(v^*, vs^2_{t_2}\right) = 1\right\} \cup \left\{\delta\left(v^*, vs^1_{t_1}\right) = t_1/2\right\}\right) \cap \left\{vs^2_{t_2-1} = vs^2_{t_2}\right\} \,\middle|\, A_{12}\right) \\
&\qquad = \mathbb{P}\left(\delta\left(v^*, vs^2_{t_2}\right) = 1 \,\middle|\, A_{12}\right) + \mathbb{P}\left(\delta\left(v^*, vs^1_{t_1}\right) = t_1/2, vs^2_{t_2-1} = vs^2_{t_2} \,\middle|\, A_{12}\right) \\
&\qquad\quad - \mathbb{P}\left(\delta\left(v^*, vs^2_{t_2}\right) = 1, \delta\left(v^*, vs^1_{t_1}\right) = t_1/2 \,\middle|\, A_{12}\right)
\end{aligned} \tag{A.5}$$

We now compute all three of these probabilities. Before we do so, we first compute the probability that $vs^2_{t_2-1} = vs^2_{t_2}$. We do this by conditioning on the value of $\delta\left(v^*, vs^2_{t_2-1}\right)$. Using (13.6) and (13.7) we have that

$$\begin{aligned}
\mathbb{P}\left(vs^2_{t_2-1} = vs^2_{t_2}\right) &= \sum_{h=1}^{(t_2-1)/2} \mathbb{P}\left(vs^2_{t_2-1} = vs^2_{t_2} \,\middle|\, \delta\left(v^*, vs^2_{t_2-1}\right) = h\right) \cdot \frac{2}{t_2-1} \\
&= \sum_{h=1}^{(t_2-1)/2} \frac{t_2+1-2h}{t_2+1} \cdot \frac{2}{t_2-1} = 1 - \frac{4}{(t_2-1)(t_2+1)} \sum_{h=1}^{(t_2-1)/2} h = 1 - \frac{1}{2} = \frac{1}{2}.
\end{aligned}$$

Turning back to the three probabilities in (A.5), notice that in all three cases the events are independent of A_{12}. So first we have that

$$\mathbb{P}\left(\delta\left(v^*, vs^2_{t_2}\right) = 1 \,\middle|\, A_{12}\right) = \mathbb{P}\left(\delta\left(v^*, vs^2_{t_2}\right) = 1\right) = \frac{2}{t_2+1}.$$

Next, by independence we have that

$$\begin{aligned}\mathbb{P}\left(\delta\left(v^*, vs^1_{t_1}\right) = t_1/2, vs^2_{t_2-1} = vs^2_{t_2} \,\middle|\, A_{12}\right) &= \mathbb{P}\left(\delta\left(v^*, vs^1_{t_1}\right) = t_1/2, vs^2_{t_2-1} = vs^2_{t_2}\right) \\ &= \mathbb{P}\left(\delta\left(v^*, vs^1_{t_1}\right) = t_1/2\right)\mathbb{P}\left(vs^2_{t_2-1} = vs^2_{t_2}\right) = \frac{2}{t_1}\cdot\frac{1}{2} = \frac{1}{t_1}.\end{aligned}$$

Finally, by using independence again, we have that

$$\begin{aligned}\mathbb{P}\left(\delta\left(v^*, vs^2_{t_2}\right) = 1, \delta\left(v^*, vs^1_{t_1}\right) = t_1/2 \,\middle|\, A_{12}\right) &= \mathbb{P}\left(\delta\left(v^*, vs^2_{t_2}\right) = 1, \delta\left(v^*, vs^1_{t_1}\right) = t_1/2\right) \\ &= \mathbb{P}\left(\delta\left(v^*, vs^2_{t_2}\right) = 1\right)\mathbb{P}\left(\delta\left(v^*, vs^1_{t_1}\right) = t_1/2\right) = \frac{2}{t_2+1}\cdot\frac{2}{t_1}.\end{aligned}$$

Plugging the previous three displays into (A.5), we have determined the first term in (A.4):

$$\mathbb{P}\left(\widehat{v}_{\mathrm{ML}} = v^*, vs^2_{t_2-1} = vs^2_{t_2} \,\middle|\, A_{12}\right) = \frac{1}{t_1} + \frac{2}{t_2+1} - \frac{4}{t_1\left(t_2+1\right)}. \tag{A.6}$$

The analysis of the second term in (A.4) is analogous to what we have just done for the first term, so we omit the details. In fact, it turns out that this second term is equal to the first term:

$$\mathbb{P}\left(\widehat{v}_{\mathrm{ML}} = v^*, vs^2_{t_2-1} \neq vs^2_{t_2} \,\middle|\, A_{12}\right) = \frac{1}{t_1} + \frac{2}{t_2+1} - \frac{4}{t_1\left(t_2+1\right)}. \tag{A.7}$$

Putting together (A.4), (A.6), and (A.7), we obtain that

$$\mathbb{P}\left(\widehat{v}_{\mathrm{ML}} = v^* \,|\, A_{12}\right) = \frac{2}{t_1} + \frac{4}{t_2+1} - \frac{8}{t_1\left(t_2+1\right)} \tag{A.8}$$

Thus putting together (A.2), (A.3), and (A.8), we obtain that

$$\mathbb{P}\left(\widehat{v}_{\mathrm{ML}} = v^*\right) = \frac{d-1}{d}\left(\frac{2}{t_1} + \frac{4}{t_2+1} - \frac{8}{t_1\left(t_2+1\right)}\right) + \frac{1}{d}\cdot\frac{4}{t_1\left(t_2+1\right)}\left(\frac{1}{d} + \frac{1}{d-1} + \frac{6}{t_2-1}\cdot\frac{1}{d-1}\right).$$

Separating the main terms and the lower order terms, we can write

$$\begin{aligned}\mathbb{P}\left(\widehat{v}_{\mathrm{ML}} = v^*\right) = \frac{d-1}{d}&\left(\frac{2}{t_1} + \frac{4}{t_2+1}\right) \\ &+ \frac{1}{d}\cdot\frac{4}{t_1\left(t_2+1\right)}\left(-2\left(d-1\right) + \frac{1}{d} + \frac{1}{d-1} + \frac{6}{t_2-1}\cdot\frac{1}{d-1}\right).\end{aligned}$$

Since $d \geq 3$ and $t_2 \geq 5$, the second term in the expression above is negative, so we have that

$$\mathbb{P}\left(\widehat{v}_{\mathrm{ML}} = v^*\right) \leq \frac{d-1}{d}\left(\frac{2}{t_1} + \frac{4}{t_2+1}\right) \leq \frac{d-1}{d}\frac{6}{\min\{t_1,t_2\}}. \qquad \square$$

A.2. **When both t_1 and t_2 are odd.**

Proof of Theorem 11.4(b) when both t_1 and t_2 are odd. We may (and will) assume in the following that $t_1, t_2 \geq 5$, since if $\min\{t_1,t_2\} \leq 3$, then the right hand side of (11.4) is greater than 1 and thus the statement is vacuously true.

Recall that we are analyzing the MLE for the *uniform protocol* given by the probabilities in (13.6) and for which we have that (13.7) holds. We start with a few observations. For $i \in \{1,2\}$, the observation $G^i_{t_i}$ is either a ball or it is not. If $G^i_{t_i}$ is a ball, then it is a ball of radius $(t_i-1)/2$ around $vs^i_{t_i-1} = vs^i_{t_i}$, and hence we can determine $vs^i_{t_i-1} = vs^i_{t_i}$. If $G^i_{t_i}$ is not a ball, then its central edge is $\left\{vs^i_{t_i-1}, vs^i_{t_i}\right\}$, and hence we can determine the set $\left\{vs^i_{t_i-1}, vs^i_{t_i}\right\}$. In any case, we may thus define $X_i(v) := \min\left\{\delta\left(v, vs^i_{t_i-1}\right), \delta\left(v, vs^i_{t_i}\right)\right\}$ and note that the function $X_i : V \mapsto \mathbb{R}$ is determined by the observation $G^i_{t_i}$.

With this notation, using the expressions in (13.5), the independence of the two observations, and substituting the expressions in (13.6) and (13.7), we can write down the likelihood function. There are four cases, depending on whether or not $G^1_{t_1}$ and $G^2_{t_2}$ are balls or not. Instead of detailing all four cases of the likelihood function, we skip straight to writing down an expression for the MLE in the four cases; this is analogous to (A.1). If $G^1_{t_1}$ and $G^2_{t_2}$ are both balls, then

$$\widehat{v}_{\mathrm{ML}} \in \underset{v \in V^1_{t_1} \cap V^2_{t_2} \setminus \left\{vs^1_{t_1}, vs^2_{t_2}\right\}}{\arg\min} \left[(X_1(v)+X_2(v))\log(d-1) - \log\left(t_1+1-2X_1(v)\right) - \log\left(t_2+1-2X_2(v)\right)\right]. \tag{A.9}$$

If $G^1_{t_1}$ is a ball and $G^2_{t_2}$ is not a ball, then

$$\widehat{v}_{\mathrm{ML}} \in \underset{v \in V^1_{t_1} \cap V^2_{t_2} \setminus \left\{vs^1_{t_1}, vs^2_{t_2}, vs^2_{t_2-1}\right\}}{\arg\min} \left[(X_1(v)+X_2(v))\log(d-1) - \log\left(t_1+1-2X_1(v)\right) - \log X_2(v)\right]. \tag{A.10}$$

If $G^1_{t_1}$ is not a ball and $G^2_{t_2}$ is a ball, then the MLE satisfies the display above with the indices 1 and 2 switched. Finally, if $G^1_{t_1}$ is not a ball and $G^2_{t_2}$ is also not a ball, then

$$\widehat{v}_{\mathrm{ML}} \in \underset{v \in V^1_{t_1} \cap V^2_{t_2} \setminus \left\{vs^1_{t_1}, vs^1_{t_1-1}, vs^2_{t_2}, vs^2_{t_2-1}\right\}}{\arg\min} \left[(X_1(v)+X_2(v))\log(d-1) - \log X_1(v) - \log X_2(v)\right]. \tag{A.11}$$

To understand the MLE better, we distinguish several cases. These are based on whether or not $G^1_{t_1}$ and $G^2_{t_2}$ are balls, as well as the distance of the sets $\left\{vs^1_{t_1-1}, vs^1_{t_1}\right\}$ and $\left\{vs^2_{t_2-1}, vs^2_{t_2}\right\}$ (and if their distance is zero, what does their intersection look like). Compared to the case where one of t_1 and t_2 is even and the other is odd, we have essentially twice as many cases to consider, because both $G^1_{t_1}$ and $G^2_{t_2}$ can be balls or not. In all cases there is a simple description of the MLE, which we detail next.

We first consider the case when $G^1_{t_1}$ and $G^2_{t_2}$ are both balls. In this case, to abbreviate notation, we let $vs^1 \equiv vs^1_{t_1-1} = vs^1_{t_1}$ and $vs^2 \equiv vs^2_{t_2-1} = vs^2_{t_2}$. We distinguish three subcases based on whether $X_2\left(vs^1\right)$ is 0, 1, or at least 2.

(1) *$G^1_{t_1}$ and $G^2_{t_2}$ are both balls, and $X_2\left(vs^1\right) = 0$.* In this case $vs^1 = vs^2$ and all three terms in (A.9) are minimized by the neighbors of $vs^1 = vs^2$. Therefore $\widehat{v}_{\mathrm{ML}}$ chooses a neighbor of $vs^1 = vs^2$ uniformly at random.

(2) *$G^1_{t_1}$ and $G^2_{t_2}$ are both balls, and $X_2\left(vs^1\right) = 1$.* In this case vs^1 and vs^2 are neighbors. Let us consider all three terms in (A.9). The function $(X_1(v) + X_2(v))\log(d-1)$ is minimized (among vertices not in $\left\{vs^1, vs^2\right\}$) by the neighbors of the set $\left\{vs^1, vs^2\right\}$. The function $-\log\left(t_1 + 1 - 2X_1(v)\right)$ is increasing in $X_1(v)$, while the function $-\log\left(t_2 + 1 - 2X_2(v)\right)$ is increasing in $X_2(v)$. Consequently, the set of minimizers of their sum (among vertices not in $\left\{vs^1, vs^2\right\}$) is contained within the neighbors of the set $\left\{vs^1, vs^2\right\}$. The precise set of minimizers depends on the relationship between t_1 and t_2. If $t_1 = t_2$, then $\widehat{v}_{\mathrm{ML}}$ chooses a neighbor of the set $\left\{vs^1, vs^2\right\}$ uniformly at random. If $t_1 > t_2$, then $\widehat{v}_{\mathrm{ML}}$ chooses one of the $d-1$ neighbors of vs^2 that is not vs^1, uniformly at random. If $t_1 < t_2$, then the indices are switched: $\widehat{v}_{\mathrm{ML}}$ chooses one of the $d-1$ neighbors of vs^1 that is not vs^2, uniformly at random.

(3) *$G^1_{t_1}$ and $G^2_{t_2}$ are both balls, and $X_2\left(vs^1\right) \geq 2$.* We again consider the three terms in (A.9). The first term $((X_1(v) + X_2(v))\log(d-1))$ is minimized on the shortest path between vs^1 and vs^2. The other two terms are increasing in $X_1(v)$ and $X_2(v)$, respectively. This implies that the minimizer of the whole expression in (A.9) lies on the shortest path between vs^1 and vs^2. Let P_{12} denote the set of vertices that are on the shortest path between vs^1 and vs^2, excluding vs^1 and vs^2. We thus have that the MLE satisfies

$$\widehat{v}_{\mathrm{ML}} \in \underset{v \in P_{12} \cap V^1_{t_1} \cap V^2_{t_2}}{\arg\max} \left(t_1 + 1 - 2X_1(v)\right)\left(t_2 + 1 - 2X_2\left(v\right)\right).$$

Next, we consider the case when $G^1_{t_1}$ is a ball and $G^2_{t_2}$ is not a ball. In this case we can again write $vs^1 \equiv vs^1_{t_1-1} = vs^1_{t_1}$ to abbreviate notation. We again distinguish three subcases based on whether $X_2\left(vs^1\right)$ is 0, 1, or at least 2.

(4) *$G^1_{t_1}$ is a ball, $G^2_{t_2}$ is not a ball, and $X_2\left(vs^1\right) = 0$.* In this case $vs^2_{t_2-1}$ and $vs^2_{t_2}$ are neighbors and $vs^1 \in \left\{vs^2_{t_2-1}, vs^2_{t_2}\right\}$. Let us consider all three terms in (A.10). The first term, $(X_1(v) + X_2(v))\log(d-1)$, is minimized (among vertices not in $\left\{vs^1_{t_1}, vs^2_{t_2-1}, vs^2_{t_2}\right\}$) by the neighbors of vs^1 that are not in $\left\{vs^2_{t_2-1}, vs^2_{t_2}\right\}$. The second term, $-\log\left(t_1 + 1 - 2X_1(v)\right)$, is an increasing function of $X_1(v)$, and hence it is also minimized (among possible vertices) by the neighbors of vs^1 that are not in $\left\{vs^2_{t_2-1}, vs^2_{t_2}\right\}$. The third term, $-\log X_2(v)$, is not minimized among the neighbors of vs^1; however, this is a lower order term compared to the first term and it can be seen that the full expression in (A.10) is minimized by the neighbors of vs^1 that are not in $\left\{vs^2_{t_2-1}, vs^2_{t_2}\right\}$. Therefore $\widehat{v}_{\mathrm{ML}}$ chooses a neighbor of vs^1 that is not in $\left\{vs^2_{t_2-1}, vs^2_{t_2}\right\}$ uniformly at random.

(5) *$G^1_{t_1}$ is a ball, $G^2_{t_2}$ is not a ball, and $X_2\left(vs^1\right) = 1$.* This is similar to Case (4) above and we omit the details for brevity. The MLE is the same: $\widehat{v}_{\mathrm{ML}}$ chooses one of the $d-1$ neighbors of vs^1 that is not in $\left\{vs^2_{t_2-1}, vs^2_{t_2}\right\}$, uniformly at random.

(6) *$G^1_{t_1}$ is a ball, $G^2_{t_2}$ is not a ball, and $X_2\left(vs^1\right) \geq 2$.* Let us again consider the three terms in (A.10), and let vs^2 denote the vertex in the set $\left\{vs^2_{t_2-1}, vs^2_{t_2}\right\}$ that is closer to vs^1. The first term, $(X_1(v) + X_2(v))\log(d-1)$, is minimized on the shortest path between vs^1 and vs^2. The second term is increasing in $X_1(v)$, while the third term is decreasing in $X_2(v)$. We also have the constraint that $v \in V^1_{t_1} \cap V^2_{t_2} \setminus \left\{vs^1, vs^2_{t_2-1}, vs^2_{t_2}\right\}$. Let P_{12} denote the set of vertices that are on the shortest path between vs^1 and vs^2, excluding vs^1 and vs^2. Define v' to be the vertex in $P_{12} \cap V^1_{t_1} \cap V^2_{t_2}$ that is closest to vs^1 (note that $P_{12} \cap V^1_{t_1} \cap V^2_{t_2}$ is nonempty, due to the assumption that $X_2\left(vs^1\right) \geq 2$). Given the constraints, v' is the unique vertex that minimizes both the first and the second terms in (A.10). Depending on the details, v' might also minimize the third term in (A.10), but even if it does not, it turns out that v' is always the overall minimizer of the expression in (A.10). Therefore $\widehat{v}_{\mathrm{ML}} = v'$.

The case when $G^1_{t_1}$ is not a ball and $G^2_{t_2}$ is a ball is identical to the above, with the indices 1 and 2 switched. Finally, we consider the case when both $G^1_{t_1}$ and $G^2_{t_2}$ are not balls. We now distinguish four subcases; these are based on whether the distance between $\left\{vs^1_{t_1-1}, vs^1_{t_1}\right\}$ and $\left\{vs^2_{t_2-1}, vs^2_{t_2}\right\}$ is

0, 1, or at least 2, and when this distance is 0, we further distinguish between when the size of the intersection of these two sets is 1 or 2.

(7) $G^1_{t_1}$ *is not a ball,* $G^2_{t_2}$ *is not a ball, and* $\left\{vs^1_{t_1-1}, vs^1_{t_1}\right\} = \left\{vs^2_{t_2-1}, vs^2_{t_2}\right\}$. In this case for any possible vertex v we have that $\ell := X_1(v) = X_2(v) \geq 1$. Thus, by (A.11), the function that we need to minimize is $\ell \mapsto 2\ell \log(d-1) - 2\log \ell$. There are now two cases to distinguish, depending on the value of d.

When $d \geq 4$, this function is minimized when $\ell = 1$. Therefore $\widehat{v}_{\mathrm{ML}}$ chooses one of the $2d-2$ neighbors of the set $\left\{vs^1_{t_1-1}, vs^1_{t_1}\right\}$, uniformly at random.

When $d = 3$, this function is minimized when $\ell \in \{1, 2\}$. Therefore $\widehat{v}_{\mathrm{ML}}$ chooses one of the $2\left(d - 1 + (d-1)^2\right) = 12$ vertices at distance 1 or 2 from the set $\left\{vs^1_{t_1-1}, vs^1_{t_1}\right\}$, uniformly at random.

(8) $G^1_{t_1}$ *is not a ball,* $G^2_{t_2}$ *is not a ball, and* $\left|\left\{vs^1_{t_1-1}, vs^1_{t_1}\right\} \cap \left\{vs^2_{t_2-1}, vs^2_{t_2}\right\}\right| = 1$. To abbreviate notation, let $H := \left\{vs^1_{t_1-1}, vs^1_{t_1}\right\} \cup \left\{vs^2_{t_2-1}, vs^2_{t_2}\right\}$ and $\widetilde{v} := \left\{vs^1_{t_1-1}, vs^1_{t_1}\right\} \cap \left\{vs^2_{t_2-1}, vs^2_{t_2}\right\}$. We can categorize the vertices in $V \setminus H$ into three groups.

There are vertices v for which $\ell := X_1(v) = X_2(v) - 1 \geq 1$. For such vertices the quantity in (A.11) is equal to $(2\ell+1)\log(d-1) - \log \ell - \log(\ell+1)$.

There are vertices v for which $\ell := X_2(v) = X_1(v) - 1 \geq 1$. For such vertices the quantity in (A.11) is also equal to $(2\ell+1)\log(d-1) - \log \ell - \log(\ell+1)$.

Finally, there are vertices v for which $\ell := X_1(v) = X_2(v) = \delta(v, \widetilde{v}) \geq 1$. For such vertices the quantity in (A.11) is equal to $2\ell \log(d-1) - 2\log \ell$ (which is the same expression as in Case (7) above).

When minimizing these quantities, there are now two cases to distinguish, depending on the value of d. When $d \geq 4$, $\widehat{v}_{\mathrm{ML}}$ chooses one of the $d-2$ neighbors of $\widetilde{v}$ not in H, uniformly at random. When $d = 3$, $\widehat{v}_{\mathrm{ML}}$ chooses one of $(d-2) + d(d-1) = 7$ nodes that is at distance 1 or 2 from $\widetilde{v}$ and is not in H, uniformly at random.

(9) $G^1_{t_1}$ *is not a ball,* $G^2_{t_2}$ *is not a ball, and the distance between* $\left\{vs^1_{t_1-1}, vs^1_{t_1}\right\}$ *and* $\left\{vs^2_{t_2-1}, vs^2_{t_2}\right\}$ *is equal to* 1. To abbreviate notation, let $H := \left\{vs^1_{t_1-1}, vs^1_{t_1}\right\} \cup \left\{vs^2_{t_2-1}, vs^2_{t_2}\right\}$, let $\widetilde{v}^1$ denote the vertex in $\left\{vs^1_{t_1-1}, vs^1_{t_1}\right\}$ that is closest to $\left\{vs^2_{t_2-1}, vs^2_{t_2}\right\}$, and define $\widetilde{v}^2$ analogously. We can categorize the vertices in $V \setminus H$ into four groups.

There are vertices v for which $\ell := X_1(v) = X_2(v) - 2 \geq 1$. For such vertices the quantity in (A.11) is equal to $(2\ell+2)\log(d-1) - \log \ell - \log(\ell+2)$.

There are vertices v for which $\ell := X_1(v) = \delta\left(v, \widetilde{v}^1\right) \geq 1$ and $X_2(v) = \delta\left(v, \widetilde{v}^2\right) = \ell + 1$. For such vertices the quantity in (A.11) is equal to $(2\ell+1)\log(d-1) - \log\ell - \log(\ell+1)$.

There are vertices v for which $\ell := X_2(v) = \delta\left(v, \widetilde{v}^2\right) \geq 1$ and $X_1(v) = \delta\left(v, \widetilde{v}^1\right) = \ell + 1$. For such vertices the quantity in (A.11) is also equal to $(2\ell+1)\log(d-1) - \log\ell - \log(\ell+1)$.

Finally, there are vertices v for which $\ell := X_2(v) = X_1(v) - 2 \geq 1$. For such vertices the quantity in (A.11) is equal to $(2\ell+2)\log(d-1) - \log\ell - \log(\ell+2)$.

Now note that whenever $d \geq 3$ and $\ell \geq 1$, we always have that $(2\ell+2)\log(d-1) - \log\ell - \log(\ell+2) > (2\ell+1)\log(d-1) - \log\ell - \log(\ell+1)$. Furthermore, note that the function $\ell \mapsto (2\ell+1)\log(d-1) - \log\ell - \log(\ell+1)$ on the domain $\ell \geq 1$ is minimized at $\ell = 1$. Putting these together we have that $\widehat{v}_{\mathrm{ML}}$ chooses one of the $2(d-2)$ nodes that are a neighbor of $\widetilde{v}^1$ or $\widetilde{v}^2$ and not in H, uniformly at random.

(10) *$G^1_{t_1}$ is not a ball, $G^2_{t_2}$ is not a ball, and the distance between $\left\{vs^1_{t_1-1}, vs^1_{t_1}\right\}$ and $\left\{vs^2_{t_2-1}, vs^2_{t_2}\right\}$ is at least* 2. Again, let $\widetilde{v}^1$ denote the vertex in $\left\{vs^1_{t_1-1}, vs^1_{t_1}\right\}$ that is closest to $\left\{vs^2_{t_2-1}, vs^2_{t_2}\right\}$, and define $\widetilde{v}^2$ analogously. Let P_{12} denote the set of vertices that are on the shortest path between $\widetilde{v}^1$ and $\widetilde{v}^2$, excluding $\widetilde{v}^1$ and $\widetilde{v}^2$.

The expression in (A.11) has three terms. The first term, $(X_1(v) + X_2(v))\log(d-1)$, is the main term, and it is minimized on P_{12}, taking on the value $\delta\left(\widetilde{v}^1, \widetilde{v}^2\right)\log(d-1)$. The other two terms are decreasing in $X_1(v)$ and $X_2(v)$, respectively. However, it turns out these are lower order terms and that almost always the whole expression in (A.11) is minimized on P_{12}, and thus the MLE satisfies

$$\widehat{v}_{\mathrm{ML}} \in \underset{v \in P_{12} \cap V^1_{t_1} \cap V^2_{t_2}}{\arg\max} X_1(v)\, X_2(v)\,.$$

There is only one exception to this: when $d = 3$ and $\delta\left(\widetilde{v}^1, \widetilde{v}^2\right) = 2$. In this case let w be the unique vertex that is at distance 1 from both $\widetilde{v}^1$ and $\widetilde{v}^2$, and let w' be the unique vertex that is at distance 2 from both $\widetilde{v}^1$ and $\widetilde{v}^2$. In this case the expression in (A.11) is minimized at w and w', so $\widehat{v}_{\mathrm{ML}}$ chooses w or w', uniformly at random.

Now that we have fully described the MLE, we can compute the probability that it is correct. We may again condition on whether or not A_{12} holds (see (13.8)) to obtain that

$$\mathbb{P}\left(\widehat{v}_{\mathrm{ML}} = v^*\right) = \mathbb{P}\left(\widehat{v}_{\mathrm{ML}} = v^* \mid A_{12}\right) \cdot \frac{d-1}{d} + \mathbb{P}\left(\widehat{v}_{\mathrm{ML}} = v^* \,\middle|\, A^C_{12}\right) \cdot \frac{1}{d}. \tag{A.12}$$

Note that if A_{12} holds then we must be in Cases (3), (6), or (10). Consequently, Cases (1), (2), (4), (5), (7), (8), and (9) imply that A_{12} does not hold.

Let us start by computing $\mathbb{P}\left(\widehat{v}_{\mathrm{ML}} = v^* \,\middle|\, A_{12}^C\right)$. Recall from above that in Cases (3) and (6) we have that $\widehat{v}_{\mathrm{ML}} \in P_{12}$, so if A_{12}^C holds, then $\widehat{v}_{\mathrm{ML}} \neq v^*$. In Case (10) we also have that $\widehat{v}_{\mathrm{ML}} \in P_{12}$, with one exception (see above), but even then we have that $\widehat{v}_{\mathrm{ML}}$ is "in between" $\left\{vs_{t_1-1}^1, vs_{t_1}^1\right\}$ and $\left\{vs_{t_2-1}^2, vs_{t_2}^2\right\}$, and so if A_{12}^C holds, then $\widehat{v}_{\mathrm{ML}} \neq v^*$. Thus only Cases (1), (2), (4), (5), (7), (8), and (9) contribute to the probability $\mathbb{P}\left(\widehat{v}_{\mathrm{ML}} = v^* \,\middle|\, A_{12}^C\right)$. In the following computations we use the expressions (13.6) and (13.7).

First, corresponding to Case (1) above: if $\delta\left(v^*, vs_{t_1}^1\right) = \delta\left(v^*, vs_{t_2}^2\right) = 1$, then the MLE is correct with probability $1/d$. This gives a contribution of $\frac{2}{t_1-1} \cdot \frac{t_1-1}{t_1+1} \cdot \frac{2}{t_2-1} \cdot \frac{t_2-1}{t_2+1} \cdot \frac{1}{d} = \frac{4}{(t_1+1)(t_2+1)} \cdot \frac{1}{d}$.

Second, corresponding to Case (2) above, we distinguish three subcases based on whether $t_1 = t_2$, $t_1 < t_2$, or $t_1 > t_2$. If $t_1 = t_2$, then if $\delta\left(v^*, vs_{t_1}^1\right) = 1$, $\delta\left(v^*, vs_{t_2-1}^2\right) = 2$, and $vs_{t_2-1}^2 = vs_{t_2}^2$, or if $\delta\left(v^*, vs_{t_2}^2\right) = 1$, $\delta\left(v^*, vs_{t_1-1}^1\right) = 2$, and $vs_{t_1-1}^1 = vs_{t_1}^1$, then the MLE is correct with probability $1/(2d-2)$. This gives a contribution of

$$\left(\frac{2}{t_1+1} \cdot \frac{2}{t_2-1} \cdot \frac{t_2-3}{t_2+1} + \frac{2}{t_2+1} \cdot \frac{2}{t_1-1} \cdot \frac{t_1-3}{t_1+1}\right) \frac{1}{2(d-1)} = \frac{4(t-3)}{(t-1)(t+1)^2} \cdot \frac{1}{d-1},$$

where $t := t_1 = t_2$. If $t_1 < t_2$, then if $\delta\left(v^*, vs_{t_1}^1\right) = 1$, $\delta\left(v^*, vs_{t_2-1}^2\right) = 2$, and $vs_{t_2-1}^2 = vs_{t_2}^2$, then the MLE is correct with probability $1/(d-1)$. This gives a contribution of

$$\frac{2}{t_1+1} \cdot \frac{2}{t_2-1} \cdot \frac{t_2-3}{t_2+1} \cdot \frac{1}{d-1} = \frac{4(t_2-3)}{(t_2-1)(t_1+1)(t_2+1)} \cdot \frac{1}{d-1}.$$

If $t_1 > t_2$, then we have the same contribution as in the display above, with the indices 1 and 2 switched. Altogether we have obtained that the contribution in every subcase is

$$\frac{4(\max\{t_1,t_2\}-3)}{(\max\{t_1,t_2\}-1)(t_1+1)(t_2+1)} \cdot \frac{1}{d-1} < \frac{4}{(t_1+1)(t_2+1)} \cdot \frac{1}{d-1}.$$

Next, we turn to Case (4) above. We have that if $\delta\left(v^*, vs_{t_1}^1\right) = 1$, $\delta\left(v^*, vs_{t_2-1}^2\right) = 1$, and $\delta\left(v^*, vs_{t_2}^2\right) = 2$, then the MLE is correct with probability $1/(d-1)$. This gives a contribution of $\frac{2}{t_1+1} \cdot \frac{2}{t_2-1} \cdot \frac{2}{t_2+1} \cdot \frac{1}{d-1}$. There is an analogous term coming from when $G_{t_1}^1$ is not a ball and $G_{t_2}^2$ is a ball, giving a contribution of $\frac{2}{t_2+1} \cdot \frac{2}{t_1-1} \cdot \frac{2}{t_1+1} \cdot \frac{1}{d-1}$. The combined contribution from the two terms is

$$\frac{4}{(t_1+1)(t_2+1)} \cdot \frac{1}{d-1}\left(\frac{2}{t_1-1} + \frac{2}{t_2-1}\right) \leq \frac{4}{(t_1+1)(t_2+1)} \cdot \frac{1}{d-1},$$

where the inequality follows from the assumption that $\min\{t_1, t_2\} \geq 5$.

Next, we turn to Case (5) above. We have that if $\delta\left(v^*, vs^1_{t_1}\right) = 1$, $\delta\left(v^*, vs^2_{t_2-1}\right) = 2$, and $\delta\left(v^*, vs^2_{t_2}\right) = 3$, then the MLE is correct with probability $1/(d-1)$. This gives a contribution of $\frac{2}{t_1+1} \cdot \frac{2}{t_2-1} \cdot \frac{4}{t_2+1} \cdot \frac{1}{d-1}$. There is an analogous term coming from when $G^1_{t_1}$ is not a ball and $G^2_{t_2}$ is a ball, giving a contribution of $\frac{2}{t_2+1} \cdot \frac{2}{t_1-1} \cdot \frac{4}{t_1+1} \cdot \frac{1}{d-1}$. The combined contribution from the two terms is

$$\frac{4}{(t_1+1)(t_2+1)} \cdot \frac{1}{d-1}\left(\frac{4}{t_1-1} + \frac{4}{t_2-1}\right) \leq \frac{4}{(t_1+1)(t_2+1)} \cdot \frac{2}{d-1},$$

where the inequality follows from the assumption that $\min\{t_1, t_2\} \geq 5$.

Next, we turn to Case (7) above, where we have to distinguish between $d \geq 4$ and $d = 3$. When $d \geq 4$, then if $\delta\left(v^*, vs^1_{t_1-1}\right) = 1$, $\delta\left(v^*, vs^1_{t_1}\right) = 2$, $\delta\left(v^*, vs^2_{t_2-1}\right) = 1$, $\delta\left(v^*, vs^2_{t_2}\right) = 2$, and $vs^1_{t_1} = vs^2_{t_2}$, then the MLE is correct with probability $1/(2d-2)$. This gives a contribution of

$$\begin{aligned}\frac{2}{t_1-1} \cdot \frac{2}{t_1+1} \cdot \frac{2}{t_2-1} \cdot \frac{2}{t_2+1} \cdot \frac{1}{d-1} \cdot \frac{1}{2(d-1)} &= \frac{4}{(t_1+1)(t_2+1)} \cdot \frac{1}{(d-1)^2} \cdot \frac{2}{(t_1-1)(t_2-1)} \\ &\leq \frac{1}{8} \cdot \frac{4}{(t_1+1)(t_2+1)} \cdot \frac{1}{(d-1)^2},\end{aligned} \tag{A.13}$$

where the inequality follows from the assumption that $\min\{t_1, t_2\} \geq 5$. When $d = 3$, there are now two situations when the MLE has a chance of being correct:

- if $\delta\left(v^*, vs^1_{t_1-1}\right) = 1$, $\delta\left(v^*, vs^1_{t_1}\right) = 2$, $\delta\left(v^*, vs^2_{t_2-1}\right) = 1$, $\delta\left(v^*, vs^2_{t_2}\right) = 2$, and $vs^1_{t_1} = vs^2_{t_2}$,
- or if $\delta\left(v^*, vs^1_{t_1-1}\right) = 2$, $\delta\left(v^*, vs^1_{t_1}\right) = 3$, $\delta\left(v^*, vs^2_{t_2-1}\right) = 2$, $\delta\left(v^*, vs^2_{t_2}\right) = 3$, $vs^1_{t_1-1} = vs^2_{t_2-1}$, and $vs^1_{t_1} = vs^2_{t_2}$;

in both cases the MLE is correct with probability $1/12$. This gives a contribution of

$$\begin{aligned}&\left(\frac{2}{t_1-1} \cdot \frac{2}{t_1+1} \cdot \frac{2}{t_2-1} \cdot \frac{2}{t_2+1} \cdot \frac{1}{2} + \frac{2}{t_1-1} \cdot \frac{4}{t_1+1} \cdot \frac{2}{t_2-1} \cdot \frac{4}{t_2+1} \cdot \frac{1}{2} \cdot \frac{1}{2}\right) \cdot \frac{1}{12} \\ &\qquad = \frac{2}{(t_1+1)(t_2+1)(t_1-1)(t_2-1)}.\end{aligned}$$

This is equal to the quantity in (A.13), when $d = 3$ is substituted. Thus no matter what $d \geq 3$ is, the contribution is always at most

$$\frac{1}{8} \cdot \frac{4}{(t_1+1)(t_2+1)} \cdot \frac{1}{(d-1)^2}.$$

Next, we turn to Case (8) above, where we again distinguish between $d \geq 4$ and $d = 3$. When $d \geq 4$, then if $\delta\left(v^*, vs^1_{t_1-1}\right) = 1$, $\delta\left(v^*, vs^1_{t_1}\right) = 2$, $\delta\left(v^*, vs^2_{t_2-1}\right) = 1$, $\delta\left(v^*, vs^2_{t_2}\right) = 2$, and $vs^1_{t_1} \neq vs^2_{t_2}$, then the MLE is correct with probability $1/(d-2)$. This gives a contribution of

$$\begin{aligned}\frac{2}{t_1-1}\cdot\frac{2}{t_1+1}\cdot\frac{2}{t_2-1}\cdot\frac{2}{t_2+1}\cdot\frac{d-2}{d-1}\cdot\frac{1}{d-2} &= \frac{4}{(t_1+1)(t_2+1)}\cdot\frac{1}{d-1}\cdot\frac{4}{(t_1-1)(t_2-1)} \\ &\leq \frac{1}{4}\cdot\frac{4}{(t_1+1)(t_2+1)}\cdot\frac{1}{d-1},\end{aligned} \tag{A.14}$$

where the inequality follows from the assumption that $\min\{t_1, t_2\} \geq 5$. When $d = 3$, there are now four situations when the MLE has a chance of being correct:

- if $\delta\left(v^*, vs^1_{t_1-1}\right) = 1$, $\delta\left(v^*, vs^1_{t_1}\right) = 2$, $\delta\left(v^*, vs^2_{t_2-1}\right) = 1$, $\delta\left(v^*, vs^2_{t_2}\right) = 2$, and $vs^1_{t_1} \neq vs^2_{t_2}$;
- or if $\delta\left(v^*, vs^1_{t_1-1}\right) = 2$, $\delta\left(v^*, vs^1_{t_1}\right) = 3$, $\delta\left(v^*, vs^2_{t_2-1}\right) = 2$, $\delta\left(v^*, vs^2_{t_2}\right) = 3$, $vs^1_{t_1-1} = vs^2_{t_2-1}$, and $vs^1_{t_1} \neq vs^2_{t_2}$;
- or if $\delta\left(v^*, vs^1_{t_1-1}\right) = 1$, $\delta\left(v^*, vs^1_{t_1}\right) = 2$, $\delta\left(v^*, vs^2_{t_2-1}\right) = 2$, $\delta\left(v^*, vs^2_{t_2}\right) = 3$, and $vs^1_{t_1} = vs^2_{t_2-1}$;
- or if $\delta\left(v^*, vs^1_{t_1-1}\right) = 2$, $\delta\left(v^*, vs^1_{t_1}\right) = 3$, $\delta\left(v^*, vs^2_{t_2-1}\right) = 1$, $\delta\left(v^*, vs^2_{t_2}\right) = 2$, and $vs^1_{t_1-1} = vs^2_{t_2}$;

in all four cases the MLE is correct with probability $1/7$. This gives a contribution of

$$\begin{aligned}&\frac{2}{t_1-1}\cdot\frac{2}{t_1+1}\cdot\frac{2}{t_2-1}\cdot\frac{2}{t_2+1}\cdot\frac{1}{2}\cdot\frac{1}{7} + \frac{2}{t_1-1}\cdot\frac{4}{t_1+1}\cdot\frac{2}{t_2-1}\cdot\frac{4}{t_2+1}\cdot\frac{1}{2}\cdot\frac{1}{2}\cdot\frac{1}{7} \\ &+ \frac{2}{t_1-1}\cdot\frac{2}{t_1+1}\cdot\frac{2}{t_2-1}\cdot\frac{4}{t_2+1}\cdot\frac{1}{2}\cdot\frac{1}{7} + \frac{2}{t_1-1}\cdot\frac{4}{t_1+1}\cdot\frac{2}{t_2-1}\cdot\frac{2}{t_2+1}\cdot\frac{1}{2}\cdot\frac{1}{7} \\ &= \frac{8}{(t_1+1)(t_2+1)(t_1-1)(t_2-1)}.\end{aligned}$$

This is equal to the quantity in (A.14), when $d = 3$ is substituted. Thus no matter what $d \geq 3$ is, the contribution is always at most

$$\frac{1}{4}\cdot\frac{4}{(t_1+1)(t_2+1)}\cdot\frac{1}{d-1}.$$

Finally, we turn to Case (9) above. There are now two situations when the MLE has a chance of being correct:

- if $\delta\left(v^*, vs^1_{t_1-1}\right) = 1$, $\delta\left(v^*, vs^1_{t_1}\right) = 2$, $\delta\left(v^*, vs^2_{t_2-1}\right) = 2$, $\delta\left(v^*, vs^2_{t_2}\right) = 3$, and $vs^1_{t_1} \neq vs^2_{t_2-1}$;
- or if $\delta\left(v^*, vs^1_{t_1-1}\right) = 2$, $\delta\left(v^*, vs^1_{t_1}\right) = 3$, $\delta\left(v^*, vs^2_{t_2-1}\right) = 1$, $\delta\left(v^*, vs^2_{t_2}\right) = 2$, and $vs^1_{t_1-1} \neq vs^2_{t_2}$;

in both cases the MLE is correct with probability $1/(2d-4)$. This gives a contribution of

$$\frac{2}{t_1-1}\cdot\frac{2}{t_1+1}\cdot\frac{2}{t_2-1}\cdot\frac{4}{t_2+1}\cdot\frac{d-2}{d-1}\cdot\frac{1}{2(d-2)} + \frac{2}{t_1-1}\cdot\frac{4}{t_1+1}\cdot\frac{2}{t_2-1}\cdot\frac{2}{t_2+1}\cdot\frac{d-2}{d-1}\cdot\frac{1}{2(d-2)}$$

$$= \frac{4}{(t_1+1)(t_2+1)} \cdot \frac{1}{d-1} \cdot \frac{8}{(t_1-1)(t_2-1)} \leq \frac{1}{2} \cdot \frac{4}{(t_1+1)(t_2+1)} \cdot \frac{1}{d-1},$$

where the inequality follows from the assumption that $\min\{t_1, t_2\} \geq 5$.

In summary, putting the contributions from all these cases together we are now ready to bound the probability $\mathbb{P}\left(\widehat{v}_{\mathrm{ML}} = v^* \,\middle|\, A_{12}^C\right)$. We have that

$$\begin{aligned}\mathbb{P}\left(\widehat{v}_{\mathrm{ML}} = v^* \,\middle|\, A_{12}^C\right) &\leq \frac{4}{(t_1+1)(t_2+1)} \left\{\frac{1}{d} + \frac{1}{d-1}\left(1+1+2+\frac{1}{8(d-1)}+\frac{1}{4}+\frac{1}{2}\right)\right\} \\ &\leq \frac{263}{24} \cdot \frac{1}{(t_1+1)(t_2+1)} \leq \frac{11}{(t_1+1)(t_2+1)}, \end{aligned} \tag{A.15}$$

where in the second inequality we used that $d \geq 3$.

We now turn to computing $\mathbb{P}\left(\widehat{v}_{\mathrm{ML}} = v^* \,|\, A_{12}\right)$. To do this, we condition on the values of $\delta\left(v^*, vs^1_{t_1-1}\right)$ and $\delta\left(v^*, vs^2_{t_2-1}\right)$. To this end, define for $1 \leq h_1 \leq (t_1-1)/2$ and $1 \leq h_2 \leq (t_2-1)/2$ the events

$$\begin{aligned} D_1(h_1) &:= \left\{\delta\left(v^*, vs^1_{t_1-1}\right) = h_1\right\}, \\ D_2(h_2) &:= \left\{\delta\left(v^*, vs^2_{t_2-1}\right) = h_2\right\}. \end{aligned}$$

The events $D_1(h_1)$ and $D_2(h_2)$ are independent and they are also independent of A_{12}, so

$$\mathbb{P}\left(D_1(h_1) \cap D_2(h_2) \,|\, A_{12}\right) = \mathbb{P}\left(D_1(h_1) \cap D_2(h_2)\right) = \mathbb{P}\left(D_1(h_1)\right)\mathbb{P}\left(D_2(h_2)\right) = \frac{2}{t_1-1} \cdot \frac{2}{t_2-1}.$$

Thus conditioning on the values of $\delta\left(v^*, vs^1_{t_1-1}\right)$ and $\delta\left(v^*, vs^2_{t_2-1}\right)$ we have that

$$\mathbb{P}\left(\widehat{v}_{\mathrm{ML}} = v^* \,|\, A_{12}\right) = \frac{4}{(t_1-1)(t_2-1)} \sum_{h_1=1}^{(t_1-1)/2} \sum_{h_2=1}^{(t_2-1)/2} \mathbb{P}\left(\widehat{v}_{\mathrm{ML}} = v^* \,|\, A_{12} \cap D_1(h_1) \cap D_2(h_2)\right). \tag{A.16}$$

So now what remains is to compute $\mathbb{P}\left(\widehat{v}_{\mathrm{ML}} = v^* \,|\, A_{12} \cap D_1(h_1) \cap D_2(h_2)\right)$ and to sum this over possible values of h_1 and h_2. To do this we further define the events

$$\begin{aligned} B_1 &:= \left\{vs^1_{t_1-1} = vs^1_{t_1}\right\}, \\ B_2 &:= \left\{vs^2_{t_2-1} = vs^2_{t_2}\right\}. \end{aligned}$$

In words, B_1 and B_2 are the events that the virtual source stays in place at the last time step in the first and the second sample, respectively. Note that B_1 and B_2 are independent, even conditioned

on $A_{12} \cap D_1(h_1) \cap D_2(h_2)$. Therefore

$$\mathbb{P}(B_1 \cap B_2 \,|\, A_{12} \cap D_1(h_1) \cap D_2(h_2)) = \mathbb{P}(B_1 \,|\, D_1(h_1))\,\mathbb{P}(B_2 \,|\, D_2(h_2)) = \frac{t_1+1-2h_1}{t_1+1} \cdot \frac{t_2+1-2h_2}{t_2+1},$$

and similarly

$$\begin{aligned}
\mathbb{P}\left(B_1^C \cap B_2 \,\middle|\, A_{12} \cap D_1(h_1) \cap D_2(h_2)\right) &= \frac{2h_1}{t_1+1} \cdot \frac{t_2+1-2h_2}{t_2+1}, \\
\mathbb{P}\left(B_1 \cap B_2^C \,\middle|\, A_{12} \cap D_1(h_1) \cap D_2(h_2)\right) &= \frac{t_1+1-2h_1}{t_1+1} \cdot \frac{2h_2}{t_2+1}, \\
\mathbb{P}\left(B_1^C \cap B_2^C \,\middle|\, A_{12} \cap D_1(h_1) \cap D_2(h_2)\right) &= \frac{2h_1}{t_1+1} \cdot \frac{2h_2}{t_2+1}.
\end{aligned}$$

By conditioning on whether or not the events B_1 and B_2 hold, we may break up the probability $\mathbb{P}(\widehat{v}_{\mathrm{ML}} = v^* \,|\, A_{12} \cap D_1(h_1) \cap D_2(h_2))$ into a sum with four terms:

$$\begin{aligned}
&\mathbb{P}(\widehat{v}_{\mathrm{ML}} = v^* \,|\, A_{12} \cap D_1(h_1) \cap D_2(h_2)) \\
&\quad = \frac{(t_1+1-2h_1)(t_2+1-2h_2)}{(t_1+1)(t_2+1)} \mathbb{P}(\widehat{v}_{\mathrm{ML}} = v^* \,|\, A_{12} \cap D_1(h_1) \cap D_2(h_2) \cap B_1 \cap B_2) && \text{(A.17)} \\
&\qquad + \frac{(2h_1)(t_2+1-2h_2)}{(t_1+1)(t_2+1)} \mathbb{P}\left(\widehat{v}_{\mathrm{ML}} = v^* \,\middle|\, A_{12} \cap D_1(h_1) \cap D_2(h_2) \cap B_1^C \cap B_2\right) && \text{(A.18)} \\
&\qquad + \frac{(t_1+1-2h_1)(2h_2)}{(t_1+1)(t_2+1)} \mathbb{P}\left(\widehat{v}_{\mathrm{ML}} = v^* \,\middle|\, A_{12} \cap D_1(h_1) \cap D_2(h_2) \cap B_1 \cap B_2^C\right) && \text{(A.19)} \\
&\qquad + \frac{4h_1h_2}{(t_1+1)(t_2+1)} \mathbb{P}\left(\widehat{v}_{\mathrm{ML}} = v^* \,\middle|\, A_{12} \cap D_1(h_1) \cap D_2(h_2) \cap B_1^C \cap B_2^C\right) && \text{(A.20)}
\end{aligned}$$

We now compute each of these four conditional probabilities in turn.

We start with (A.18) and (A.19), as these are the simplest cases among the four. Given the event $A_{12} \cap D_1(h_1) \cap D_2(h_2) \cap B_1 \cap B_2^C$ in (A.19), Case (6) describes the MLE. Specifically, if v' denotes the vertex in $P_{12} \cap V_{t_1}^1 \cap V_{t_2}^2$ that is closest to vs^1, then we have that $\widehat{v}_{\mathrm{ML}} = v'$. Therefore in this case $\widehat{v}_{\mathrm{ML}} = v^*$ if and only if $h_1 = 1$ or $h_2 = (t_2-1)/2$. Thus we have that

$$\begin{aligned}
\mathbb{P}\left(\widehat{v}_{\mathrm{ML}} = v^* \,\middle|\, A_{12} \cap D_1(h_1) \cap D_2(h_2) \cap B_1 \cap B_2^C\right) &= \mathbf{1}_{\{h_1=1\} \cup \{h_2=(t_2-1)/2\}} \\
&= \mathbf{1}_{\{h_1=1\}} + \mathbf{1}_{\{h_2=(t_2-1)/2\}} - \mathbf{1}_{\{h_1=1\} \cap \{h_2=(t_2-1)/2\}}.
\end{aligned}$$

Plugging this back into (A.19) and summing over h_1 and h_2 we obtain that

$$\sum_{h_1=1}^{(t_1-1)/2} \sum_{h_2=1}^{(t_2-1)/2} \frac{(t_1+1-2h_1)(2h_2)}{(t_1+1)(t_2+1)} \mathbb{P}\left(\widehat{v}_{\mathrm{ML}} = v^* \,\middle|\, A_{12} \cap D_1(h_1) \cap D_2(h_2) \cap B_1 \cap B_2^C\right)$$

$$= \frac{4}{(t_1+1)(t_2+1)} \sum_{h_1=1}^{(t_1-1)/2} \sum_{h_2=1}^{(t_2-1)/2} \left(\frac{t_1+1}{2} - h_1 \right) h_2 \mathbf{1}_{\{h_1=1\} \cup \{h_2=(t_2-1)/2\}}$$

$$= \frac{4}{(t_1+1)(t_2+1)} \cdot \frac{t_1-1}{2} \sum_{h_2=1}^{(t_2-1)/2} h_2 + \frac{4}{(t_1+1)(t_2+1)} \cdot \frac{t_2-1}{2} \sum_{h_1=1}^{(t_1-1)/2} \left(\frac{t_1+1}{2} - h_1 \right)$$
$$- \frac{4}{(t_1+1)(t_2+1)} \cdot \frac{t_1-1}{2} \cdot \frac{t_2-1}{2}$$
$$= \frac{(t_1-1)(t_2-1)}{4(t_1+1)} + \frac{(t_1-1)(t_2-1)}{4(t_2+1)} - \frac{(t_1-1)(t_2-1)}{(t_1+1)(t_2+1)}.$$

Multiplying this expression by $4/\{(t_1-1)(t_2-1)\}$ we thus see that the contribution to (A.16) from (A.19) is

$$\frac{1}{t_1+1} + \frac{1}{t_2+1} - \frac{4}{(t_1+1)(t_2+1)}. \tag{A.21}$$

Observe that (A.18) is analogous to (A.19) with the two samples switched. Since the expression in (A.21) is symmetric with respect to t_1 and t_2, this means that the contribution to (A.16) from (A.18) is also equal to the expression in (A.21).

We now turn to the expression in (A.20). Given the event $A_{12} \cap D_1(h_1) \cap D_2(h_2) \cap B_1^C \cap B_2^C$, Case (10) describes the MLE. In particular, note that on this event we have that $X_1(v) + X_2(v) = h_1 + h_2$ for every $v \in P_{12}$, and thus $X_1(v)X_2(v) = X_1(v)(h_1 + h_2 - X_1(v))$. Letting $d := X_1(v)$ to abbreviate notation, note that the function $d \mapsto d(h_1 + h_2 - d)$ is a quadratic function that is maximized (among integers) at $d = (h_1+h_2)/2$ if h_1+h_2 is even, and at $d = (h_1+h_2-1)/2$ and $d = (h_1+h_2+1)/2$ if h_1+h_2 is odd. This allows us to understand the MLE and the expression in (A.20) as follows:

- If $h_1 = h_2 = 1$, then if $d = 3$ then the MLE is correct with probability $1/2$, and if $d \geq 4$ then the MLE is correct with probability 1. In either case we can bound this probability by 1.
- If $2 < h_1 + h_2 \leq \min\{t_1, t_2\} - 1$ and $h_1 + h_2$ is even, then $\widehat{v}_{\mathrm{ML}}$ is the unique vertex v such that $X_1(v) = X_2(v) = (h_1+h_2)/2$. Thus in this case $\widehat{v}_{\mathrm{ML}} = v^*$ if and only if $h_1 = h_2$.
- If $2 < h_1 + h_2 \leq \min\{t_1, t_2\} - 1$ and $h_1 + h_2$ is odd, then $\widehat{v}_{\mathrm{ML}}$ picks uniformly at random among the two vertices for which $\{X_1(v), X_2(v)\} = \{(h_1+h_2-1)/2, (h_1+h_2+1)/2\}$. Thus in this case the MLE is correct with probability $1/2$ if $|h_1 - h_2| = 1$, and not correct otherwise.
- If $h_1 + h_2 \geq \min\{t_1, t_2\}$ (note that this can only occur if $t_1 \neq t_2$), then if $v \in P_{12}$ is such that $X_1(v) \in \{\lfloor (h_1+h_2)/2 \rfloor, \lceil (h_1+h_2)/2 \rceil\}$, then $v \notin V_{t_1}^1 \cap V_{t_2}^2$. Therefore, since $d \mapsto d(h_1 + h_2 - d)$ is a quadratic function, $\widehat{v}_{\mathrm{ML}}$ is the unique vertex $v \in P_{12} \cap V_{t_1}^1 \cap V_{t_2}^2$

such that $X_1(v)$ is closest to $\{\lfloor (h_1+h_2)/2 \rfloor, \lceil (h_1+h_2)/2 \rceil\}$. To understand this better, assume (without loss of generality) that $t_1 \le t_2$. Then we have that $\widehat{v}_{\mathrm{ML}} = v^*$ if and only if $h_1 = (t_1-1)/2$.

Altogether we have obtained, assuming $t_1 \le t_2$, that

$$\mathbb{P}\left(\widehat{v}_{\mathrm{ML}} = v^* \,\middle|\, A_{12} \cap D_1(h_1) \cap D_2(h_2) \cap B_1^C \cap B_2^C\right) \le \mathbf{1}_{\{h_1=h_2\}} + \frac{1}{2}\mathbf{1}_{\{|h_1-h_2|=1, h_1+h_2 \le t_1-1\}} + \mathbf{1}_{\{h_1=(t_1-1)/2, h_1+h_2 \ge t_1\}}.$$

Multiplying the right hand side by $h_1 h_2$ and summing over h_1 and h_2, we obtain that

$$\begin{aligned}
&\sum_{h_1=1}^{(t_1-1)/2} \sum_{h_2=1}^{(t_2-1)/2} h_1 h_2 \left(\mathbf{1}_{\{h_1=h_2\}} + \frac{1}{2}\mathbf{1}_{\{|h_1-h_2|=1, h_1+h_2 \le t_1-1\}} + \mathbf{1}_{\{h_1=(t_1-1)/2, h_1+h_2 \ge t_1\}}\right) \\
&\qquad = \sum_{h=1}^{(t_1-1)/2} h^2 + \sum_{h=1}^{(t_1-3)/2} h(h+1) + \frac{t_1-1}{2} \sum_{h_2=(t_1+1)/2}^{(t_2-1)/2} h_2 \\
&\qquad = \frac{(t_1-1)\left[(t_1-3)(t_1+1) + 3(t_2-1)(t_2+1)\right]}{48}.
\end{aligned}$$

Multiplying this by $16/\{(t_1-1)(t_2-1)(t_1+1)(t_2+1)\}$ we thus see that the contribution to (A.16) from (A.20) is at most

$$\frac{(t_1-3)(t_1+1) + 3(t_2-1)(t_2+1)}{3(t_2-1)(t_1+1)(t_2+1)} = \frac{1}{t_1+1} + \frac{t_1-3}{3(t_2-1)(t_2+1)} \le \frac{1}{t_1+1} + \frac{1/3}{t_2+1}.$$

Recall that here we assumed that $t_1 \le t_2$, so in general the contribution to (A.16) from (A.20) is at most

$$\frac{1}{\min\{t_1,t_2\}+1} + \frac{1/3}{\max\{t_1,t_2\}+1}. \tag{A.22}$$

The expression in (A.17) is similar to that in (A.20); in fact, it turns out that the contribution to (A.16) from (A.17) is also at most the quantity in (A.22). Since the analysis of (A.17) is analogous to that of (A.20) done above, we omit it for brevity.

Putting everything together, in particular (A.16), the cases (A.17)—(A.20), and the corresponding contributions (A.21) and (A.22), and recalling that both of these contributions should be counted twice, we obtain that

$$\mathbb{P}\left(\widehat{v}_{\mathrm{ML}} = v^* \,|\, A_{12}\right) \le \frac{2}{t_1+1} + \frac{2}{t_2+1} + \frac{2}{\min\{t_1,t_2\}+1} + \frac{2/3}{\max\{t_1,t_2\}+1} - \frac{8}{(t_1+1)(t_2+1)}$$

$$\leq \frac{6+2/3}{\min\{t_1,t_2\}+1} - \frac{8}{(t_1+1)(t_2+1)}. \tag{A.23}$$

Now finally putting together (A.12), (A.15), and (A.23), we obtain that

$$\begin{aligned}\mathbb{P}(\widehat{v}_{\mathrm{ML}} = v^*) &\leq \frac{d-1}{d}\left(\frac{6+2/3}{\min\{t_1,t_2\}+1} - \frac{8}{(t_1+1)(t_2+1)}\right) + \frac{1}{d}\cdot\frac{11}{(t_1+1)(t_2+1)} \\ &= \frac{d-1}{d}\cdot\frac{6+2/3}{\min\{t_1,t_2\}+1} + \frac{11-8(d-1)}{d(t_1+1)(t_2+1)}.\end{aligned}$$

Since $d \geq 3$, we have that $11 - 8(d-1) < 0$, so the second term above is negative. Therefore

$$\mathbb{P}(\widehat{v}_{\mathrm{ML}} = v^*) \leq \frac{d-1}{d}\cdot\frac{6+2/3}{\min\{t_1,t_2\}+1},$$

which concludes the proof. □

References

[1] G. Amir and O. Gurel-Gurevich. On fixation of activated random walks. *Electron. Commun. Probab.*, pages no. 12, 119–123, 2010.

[2] Greg W. Anderson, Alice Guionnet, and Ofer Zeitouni. *An Introduction to Random Matrices*. Cambridge University Press, 2010.

[3] Greg W. Anderson and Ofer Zeitouni. A CLT for a band matrix model. *Probability Theory and Related Fields*, 134(2):283–338, 2006.

[4] Riddhipratim Basu, Shirshendu Ganguly, and Christopher Hoffman. Non-fixation of symmetric activated random walk on the line for small sleep rate. To appear, Comm. Math. Phys., Preprint Arxiv 1508.05677.

[5] Blind. https://www.teamblind.com. Accessed 15 June, 2020.

[6] Sébastien Bubeck, Jian Ding, Ronen Eldan, and Miklós Z. Rácz. Testing for high-dimensional geometry in random graphs. *Random Structures & Algorithms*, 49(3):503–532, 2016.

[7] Sébastien Bubeck and Shirshendu Ganguly. Entropic CLT and phase transition in high-dimensional Wishart matrices. Preprint available at http://arxiv.org/abs/1509.03258, 2015.

[8] Kechao Cai, Hong Xie, and John C.S. Lui. Information spreading forensics via sequential dependent snapshots. *IEEE/ACM Transactions on Networking*, 26(1):478–491, 2018.

[9] Luc Devroye, András György, Gábor Lugosi, and Frederic Udina. High-dimensional random geometric graphs and their clique number. *Electronic Journal of Probability*, 16:2481–2508, 2011.

[10] P. Diaconis and W. Fulton. A growth model, a game, an algebra, Lagrange inversion, and characteristic classes. *Rend. Sem. Mat. Univ. Politec. Torino*, 49(1):95–119, 1991.

[11] R. Dickman. Nonequilibrium phase transitions in epidemics and sandpiles. *Physica A*, 306:90–97, 2002.

[12] R. Dickman, M. Alava, M.A. Muñoz, J. Peltola, A. Vespignani, and S. Zapperi. Critical behaviour of a one-dimensional fixed-energy sandpile. *Phys. Rev. E*, 64:56104, 2001.

[13] R. Dickman, M.A. Muñoz, A. Vespignani, and S. Zapperi. Paths to self-organized criticality. *Braz. J. Phys.*, 30:27, 2000.

[14] R. Dickman, A. Vespignani, and S. Zapperi. Self-organized criticality as an absorbing-state phase transition. *Physical Review E*, 57:5095–5105, 1998.

[15] Ronald Dickman, Leonardo T. Rolla, and Vladas Sidoravicius. Activated random walkers: Facts, conjectures and challenges. *Journal of Statistical Physics*, 138(1-3):126–142, 2010.

[16] Noureddine El Karoui. On the largest eigenvalue of Wishart matrices with identity covariance when n, p and $p/n \to \infty$. *arXiv preprint math/0309355*, 2003.

[17] Noureddine El Karoui. Tracy-Widom limit for the largest eigenvalue of a large class of complex sample covariance matrices. *The Annals of Probability*, pages 663–714, 2007.

[18] Ronen Eldan and Dan Mikulincer. Information and dimensionality of anisotropic random geometric graphs. Preprint available at https://arxiv.org/abs/1609.02490, 2016.

[19] Kimmo Eriksson. Chip-firing games on mutating graphs. *SIAM Journal on Discrete Mathematics*, 9(1):118–128, 1996.

[20] Giulia Fanti, Peter Kairouz, Sewoong Oh, Kannan Ramchandran, and Pramod Viswanath. Metadata-conscious anonymous messaging. In *Proceedings of the 33rd International Conference on Machine Learning (ICML)*, volume 33, pages 108–116, 2016.

[21] Giulia Fanti, Peter Kairouz, Sewoong Oh, Kannan Ramchandran, and Pramod Viswanath. Rumor Source Obfuscation on Irregular Trees. In *ACM SIGMETRICS Performance Evaluation Review*, volume 44, pages 153–164, 2016.

[22] Giulia Fanti, Peter Kairouz, Sewoong Oh, Kannan Ramchandran, and Pramod Viswanath. Hiding the Rumor Source. *IEEE Transactions on Information Theory*, 63(10):6679–6713, 2017.

[23] Giulia Fanti, Peter Kairouz, Sewoong Oh, and Pramod Viswanath. Spy vs. Spy: Rumor Source Obfuscation. In *ACM SIGMETRICS*, volume 43, pages 271–284. ACM, 2015.

[24] Anne Fey, Lionel Levine, and David B Wilson. Driving sandpiles to criticality and beyond. *Physical review letters*, 104(14):145703, 2010.

[25] Bob Hough, Dan Jerison, and Lionel Levine. Sandpiles on the square lattice. *Preprint arXiv:1703.00827*, 2017.

[26] Svante Janson. Tail bounds for sums of geometric and exponential random variables. *Statistics and Probability Letters*, 135:1–6, 04 2018.

[27] Tiefeng Jiang and Danning Li. Approximation of Rectangular Beta-Laguerre Ensembles and Large Deviations. *Journal of Theoretical Probability*, 28:804–847, 2015.

[28] Kurt Johansson. On fluctuations of eigenvalues of random Hermitian matrices. *Duke Math. J.*, 91(1):151–204, 1998.

[29] Iain M. Johnstone. On the distribution of the largest eigenvalue in principal components analysis. *Annals of Statistics*, 29(2):295–327, 2001.

[30] H. Kesten and V. Sidoravicius. Branching random walk with catalysts. *Elec. J. Probab.*, 8:1–51, 2003.

[31] H. Kesten and V. Sidoravicius. The spread of a rumor or infection in a moving population. *Ann. Probab.*, 33:2402–2462, 2005.

[32] H. Kesten and V. Sidoravicius. A phase transition in a model for the spread of an infection. *Illinois J. Math.*, 50:547–634, 2006.

[33] H. Kesten and V. Sidoravicius. A shape theorem for the spread of an infection. *Ann. Math.*, 167:701–766, 2008.

[34] Justin Khim and Po-Ling Loh. Confidence sets for the source of a diffusion in regular trees. *IEEE Transactions on Network Science and Engineering*, 4(1):27–40, 2017.

[35] Ankit Kumar, Vivek S. Borkar, and Nikhil Karamchandani. Temporally Agnostic Rumor-Source Detection. *IEEE Transactions on Signal and Information Processing over Networks*, 3(2):316–329, 2017.

[36] Lionel Levine. Threshold state and a conjecture of poghosyan, poghosyan, priezzhev and ruelle. *Communications in Mathematical Physics*, 335(2):1003–1017, 2015.

[37] Lionel Levine and Yuval Peres. Internal erosion and the exponent 3/4. Available at http://www.math.cornell.edu/~levine/erosion.pdf.

[38] Sven Lübeck. Universal scaling behavior of non-equilibrium phase transitions. *International Journal of Modern Physics B*, 18(31n32):3977–4118, 2004.

[39] Wuqiong Luo, Wee Peng Tay, and Mei Leng. Infection Spreading and Source Identification: A Hide and Seek Game. *IEEE Transactions on Signal Processing*, 64(16):4228–4243, 2016.

[40] S.S. Manna. Large-scale simulation of avalanche cluster distribution in sand pile model. *J. Stat. Phys.*, 59:509–521, 1990.

[41] S.S. Manna. Two-state model of self-organized criticality. *J.Phys. A, Math. Gen.*, 24:L363–L369, 1991.

[42] Leonardo T. Rolla and Vladas Sidoravicius. Absorbing-state phase transition for driven-dissipative stochastic dynamics on $\mathbb{Z}$. *Inventiones mathematicae*, 188(1):127–150, 2012.

[43] Secret. https://en.wikipedia.org/wiki/Secret_(app). Accessed 15 June, 2020.

[44] Devavrat Shah and Tauhid Zaman. Detecting Sources of Computer Viruses in Networks: Theory and Experiment. In *ACM SIGMETRICS Performance Evaluation Review*, volume 38, pages 203–214, 2010.

[45] Devavrat Shah and Tauhid Zaman. Rumors in a Network: Who's the Culprit? *IEEE Transactions on Information Theory*, 57(8):5163–5181, 2011.

[46] Devavrat Shah and Tauhid Zaman. Finding rumor sources on random trees. *Operations Research*, 64(3):736–755, 2016.

[47] Eric Shellef. Nonfixation for activated random walks. *ALEA*, 7:137–149, 2010.

[48] V. Sidoravicius and A. Teixeira. Absorbing-state transition for stochastic sandpiles and activated random walks. *Electronic Journal of Probability*, 22(33), 2017.

[49] Sam Spencer and Rayadurgam Srikant. On the impossibility of localizing multiple rumor sources in a line graph. *ACM SIGMETRICS Performance Evaluation Review*, 43(2):66–68, 2015.

[50] Brunella Spinelli, Elisa Celis, and Patrick Thiran. A general framework for sensor placement in source localization. *IEEE Transactions on Network Science and Engineering*, 6(2):86–102, 2019.

[51] Anirudh Sridhar and H. Vincent Poor. Bayes-optimal Methods for Finding the Source of a Cascade. Preprint available at http://arxiv.org/abs/2001.11942, 2020.

[52] Anirudh Sridhar and H. Vincent Poor. Sequential Estimation of Network Cascades. Preprint available at http://arxiv.org/abs/1912.03800, 2020.

[53] Alexandre Stauffer and Lorenzo Taggi. Critical density of activated random walks on transitive graphs. *Annals of Probability, to appear*, 2017.

[54] Leonardo T. Rolla and Laurent Tournier. Non-fixation for biased activated random walks. *Annales of the Henri Poincaré Institute - Probability and Statistics*, 54(2):938–951, 2018.

[55] L. Taggi. Absorbing-state phase transition in biased activated random walk. *Electronic Journal of Probability*, 2016(13), 2016.

[56] Wenchang Tang, Feng Ji, and Wee Peng Tay. Estimating Infection Sources in Networks Using Partial Timestamps. *IEEE Transactions on Information Forensics and Security*, 13(12):3035–3049, 2018.

[57] Alessandro Vespignani, Ronald Dickman, Miguel A. Muñoz, and Stefano Zapperi. Driving, conservation, and absorbing states in sandpiles. *Phys. Rev. Lett.*, 81:5676–5679, 1998.

[58] Alessandro Vespignani, Ronald Dickman, Miguel A. Muñoz, and Stefano Zapperi. Absorbing-state phase transitions in fixed-energy sandpiles. *Phys. Rev. E*, 62:4564–4582, 2000.

[59] Ronaldo Vidigal and Ronald Dickman. Asymptotic behavior of the order parameter in a stochastic sandpile. *Journal of Statistical Physics*, 118(1):1–25, 2005.

[60] Zhaoxu Wang, Wenxiang Dong, Wenyi Zhang, and Chee Wei Tan. Rumor Source Detection with Multiple Observations: Fundamental Limits and Algorithms. In *ACM SIGMETRICS Performance Evaluation Review*, volume 42, pages 1–13, 2014.

[61] Whisper. http://whisper.sh/. Accessed 15 June, 2020.

[62] John Wishart. The Generalised Product Moment Distribution in Samples from a Normal Multivariate Population. *Biometrika*, 20A(1/2):32–52, 1928.

[63] Yik Yak. https://en.wikipedia.org/wiki/Yik_Yak. Accessed 15 June, 2020.